Chapter 6
Viscous Flow in Ducts

Motivation. This chapter is completely devoted to an important practical fluids engineering problem: flow in ducts with various velocities, various fluids, and various duct shapes. Piping systems are encountered in almost every engineering design and thus have been studied extensively. There is a small amount of theory plus a large amount of experimentation.

The basic piping problem is this: Given the pipe geometry and its added components (such as fittings, valves, bends, and diffusers) plus the desired flow rate and fluid properties, what pressure drop is needed to drive the flow? Of course, it may be stated in alternative form: Given the pressure drop available from a pump, what flow rate will ensue? The correlations discussed in this chapter are adequate to solve most such piping problems.

This chapter is for incompressible flow; Chap. 9 treats compressible pipe flow.

6.1 Reynolds Number Regimes

Now that we have derived and studied the basic flow equations in Chap. 4, you would think that we could just whip off myriad beautiful solutions illustrating the full range of fluid behavior, of course expressing all these educational results in dimensionless form, using our new tool from Chap. 5, dimensional analysis.

The fact of the matter is that no general analysis of fluid motion yet exists. There are several dozen known particular solutions, there are many approximate digital computer solutions, and there are a great many experimental data. There is a lot of theory available if we neglect such important effects as viscosity and compressibility (Chap. 8), but there is no general theory and there may never be. The reason is that a profound and vexing change in fluid behavior occurs at moderate Reynolds numbers. The flow ceases being smooth and steady (*laminar*) and becomes fluctuating and agitated (*turbulent*). The changeover is called *transition* to turbulence. In Fig. 5.3*a* we saw that transition on the cylinder and sphere occurred at about $Re = 3 \times 10^5$, where the sharp drop in the drag coefficient appeared. Transition depends on many effects, such as wall roughness (Fig. 5.3*b*) or fluctuations in the inlet stream, but the primary parameter is the Reynolds number. There are a great many data on transition but only a small amount of theory [1 to 3].

Fig. 6.1 The three regimes of viscous flow: (*a*) laminar flow at low Re; (*b*) transition at intermediate Re; (*c*) turbulent flow at high Re.
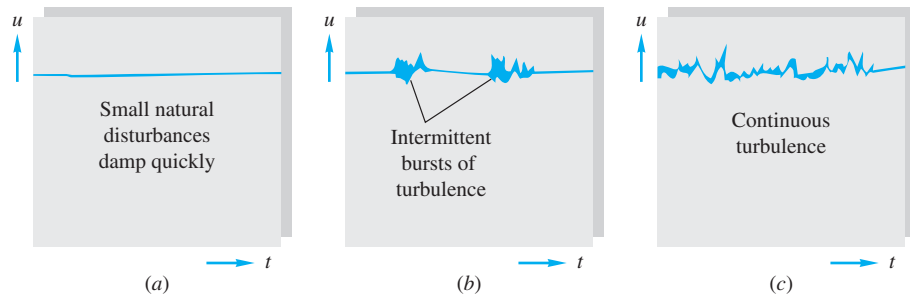
Turbulence can be detected from a measurement by a small, sensitive instrument such as a hot-wire anemometer (Fig. 6.29*e*) or a piezoelectric pressure transducer. The flow will appear steady on average but will reveal rapid, random fluctuations if turbulence is present, as sketched in Fig. 6.1. If the flow is laminar, there may be occasional natural disturbances that damp out quickly (Fig. 6.1*a*). If transition is occurring, there will be sharp bursts of intermittent turbulent fluctuation (Fig. 6.1*b*) as the increasing Reynolds number causes a breakdown or instability of laminar motion. At sufficiently large Re, the flow will fluctuate continually (Fig. 6.1*c*) and is termed *fully turbulent*. The fluctuations, typically ranging from 1 to 20 percent of the average velocity, are not strictly periodic but are random and encompass a continuous range, or spectrum, of frequencies. In a typical wind tunnel flow at high Re, the turbulent frequency ranges from 1 to 10,000 Hz, and the wavelength ranges from about 0.01 to 400 cm.

EXAMPLE 6.1

The accepted transition Reynolds number for flow in a circular pipe is $Re_{d,crit} \approx 2300$. For flow through a 5-cm-diameter pipe, at what velocity will this occur at 20°C for (*a*) airflow and (*b*) water flow?

Solution

Almost all pipe flow formulas are based on the *average* velocity $V = Q/A$, not centerline or any other point velocity. Thus transition is specified at $\rho V d / \mu \approx 2300$. With d known, we introduce the appropriate fluid properties at 20°C from Tables A.3 and A.4:

(*a*) Air: $\quad \dfrac{\rho V d}{\mu} = \dfrac{(1.205 \text{ kg/m}^3)V(0.05 \text{ m})}{1.80 \text{ E-5 kg/(m} \cdot \text{s)}} = 2300 \quad$ or $\quad V \approx 0.7\,\dfrac{\text{m}}{\text{s}}$

(*b*) Water: $\quad \dfrac{\rho V d}{\mu} = \dfrac{(998 \text{ kg/m}^3)V(0.05 \text{ m})}{0.001 \text{ kg/(m} \cdot \text{s)}} = 2300 \quad$ or $\quad V = 0.046\,\dfrac{\text{m}}{\text{s}}$

These are very low velocities, so most engineering air and water pipe flows are turbulent, not laminar. We might expect laminar duct flow with more viscous fluids such as lubricating oils or glycerin.

In free-surface flows, turbulence can be observed directly. Figure 6.2 shows liquid flow issuing from the open end of a tube. The low-Reynolds-number jet (Fig. 6.2*a*) is smooth and laminar, with the fast center motion and slower wall flow forming different trajectories
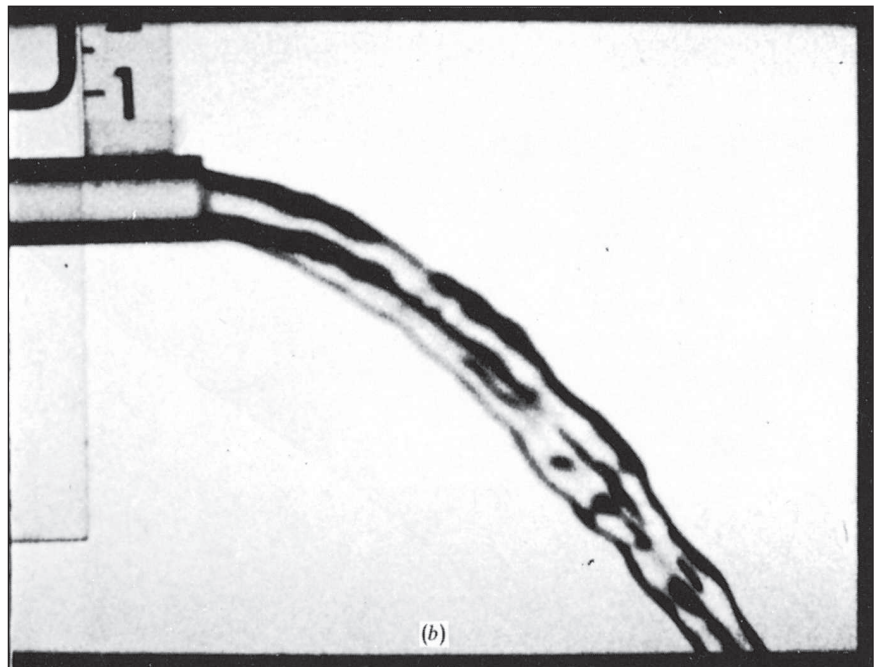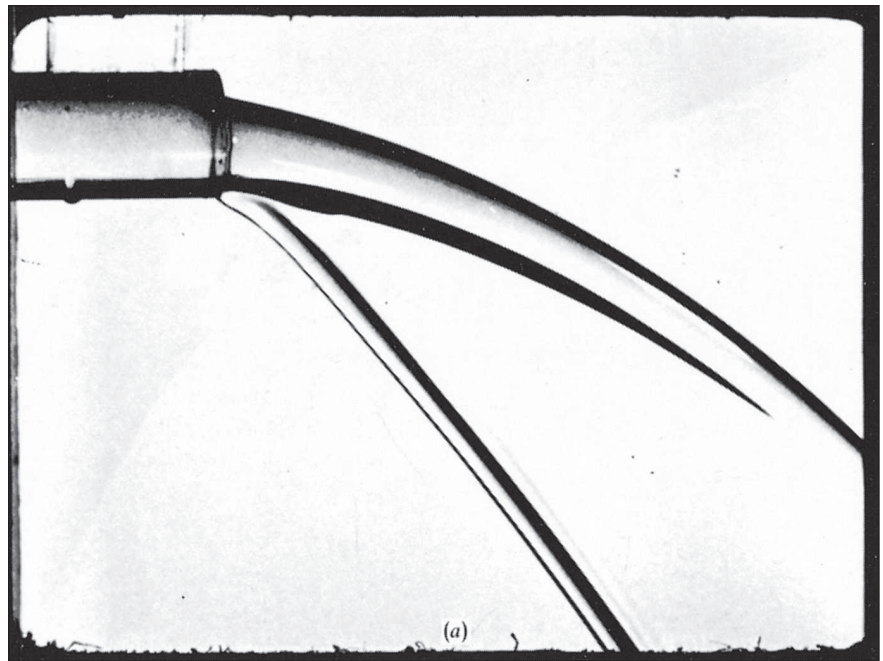
Fig. 6.2 Flow issuing at constant speed from a pipe: (*a*) high-viscosity, low-Reynolds-number, laminar flow; (*b*) low-viscosity, high-Reynolds-number, turbulent flow. Note the ragged, disorderly shape of the jet. *(National Committee for Fluid Mechanics Films, Education Development Center, Inc., © 1972.)*
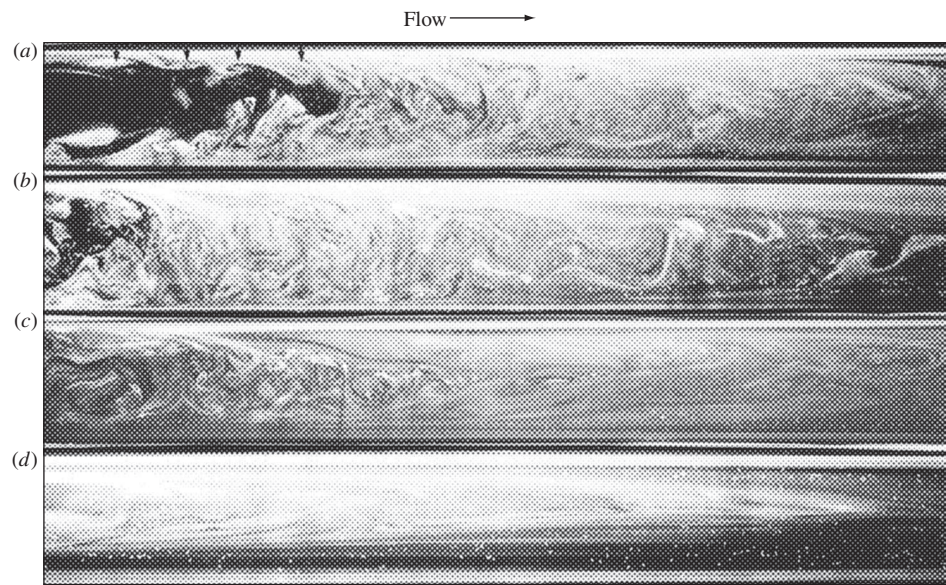
Flow ⟶

(a)

(b)

(c)

Fig. 6.3 Formation of a turbulent
puff in pipe flow: (*a*) and (*b*) near the
entrance; (*c*) somewhat downstream;
(*d*) far downstream. *(Courtesy of
Cambridge University Press–P. R.
Bandyopadhyay, "Aspects of the
Equilibrium Puff in Transitional Pipe
Flow," Journal of Fluid Mechanics,
vol. 163, 1986, pp. 439–458.)*

(d)

joined by a liquid sheet. The higher-Reynolds-number turbulent flow (Fig. 6.2*b*) is
unsteady and irregular but, when averaged over time, is steady and predictable.

How did turbulence form inside the pipe? The laminar parabolic flow profile, which
is similar to Eq. (4.137), became unstable and, at $\text{Re}_d \approx 2300$, began to form "slugs"
or "puffs" of intense turbulence. A puff has a fast-moving front and a slow-moving
rear and may be visualized by experimenting with glass tube flow. Figure 6.3 shows
a puff as photographed by Bandyopadhyay [45]. Near the entrance (Fig. 6.3*a* and *b*)
there is an irregular laminar–turbulent interface, and vortex roll-up is visible. Further
downstream (Fig. 6.3*c*) the puff becomes fully turbulent and very active, with helical
motions visible. Far downstream (Fig. 6.3*d*) the puff is cone-shaped and less active,
with a fuzzy, ill-defined interface, sometimes called the "relaminarization" region.

A complete description of the statistical aspects of turbulence is given in Ref. 1, while
theory and data on transition effects are given in Refs. 2 and 3. At this introductory level
we merely point out that the primary parameter affecting transition is the Reynolds
number. If $\text{Re} = UL/\nu$, where U is the average stream velocity and L is the "width," or
transverse thickness, of the shear layer, the following approximate ranges occur:

$$0 < \text{Re} < \quad 1\text{: highly viscous laminar "creeping" motion}$$
$$1 < \text{Re} < 100\text{: laminar, strong Reynolds number dependence}$$
$$100 < \text{Re} < 10^3\text{: laminar, boundary layer theory useful}$$
$$10^3 < \text{Re} < 10^4\text{: transition to turbulence}$$
$$10^4 < \text{Re} < 10^6\text{: turbulent, moderate Reynolds number dependence}$$
$$10^6 < \text{Re} < \quad\infty\ \text{: turbulent, slight Reynolds number dependence}$$

These representative ranges vary somewhat with flow geometry, surface roughness,
and the level of fluctuations in the inlet stream. The great majority of our analyses
are concerned with laminar flow or with turbulent flow, and one should not normally
design a flow operation in the transition region.

Historical Outline

Since turbulent flow is more prevalent than laminar flow, experimenters have observed turbulence for centuries without being aware of the details. Before 1930 flow instruments were too insensitive to record rapid fluctuations, and workers simply reported mean values of velocity, pressure, force, and so on. But turbulence can change the mean values dramatically, as with the sharp drop in drag coefficient in Fig. 5.3. A German engineer named G. H. L. Hagen first reported in 1839 that there might be *two* regimes of viscous flow. He measured water flow in long brass pipes and deduced a pressure-drop law:

$$\Delta p = (\text{const}) \frac{LQ}{R^4} + \text{entrance effect} \tag{6.1}$$

This is exactly our laminar flow scaling law from Example 5.4, but Hagen did not realize that the constant was proportional to the fluid viscosity.

The formula broke down as Hagen increased Q beyond a certain limit—that is, past the critical Reynolds number—and he stated in his paper that there must be a second mode of flow characterized by "strong movements of water for which Δp varies as the second power of the discharge. . . ." He admitted that he could not clarify the reasons for the change.

A typical example of Hagen's data is shown in Fig. 6.4. The pressure drop varies linearly with $V = Q/A$ up to about 1.1 ft/s, where there is a sharp change. Above about
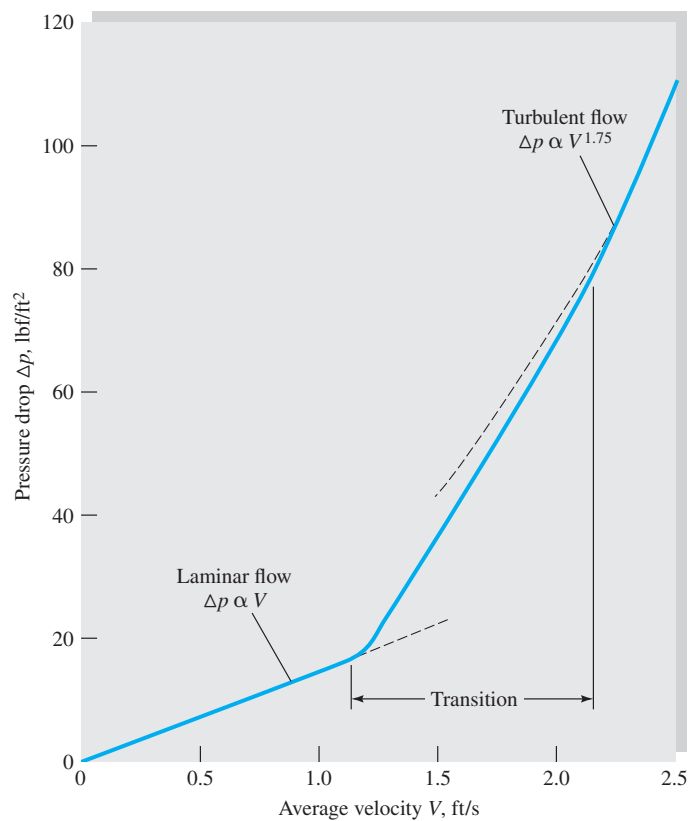

Fig. 6.4 Experimental evidence of transition for water flow in a $\frac{1}{4}$-in smooth pipe 10 ft long.
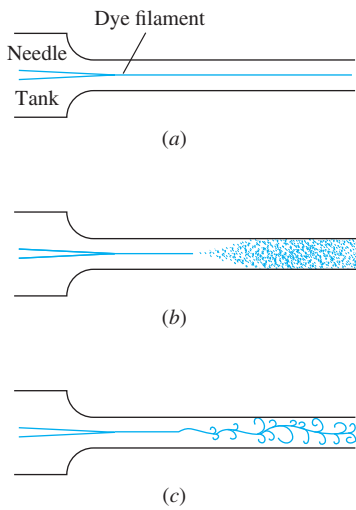
(a)

(b)

(c)

Fig. 6.5 Reynolds' sketches of pipe flow transition: (*a*) low-speed, laminar flow; (*b*) high-speed, turbulent flow; (*c*) spark photograph of condition (*b*).

Source: Reynolds, "An Experimental Investigation of the Circumstances which Determine Whether the Motion of Water Shall Be Direct or Sinuous and of the Law of Resistance in Parallel Channels," Phil. Trans. R. Soc., vol. 174, 1883, pp. 935–982.

$V = 2.2$ ft/s the pressure drop is nearly quadratic with V. The actual power $\Delta p \propto V^{1.75}$ seems impossible on dimensional grounds but is easily explained when the dimensionless pipe flow data (Fig. 5.10) are displayed.

In 1883 Osborne Reynolds, a British engineering professor, showed that the change depended on the parameter $\rho V d/\mu$, now named in his honor. By introducing a dye streak into a pipe flow, Reynolds could observe transition and turbulence. His sketches [4] of the flow behavior are shown in Fig. 6.5.

If we examine Hagen's data and compute the Reynolds number at $V = 1.1$ ft/s, we obtain $Re_d = 2100$. The flow became fully turbulent, $V = 2.2$ ft/s, at $Re_d = 4200$. The accepted design value for pipe flow transition is now taken to be

$$Re_{d,\text{crit}} \approx 2300 \tag{6.2}$$

This is accurate for commercial pipes (Fig. 6.13), although with special care in providing a rounded entrance, smooth walls, and a steady inlet stream, $Re_{d,\text{crit}}$ can be delayed until much higher values. The study of transition in pipe flow, both experimentally and theoretically, continues to be a fascinating topic for researchers, as discussed in a recent review article [55]. *Note:* The value of 2300 is for transition in *pipes.* Other geometries, such as plates, airfoils, cylinders, and spheres, have completely different transition Reynolds numbers.

Transition also occurs in external flows around bodies such as the sphere and cylinder in Fig. 5.3. Ludwig Prandtl, a German engineering professor, showed in 1914 that the thin boundary layer surrounding the body was undergoing transition from laminar to turbulent flow. Thereafter the force coefficient of a body was acknowledged to be a function of the Reynolds number [Eq. (5.2)].

There are now extensive theories and experiments of laminar flow instability that explain why a flow changes to turbulence. Reference 5 is an advanced textbook on this subject.

Laminar flow theory is now well developed, and many solutions are known [2, 3], but no analyses can simulate the fine-scale random fluctuations of turbulent flow.[1] Therefore most turbulent flow theory is semiempirical, based on dimensional analysis and physical reasoning; it is concerned with the mean flow properties only and the mean of the fluctuations, not their rapid variations. The turbulent flow "theory" presented here in Chaps. 6 and 7 is unbelievably crude yet surprisingly effective. We shall attempt a rational approach that places turbulent flow analysis on a firm physical basis.

6.2 Internal versus External Viscous Flows

Both laminar and turbulent flow may be either internal (that is, "bounded" by walls) or external and unbounded. This chapter treats internal flows, and Chap. 7 studies external flows.

An internal flow is constrained by the bounding walls, and the viscous effects will grow and meet and permeate the entire flow. Figure 6.6 shows an internal flow in a long duct. There is an *entrance region* where a nearly inviscid upstream flow converges and enters the tube. Viscous boundary layers grow downstream, retarding the

---

[1]However, direct numerical simulation (DNS) of low-Reynolds-number turbulence is now quite common [32].
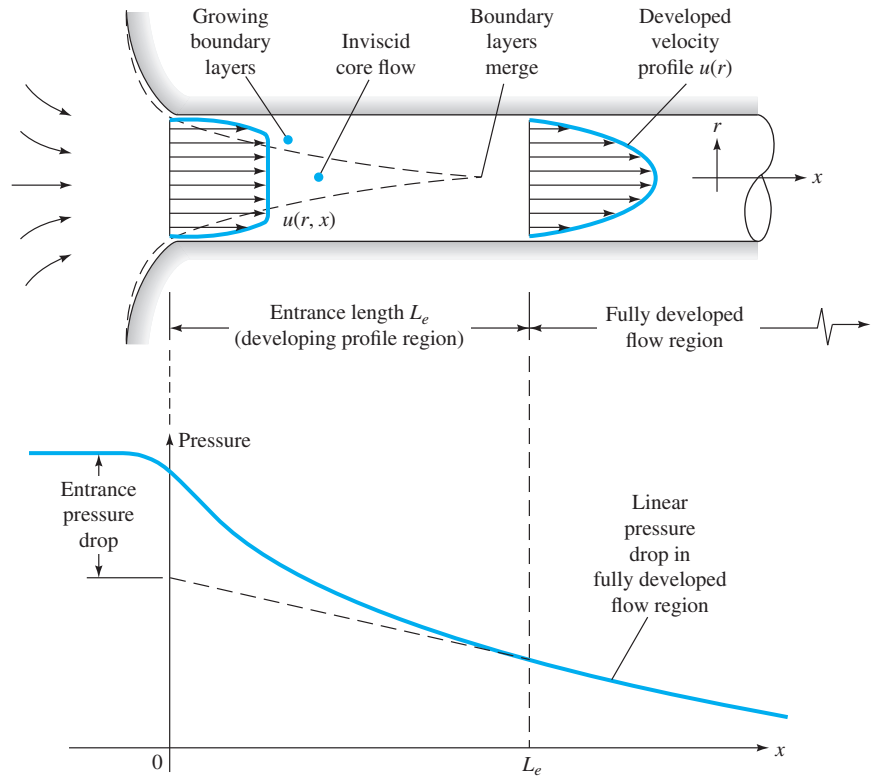
Fig. 6.6 Developing velocity profiles and pressure changes in the entrance of a duct flow.

axial flow $u(r, x)$ at the wall and thereby accelerating the center core flow to maintain the incompressible continuity requirement

$$Q = \int u \, dA = \text{const} \tag{6.3}$$

At a finite distance from the entrance, the boundary layers merge and the inviscid core disappears. The tube flow is then entirely viscous, and the axial velocity adjusts slightly further until at $x = L_e$ it no longer changes with x and is said to be *fully developed, $u \approx u(r)$* only. Downstream of $x = L_e$ the velocity profile is constant, the wall shear is constant, and the pressure drops linearly with x, for either laminar or turbulent flow. All these details are shown in Fig. 6.6.

Dimensional analysis shows that the Reynolds number is the only parameter affecting entrance length. If

$$L_e = f(d, V, \rho, \mu) \qquad V = \frac{Q}{A}$$

then

$$\frac{L_e}{d} = g\left(\frac{\rho V d}{\mu}\right) = g(\text{Re}_d) \tag{6.4}$$

For laminar flow [2, 3], the accepted correlation is

$$\frac{L_e}{d} \approx 0.06 \, \text{Re}_d \qquad \text{laminar} \tag{6.5}$$

The maximum laminar entrance length, at $Re_{d,crit} = 2300$, is $L_e = 138d$, which is the longest development length possible.

In turbulent flow, the boundary layers grow faster, and L_e is relatively shorter. For decades, the writer has favored a sixth-power-law estimate, $L_e/d \approx 4.4\,Re_d^{1/6}$, but recent CFD results, communicated by Fabien Anselmet, and separately by Sukanta Dash, indicate that a better turbulent entrance-length correlation is

$$\frac{L_e}{d} \approx 1.6\,Re_d^{1/4} \quad \text{for} \quad Re_d \leq 10^7 \tag{6.6}$$

Some computed turbulent entrance-length estimates are thus

Re_d	4000	10^4	10^5	10^6	10^7
L_e/d	13	16	28	51	90

Now 90 diameters may seem "long," but typical pipe flow applications involve an L/d value of 1000 or more, in which case the entrance effect may be neglected and a simple analysis made for fully developed flow. This is possible for both laminar and turbulent flows, including rough walls and noncircular cross sections.

EXAMPLE 6.2

A $\frac{1}{2}$-in-diameter water pipe is 60 ft long and delivers water at 5 gal/min at 20°C. What fraction of this pipe is taken up by the entrance region?

Solution

Convert

$$Q = (5 \text{ gal/min})\frac{0.00223 \text{ ft}^3/\text{s}}{1 \text{ gal/min}} = 0.0111 \text{ ft}^3/\text{s}$$

The average velocity is

$$V = \frac{Q}{A} = \frac{0.0111 \text{ ft}^3/\text{s}}{(\pi/4)[(\frac{1}{2}/12) \text{ ft}]^2} = 8.17 \text{ ft/s}$$

From Table 1.4 read for water $\nu = 1.01 \times 10^{-6} \text{ m}^2/\text{s} = 1.09 \times 10^{-5} \text{ ft}^2/\text{s}$. Then the pipe Reynolds number is

$$Re_d = \frac{Vd}{\nu} = \frac{(8.17 \text{ ft/s})[(\frac{1}{2}/12) \text{ ft}]}{1.09 \times 10^{-5} \text{ ft}^2/\text{s}} = 31,300$$

This is greater than 4000; hence the flow is fully turbulent, and Eq. (6.6) applies for entrance length:

$$\frac{L_e}{d} \approx 1.6\,Re_d^{1/4} = (1.6)(31,300)^{1/4} = 21$$

The actual pipe has $L/d = (60 \text{ ft})/[(\frac{1}{2}/12)\text{ft}] = 1440$. Hence the entrance region takes up the fraction

$$\frac{L_e}{L} = \frac{21}{1440} = 0.015 = 1.5\% \qquad\qquad Ans.$$

This is a very small percentage, so we can reasonably treat this pipe flow as essentially fully developed.

Shortness can be a virtue in duct flow if one wishes to maintain the inviscid core. For example, a "long" wind tunnel would be ridiculous, since the viscous core would invalidate the purpose of simulating free-flight conditions. A typical laboratory low-speed wind tunnel test section is 1 m in diameter and 5 m long, with $V = 30$ m/s. If we take $\nu_{air} = 1.51 \times 10^{-5}$ m²/s from Table 1.4, then $Re_d = 1.99 \times 10^6$ and, from Eq. (6.6), $L_e/d \approx 49$. The test section has $L/d = 5$, which is much shorter than the development length. At the end of the section the wall boundary layers are only 10 cm thick, leaving 80 cm of inviscid core suitable for model testing.

An external flow has no restraining walls and is free to expand no matter how thick the viscous layers on the immersed body may become. Thus, far from the body the flow is nearly inviscid, and our analytical technique, treated in Chap. 7, is to patch an inviscid-flow solution onto a viscous boundary-layer solution computed for the wall region. There is no external equivalent of fully developed internal flow.

6.3 Head Loss—The Friction Factor

When applying pipe flow formulas to practical problems, it is customary to use a control volume analysis. Consider incompressible steady flow between sections 1 and 2 of the inclined constant-area pipe in Fig. 6.7. The one-dimensional continuity relation, Eq. (3.30), reduces to

$$Q_1 = Q_2 = \text{const} \quad \text{or} \quad V_1 = V_2 = V$$

since the pipe is of constant area. The steady flow energy equation (3.75) becomes

$$\left(\frac{p}{\rho g} + \alpha \frac{V^2}{2g} + z \right)_1 = \left(\frac{p}{\rho g} + \alpha \frac{V^2}{2g} + z \right)_2 + h_f \tag{6.7}$$
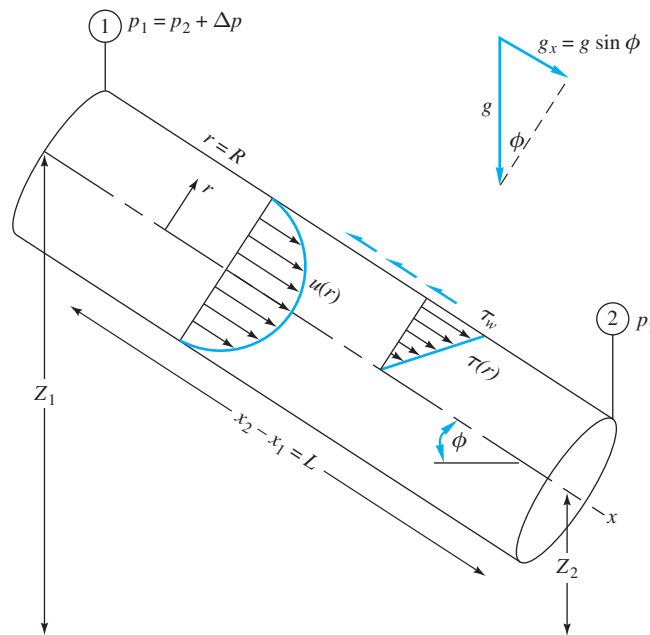

Fig. 6.7 Control volume, just inside the pipe wall, of steady, fully developed flow between two sections in an inclined pipe.

since there is no pump or turbine between 1 and 2. For fully developed flow, the velocity profile shape is the same at sections 1 and 2. Thus $\alpha_1 = \alpha_2$ and, since $V_1 = V_2$, Eq. (6.7) reduces to head loss versus pressure drop and elevation change:

$$h_f = (z_1 - z_2) + \left(\frac{p_1}{\rho g} - \frac{p_2}{\rho g} \right) = \Delta z + \frac{\Delta p}{\rho g} \tag{6.8}$$

The pipe head loss equals the change in the sum of pressure and gravity head—that is, the change in height of the hydraulic grade line (HGL).

Finally, apply the momentum relation (3.40) to the control volume in Fig. 6.7, accounting for applied x-directed forces due to pressure, gravity, and shear:

$$\sum F_x = \Delta p \, (\pi R^2) + \rho g (\pi R^2) L \sin \phi - \tau_w (2 \pi R) L = \dot{m}(V_2 - V_1) = 0 \tag{6.9a}$$

Rearrange this and we find that the head loss is also related to wall shear stress:

$$\Delta z + \frac{\Delta p}{\rho g} = h_f = \frac{2 \tau_w}{\rho g} \frac{L}{R} = \frac{4 \tau_w}{\rho g} \frac{L}{d} \tag{6.9b}$$

where we have substituted $\Delta z = L \sin \phi$ from the geometry of Fig. 6.7. Note that, regardless of whether the pipe is horizontal or tilted, the head loss is proportional to the wall shear stress.

How should we correlate the head loss for pipe flow problems? The answer was given a century and a half ago by Julius Weisbach, a German professor who in 1850 published the first modern textbook on hydrodynamics. Equation (6.9b) shows that h_f is proportional to (L/d), and data such as Hagen's in Fig. 6.6 show that, for turbulent flow, h_f is approximately proportional to V^2. The proposed correlation, still as effective today as in 1850, is

$$h_f = f \frac{L}{d} \frac{V^2}{2g} \quad \text{where} \quad f = \text{fcn}(\text{Re}_d, \frac{\varepsilon}{d}, \text{duct shape}) \tag{6.10}$$

The dimensionless parameter f is called the *Darcy friction factor,* after Henry Darcy (1803–1858), a French engineer whose pipe flow experiments in 1857 first established the effect of roughness on pipe resistance. The quantity ε is the wall roughness height, which is important in turbulent (but not laminar) pipe flow. We added the "duct shape" effect in Eq. (6.10) to remind us that square and triangular and other noncircular ducts have a somewhat different friction factor than a circular pipe. Actual data and theory for friction factors will be discussed in the sections that follow.

By equating Eqs. (6.9) and (6.10) we find an alternative form for friction factor:

$$f = \frac{8 \tau_w}{\rho V^2} \tag{6.11}$$

For noncircular ducts, we must interpret τ_w to be an average value around the duct perimeter. For this reason Eq. (6.10) is preferred as a unified definition of the Darcy friction factor.

6.4 Laminar Fully Developed Pipe Flow

Analytical solutions can be readily derived for laminar flows, either circular or noncircular. Consider fully developed *Poiseuille* flow in a round pipe of diameter d, radius R. Complete analytical results were given in Sec. 4.10. Let us review those formulas here:

$$u = u_{max}\left(1 - \frac{r^2}{R^2}\right) \quad \text{where} \quad u_{max} = \left(-\frac{dp}{dx}\right)\frac{R^2}{4\mu} \quad \text{and} \quad \left(-\frac{dp}{dx}\right) = \left(\frac{\Delta p + \rho g \Delta z}{L}\right)$$

$$V = \frac{Q}{A} = \frac{u_{max}}{2} = \left(\frac{\Delta p + \rho g \Delta z}{L}\right)\frac{R^2}{8\mu}$$

$$Q = \int u\,dA = \pi R^2 V = \frac{\pi R^4}{8\mu}\left(\frac{\Delta p + \rho g \Delta z}{L}\right) \tag{6.12}$$

$$\tau_w = \left|\mu\frac{du}{dr}\right|_{r=R} = \frac{4\mu V}{R} = \frac{8\mu V}{d} = \frac{R}{2}\left(\frac{\Delta p + \rho g \Delta z}{L}\right)$$

$$h_f = \frac{32\mu L V}{\rho g d^2} = \frac{128\mu L Q}{\pi \rho g d^4}$$

The paraboloid velocity profile has an average velocity V which is one-half of the maximum velocity. The quantity Δp is the pressure *drop* in a pipe of length L; that is, (dp/dx) is negative. These formulas are valid whenever the pipe Reynolds number, $Re_d = \rho V d/\mu$, is less than about 2300. Note that τ_w is proportional to V (see Fig. 6.6) and is independent of density because the fluid acceleration is zero. Neither of these is true in turbulent flow.

With wall shear stress known, the Poiseuille flow friction factor is easily determined:

$$f_{lam} = \frac{8\tau_{w,lam}}{\rho V^2} = \frac{8(8\mu V/d)}{\rho V^2} = \frac{64}{\rho V d/\mu} = \frac{64}{Re_d} \tag{6.13}$$

In laminar flow, the pipe friction factor decreases inversely with Reynolds number. This famous formula is effective, but often the algebraic relations of Eqs. (6.12) are more direct for problems.

EXAMPLE 6.3

An oil with $\rho = 900$ kg/m^3 and $\nu = 0.0002$ m^2/s flows upward through an inclined pipe as shown in Fig. E6.3. The pressure and elevation are known at sections 1 and 2, 10 m apart. Assuming steady laminar flow, (a) verify that the flow is up, (b) compute h_f between 1 and 2, and compute (c) Q, (d) V, and (e) Re_d. Is the flow really laminar?
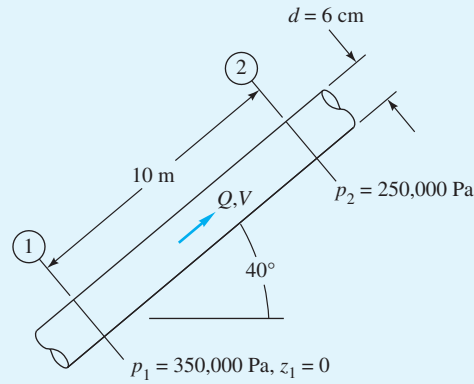
Solution

Part (a)

For later use, calculate

$$\mu = \rho\nu = (900 \text{ kg/m}^3)(0.0002 \text{ m}^2/\text{s}) = 0.18 \text{ kg/(m·s)}$$

$$z_2 = \Delta L \sin 40° = (10 \text{ m})(0.643) = 6.43 \text{ m}$$

E6.3

The flow goes in the direction of falling HGL; therefore, compute the hydraulic grade-line height at each section:

$$\text{HGL}_1 = z_1 + \frac{p_1}{\rho g} = 0 + \frac{350{,}000}{900(9.807)} = 39.65 \text{ m}$$

$$\text{HGL}_2 = z_2 + \frac{p_2}{\rho g} = 6.43 + \frac{250{,}000}{900(9.807)} = 34.75 \text{ m}$$

The HGL is lower at section 2; hence the flow is up from 1 to 2 as assumed. *Ans. (a)*

Part (b)   The head loss is the change in HGL:

$$h_f = \text{HGL}_1 - \text{HGL}_2 = 39.65 \text{ m} - 34.75 \text{ m} = 4.9 \text{ m} \qquad \textit{Ans. (b)}$$

Half the length of the pipe is quite a large head loss.

Part (c)   We can compute Q from the various laminar flow formulas, notably Eq. (6.12):

$$Q = \frac{\pi \rho g d^4 h_f}{128 \mu L} = \frac{\pi (900)(9.807)(0.06)^4 (4.9)}{128(0.18)(10)} = 0.0076 \text{ m}^3/\text{s} \qquad \textit{Ans. (c)}$$

**Part (d)**   Divide Q by the pipe area to get the average velocity:

$$V = \frac{Q}{\pi R^2} = \frac{0.0076}{\pi (0.03)^2} = 2.7 \text{ m/s} \qquad \textit{Ans. (d)}$$

Part (e)   With V known, the Reynolds number is

$$\text{Re}_d = \frac{Vd}{\nu} = \frac{2.7(0.06)}{0.0002} = 810 \qquad \textit{Ans. (e)}$$

This is well below the transition value $\text{Re}_d = 2300$, so we are fairly certain the flow is laminar. Notice that by sticking entirely to consistent SI units (meters, seconds, kilograms, newtons) for all variables we avoid the need for any conversion factors in the calculations.
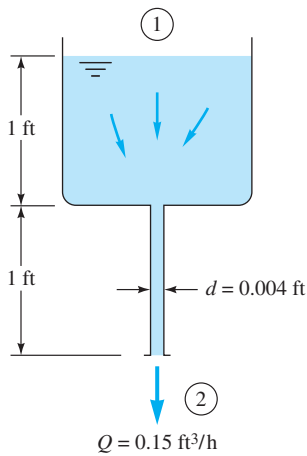
$Q = 0.15\ \text{ft}^3/\text{h}$

E6.4

EXAMPLE 6.4

A liquid of specific weight $\rho g = 58\ \text{lbf/ft}^3$ flows by gravity through a 1-ft tank and a 1-ft capillary tube at a rate of 0.15 ft³/h, as shown in Fig. E6.4. Sections 1 and 2 are at atmospheric pressure. Neglecting entrance effects and friction in the large tank, compute the viscosity of the liquid.

Solution

- *System sketch:* Figure E6.4 shows $L = 1$ ft, $d = 0.004$ ft, and $Q = 0.15$ ft³/h.
- *Assumptions:* Laminar, fully developed, incompressible (Poiseuille) pipe flow. Atmospheric pressure at sections 1 and 2. Negligible velocity at surface, $V_1 \approx 0$.
- *Approach:* Use continuity and energy to find the head loss and thence the viscosity.
- *Property values:* Given $\rho g = 58\ \text{lbf/ft}^3$, figure out $\rho = 58/32.2 = 1.80\ \text{slug/ft}^3$ if needed.
- *Solution step 1:* From continuity and the known flow rate, determine V_2:

$$V_2 = \frac{Q}{A_2} = \frac{Q}{(\pi/4)d^2} = \frac{(0.15/3600)\text{ft}^3/\text{s}}{(\pi/4)(0.004\ \text{ft})^2} = 3.32\ \text{ft/s}$$

Write the energy equation between 1 and 2, canceling terms, and find the head loss:

$$\frac{p_1}{\rho g} + \frac{\alpha_1 V_1^2}{2g} + z_1 = \frac{p_2}{\rho g} + \frac{\alpha_2 V_2^2}{2g} + z_2 + h_f$$

or
$$h_f = z_1 - z_2 - \frac{\alpha_2 V_2^2}{2g} = 2.0\ \text{ft} - 0\ \text{ft} - \frac{(2.0)(3.32\ \text{ft/s})^2}{2(32.2\ \text{ft/s}^2)} = 1.66\ \text{ft}$$

- *Comment:* We introduced $\alpha_2 = 2.0$ for laminar pipe flow from Eq. (3.76). If we forgot α_2, we would have calculated $h_f = 1.83$ ft, a 10 percent error.
- *Solution step 2:* With head loss known, the viscosity follows from the laminar formula in Eqs. (6.12):

$$h_f = 1.66\ \text{ft} = \frac{32\,\mu L V}{(\rho g)d^2} = \frac{32\mu(1.0\ \text{ft})(3.32\ \text{ft/s})}{(58\ \text{lbf/ft}^3)(0.004\ \text{ft})^2} \quad \text{solve for } \mu = 1.45\ \text{E-5}\ \frac{\text{slug}}{\text{ft-s}} \quad Ans.$$

- *Comments:* We didn't need the value of ρ—the formula contains ρg, but who knew? Note also that L in this formula is the *pipe length* of 1 ft, not the total elevation change.
- *Final check:* Calculate the Reynolds number to see if it is less than 2300 for laminar flow:

$$\text{Re}_d = \frac{\rho V d}{\mu} = \frac{(1.80\ \text{slug/ft}^3)(3.32\ \text{ft/s})(0.004\ \text{ft})}{(1.45\ \text{E-5 slug/ft-s})} \approx 1650 \quad \text{Yes, laminar.}$$

- *Comments:* So we did need ρ after all to calculate Re_d.
- *Unexpected comment:* For this head loss, there is a *second* (turbulent) solution, as we shall see in Example 6.8.

6.5 Turbulence Modeling

Throughout this chapter we assume constant density and viscosity and no thermal interaction, so that only the continuity and momentum equations are to be solved for velocity and pressure

Continuity:
$$\frac{\partial u}{\partial x} + \frac{\partial v}{\partial y} + \frac{\partial w}{\partial z} = 0$$

(6.14)

Momentum:
$$\rho\, \frac{d\mathbf{V}}{dt} = -\nabla p + \rho \mathbf{g} + \mu\, \nabla^2 \mathbf{V}$$

subject to no slip at the walls and known inlet and exit conditions. (We shall save our free-surface solutions for Chap. 10.)

We will not work with the differential energy relation, Eq. (4.53), in this chapter, but it is very important, both for heat transfer calculations and for general understanding of duct flow processes. There is work being done by pressure forces to drive the fluid through the duct. Where does this energy go? There is no work done by the wall shear stresses, because the velocity at the wall is zero. The answer is that pressure work is balanced by viscous dissipation in the interior of the flow. The integral of the dissipation function Φ, from Eq. (4.50), over the flow field will equal the pressure work. An example of this fundamental viscous flow energy balance is given in Problem C6.7.

Both laminar and turbulent flows satisfy Eqs. (6.14). For laminar flow, where there are no random fluctuations, we go right to the attack and solve them for a variety of geometries [2, 3], leaving many more, of course, for the problems.

Reynolds' Time-Averaging Concept

For turbulent flow, because of the fluctuations, every velocity and pressure term in Eqs. (6.14) is a rapidly varying random function of time and space. At present our mathematics cannot handle such instantaneous fluctuating variables. No single pair of random functions $\mathbf{V}(x, y, z, t)$ and $p(x, y, z, t)$ is known to be a solution to Eqs. (6.14). Moreover, our attention as engineers is toward the average or *mean* values of velocity, pressure, shear stress, and the like in a high-Reynolds-number (turbulent) flow. This approach led Osborne Reynolds in 1895 to rewrite Eqs. (6.14) in terms of mean or time-averaged turbulent variables.

The time mean $\bar{u}$ of a turbulent function $u(x, y, z, t)$ is defined by

$$\bar{u} = \frac{1}{T} \int_0^T u \, dt \tag{6.15}$$

where T is an averaging period taken to be longer than any significant period of the fluctuations themselves. The mean values of turbulent velocity and pressure are illustrated in Fig. 6.8. For turbulent gas and water flows, an averaging period $T \approx 5$ s is usually quite adequate.
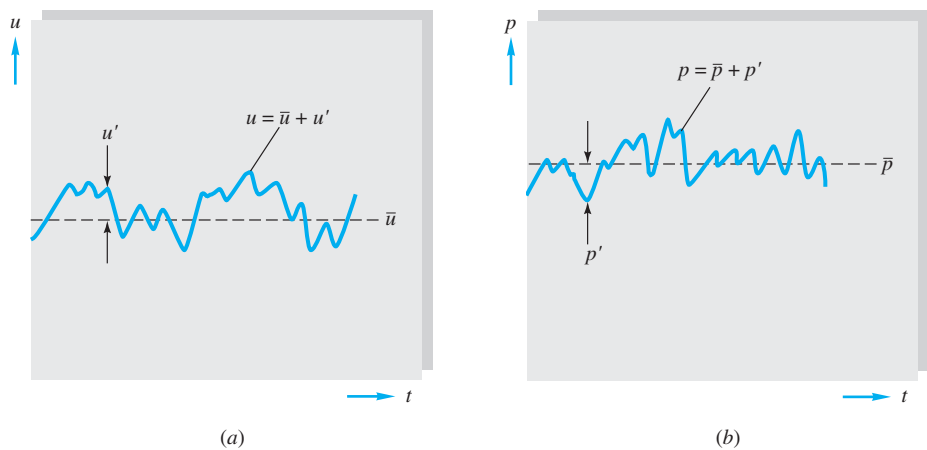

Fig. 6.8 Definition of mean and fluctuating turbulent variables: (*a*) velocity; (*b*) pressure.

The *fluctuation* u' is defined as the deviation of u from its average value

$$u' = u - \bar{u} \tag{6.16}$$

also shown in Fig. 6.8. It follows by definition that a fluctuation has zero mean value:

$$\bar{u'} = \frac{1}{T} \int_0^T (u - \bar{u}) \, dt = \bar{u} - \bar{u} = 0 \tag{6.17}$$

However, the mean square of a fluctuation is not zero and is a measure of the *intensity* of the turbulence:

$$\overline{u'^2} = \frac{1}{T} \int_0^T u'^2 \, dt \neq 0 \tag{6.18}$$

Nor in general are the mean fluctuation products such as $\overline{u'v'}$ and $\overline{u'p'}$ zero in a typical turbulent flow.

Reynolds' idea was to split each property into mean plus fluctuating variables:

$$u = \bar{u} + u' \quad v = \bar{v} + v' \quad w = \bar{w} + w' \quad p = \bar{p} + p' \tag{6.19}$$

Substitute these into Eqs. (6.14), and take the time mean of each equation. The continuity relation reduces to

$$\frac{\partial \bar{u}}{\partial x} + \frac{\partial \bar{v}}{\partial y} + \frac{\partial \bar{w}}{\partial z} = 0 \tag{6.20}$$

which is no different from a laminar continuity relation.

However, each component of the momentum equation (6.14*b*), after time averaging, will contain mean values plus three mean products, or *correlations,* of fluctuating velocities. The most important of these is the momentum relation in the mainstream, or *x*, direction, which takes the form

$$\rho \frac{d\bar{u}}{dt} = -\frac{\partial \bar{p}}{\partial x} + \rho g_x + \frac{\partial}{\partial x}\left(\mu \frac{\partial \bar{u}}{\partial x} - \rho \overline{u'^2}\right)$$
$$+ \frac{\partial}{\partial y}\left(\mu \frac{\partial \bar{u}}{\partial y} - \rho \overline{u'v'}\right) + \frac{\partial}{\partial z}\left(\mu \frac{\partial \bar{u}}{\partial z} - \rho \overline{u'w'}\right) \tag{6.21}$$

The three correlation terms $-\rho \overline{u'^2}$, $-\rho \overline{u'v'}$, and $-\rho \overline{u'w'}$ are called *turbulent stresses* because they have the same dimensions and occur right alongside the newtonian (laminar) stress terms $\mu(\partial \bar{u}/\partial x)$ and so on.

The turbulent stresses are unknown a priori and must be related by experiment to geometry and flow conditions, as detailed in Refs. 1 to 3. Fortunately, in duct and boundary layer flow, the stress $-\rho \overline{u'v'}$, associated with direction *y* normal to the wall is dominant, and we can approximate with excellent accuracy a simpler streamwise momentum equation

$$\rho \frac{d\bar{u}}{dt} \approx -\frac{\partial \bar{p}}{\partial x} + \rho g_x + \frac{\partial \tau}{\partial y} \tag{6.22}$$

where

$$\tau = \mu \frac{\partial \bar{u}}{\partial y} - \rho \overline{u'v'} = \tau_{\text{lam}} + \tau_{\text{turb}} \tag{6.23}$$
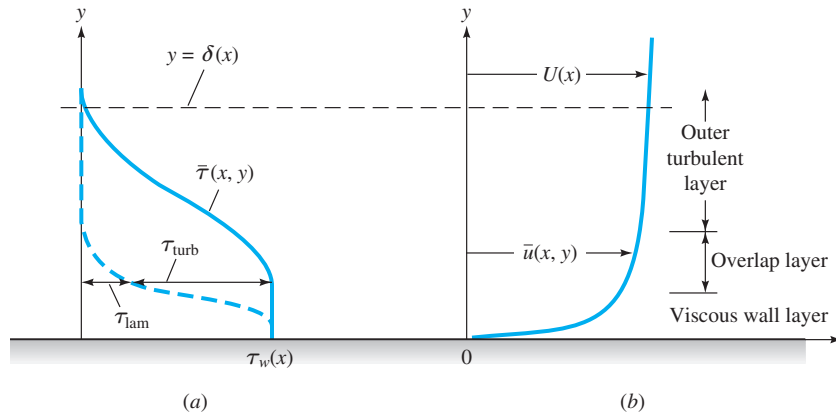
Fig. 6.9 Typical velocity and shear distributions in turbulent flow near a wall: (*a*) shear; (*b*) velocity.

Figure 6.9 shows the distribution of τ_{lam} and τ_{turb} from typical measurements across a turbulent shear layer near a wall. Laminar shear is dominant near the wall (the *wall layer*), and turbulent shear dominates in the *outer layer*. There is an intermediate region, called the *overlap layer,* where both laminar and turbulent shear are important. These three regions are labeled in Fig. 6.9.

In the outer layer τ_{turb} is two or three orders of magnitude greater than τ_{lam}, and vice versa in the wall layer. These experimental facts enable us to use a crude but very effective model for the velocity distribution $\bar{u}(y)$ across a turbulent wall layer.

The Logarithmic Overlap Law

We have seen in Fig. 6.9 that there are three regions in turbulent flow near a wall:

1. Wall layer: Viscous shear dominates.
2. Outer layer: Turbulent shear dominates.
3. Overlap layer: Both types of shear are important.

From now on let us agree to drop the overbar from velocity $\bar{u}$. Let τ_w be the wall shear stress, and let δ and U represent the thickness and velocity at the edge of the outer layer, $y = \delta$.

For the wall layer, Prandtl deduced in 1930 that u must be independent of the shear layer thickness:

$$u = f(\mu, \tau_w, \rho, y) \tag{6.24}$$

By dimensional analysis, this is equivalent to

$$u^+ = \frac{u}{u^*} = F\left(\frac{yu^*}{\nu}\right) \qquad u^* = \left(\frac{\tau_w}{\rho}\right)^{1/2} \tag{6.25}$$

Equation (6.25) is called the *law of the wall,* and the quantity u^* is termed the *friction velocity* because it has dimensions $\{LT^{-1}\}$, although it is not actually a flow velocity.

Subsequently, Kármán in 1933 deduced that u in the outer layer is independent of molecular viscosity, but its deviation from the stream velocity U must depend on the layer thickness δ and the other properties:

$$(U - u)_{\text{outer}} = g(\delta, \tau_w, \rho, y) \tag{6.26}$$

Again, by dimensional analysis we rewrite this as

$$\frac{U - u}{u^*} = G\left(\frac{y}{\delta}\right) \tag{6.27}$$

where u^* has the same meaning as in Eq. (6.25). Equation (6.27) is called the *velocity-defect law* for the outer layer.

Both the wall law (6.25) and the defect law (6.27) are found to be accurate for a wide variety of experimental turbulent duct and boundary layer flows [Refs. 1 to 3]. They are different in form, yet they must overlap smoothly in the intermediate layer. In 1937 C. B. Millikan showed that this can be true only if the overlap layer velocity varies logarithmically with y:

$$\boxed{\frac{u}{u^*} = \frac{1}{\kappa} \ln \frac{yu^*}{\nu} + B \quad \text{overlap layer}} \tag{6.28}$$

Over the full range of turbulent smooth wall flows, the dimensionless constants κ and B are found to have the approximate values $\kappa \approx 0.41$ and $B \approx 5.0$. Equation (6.28) is called the *logarithmic overlap layer*.

Thus by dimensional reasoning and physical insight we infer that a plot of u versus $\ln y$ in a turbulent shear layer will show a curved wall region, a curved outer region, and a straight-line logarithmic overlap. Figure 6.10 shows that this is exactly the case.
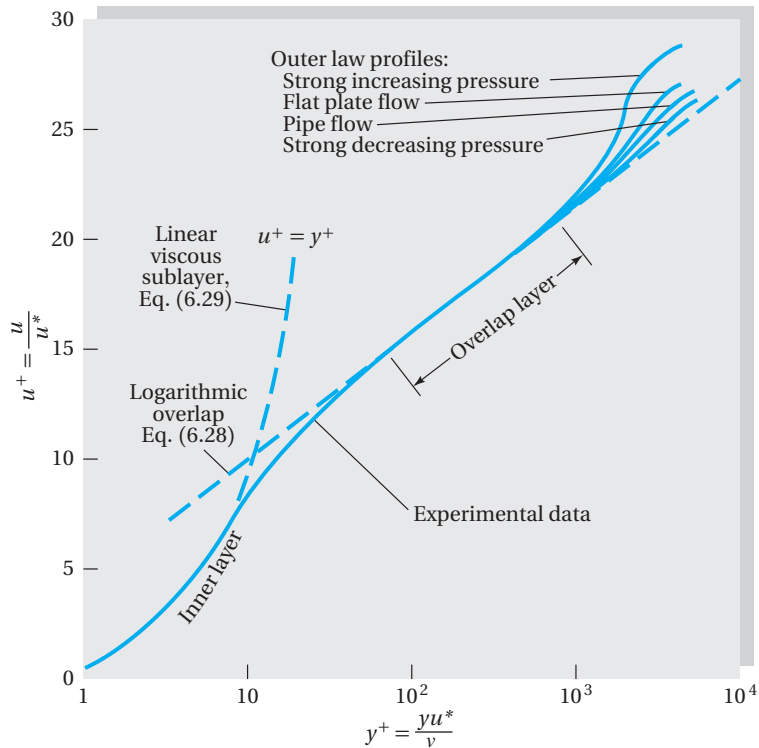

Fig. 6.10 Experimental verification of the inner, outer, and overlap layer laws relating velocity profiles in turbulent wall flow.

The four outer-law profiles shown all merge smoothly with the logarithmic overlap law but have different magnitudes because they vary in external pressure gradient. The wall law is unique and follows the linear viscous relation

$$u^+ = \frac{u}{u^*} = \frac{yu^*}{\nu} = y^+ \tag{6.29}$$

from the wall to about $y^+ = 5$, thereafter curving over to merge with the logarithmic law at about $y^+ = 30$.

Believe it or not, Fig. 6.10, which is nothing more than a shrewd correlation of velocity profiles, is the basis for most existing "theory" of turbulent shear flows. Notice that we have not solved any equations at all but have merely expressed the streamwise velocity in a neat form.

There is serendipity in Fig. 6.10: The logarithmic law (6.28), instead of just being a short overlapping link, actually approximates nearly the entire velocity profile, except for the outer law when the pressure is increasing strongly downstream (as in a diffuser). The inner wall law typically extends over less than 2 percent of the profile and can be neglected. Thus we can use Eq. (6.28) as an excellent approximation to solve nearly every turbulent flow problem presented in this and the next chapter. Many additional applications are given in Refs. 2 and 3.

Advanced Modeling Concepts

Turbulence modeling is a very active field. Scores of papers have been published to more accurately simulate the turbulent stresses in Eq. (6.21) and their y and z components. This research, now available in advanced texts [1, 13, 19], goes well beyond the present book, which is confined to the use of the logarithmic law (6.28) for pipe and boundary layer problems. For example, L. Prandtl, who invented boundary layer theory in 1904, later proposed an *eddy viscosity* model of the Reynolds stress term in Eq. (6.23):

$$-\rho \, \overline{u'v'} = \tau_{\text{turb}} \approx \mu_t \frac{du}{dy} \qquad \text{where} \qquad \mu_t \approx \rho \, l^2 \left| \frac{du}{dy} \right| \tag{6.30}$$

The term μ_t, which is a property of the *flow,* not the fluid, is called the *eddy viscosity* and can be modeled in various ways. The most popular form is Eq. (6.30), where l is called the *mixing length* of the turbulent eddies (analogous to mean free path in molecular theory). Near a solid wall, l is approximately proportional to distance from the wall, and Kármán suggested

$$l \approx \kappa y \quad \text{where} \quad \kappa = \text{Kármán's constant} \approx 0.41 \tag{6.31}$$

As a homework assignment, Prob. P6.40, you may show that Eqs. (6.30) and (6.31) lead to the logarithmic law (6.28) near a wall.

Modern turbulence models approximate three-dimensional turbulent flows and employ additional partial differential equations for such quantities as the turbulence kinetic energy, the turbulent dissipation, and the six Reynolds stresses. For details, see Refs. 1, 13, and 19.

$u(y)$

$u_0 = 5$ m/s

$y = R$

y

r

$r = R = 7$ cm
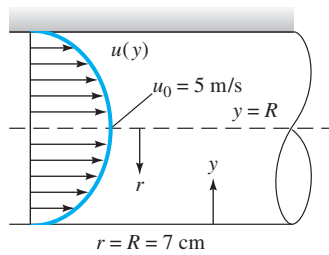
E6.5

EXAMPLE 6.5

Air at 20°C flows through a 14-cm-diameter tube under fully developed conditions. The centerline velocity is $u_0 = 5$ m/s. Estimate from Fig. 6.10 (a) the friction velocity u^* and (b) the wall shear stress τ_w.

Solution

- *System sketch:* Figure E6.5 shows turbulent pipe flow with $u_0 = 5$ m/s and $R = 7$ cm.
- *Assumptions:* Figure 6.10 shows that the logarithmic law, Eq. (6.28), is reasonable all the way to the center of the tube.
- *Approach:* Use Eq. (6.28) to estimate the unknown friction velocity u^*.
- *Property values:* For air at 20°C, $\rho = 1.205$ kg/m^3 and $\nu = 1.51$ E-5 m^2/s.
- *Solution step:* Insert all the given data into Eq. (6.28) at $y = R$ (the centerline). The only unknown is u^*:

$$\frac{u_0}{u^*} = \frac{1}{\kappa} \ln\left(\frac{Ru^*}{\nu}\right) + B \quad \text{or} \quad \frac{5.0 \text{ m/s}}{u^*} = \frac{1}{0.41} \ln\left[\frac{(0.07 \text{ m})u^*}{1.51 \text{ E-5 m}^2/\text{s}}\right] + 5$$

Although the logarithm makes it awkward, one can solve this either by hand or by Excel iteration. There is an automatic iteration procedure in Excel—File, Excel Options, Formulas, Enable iterative calculation—but here we simply show how to iterate by repeat calculations, copied and pasted downward. For a single unknown, in this case u^*, we only need two columns, one for the unknown and one for the equation. The writer hopes that the following copy-and-iterate procedure is clear:

	A	B
	Here place the first guess for u*:	Here place the equation that solves for u*:
1	1.0	=(5.0/(1/0.41*ln(0.07*a**1**/1.51E-5)+5))
2	=B1 (the number, not the equation)	Copy B1 equation and place here
3	Copy A2 here	Copy B2 here
4	Keep copying down…	Keep copying down until convergence

Note that B2 uses the *cell* location for u^*, A1, not the notation u^*. Here are the actual numbers, not instructions or equations, for this problem:

A	B
1.0000	0.1954
0.1954	0.2314
0.2314	0.2271
0.2271	0.2275
0.2275	0.2275

The solution for u^* has converged to 0.2275. To three decimal places,

$$u^* \approx 0.228 \text{ m/s} \qquad \qquad Ans. (a)$$

$$\tau_w = \rho u^{*2} = (1.205)(0.228)^2 \approx 0.062 \text{ Pa} \qquad Ans. (b)$$

- *Comments:* The logarithmic law solved everything! This is a powerful technique, using an experimental velocity correlation to approximate general turbulent flows. You may check that the Reynolds number Re$_d$ is about 40,000, definitely turbulent flow.

6.6 Turbulent Pipe Flow

For turbulent pipe flow we need not solve a differential equation but instead proceed with the logarithmic law, as in Example 6.5. Assume that Eq. (6.28) correlates the local mean velocity $u(r)$ all the way across the pipe

$$\frac{u(r)}{u^*} \approx \frac{1}{\kappa} \ln \frac{(R-r)u^*}{\nu} + B \tag{6.32}$$

where we have replaced y with $R - r$. Compute the average velocity from this profile:

$$
\begin{aligned}
V = \frac{Q}{A} &= \frac{1}{\pi R^2} \int_0^R u^* \left[\frac{1}{\kappa} \ln \frac{(R-r)u^*}{\nu} + B \right] 2\pi r \, dr \\
&= \frac{1}{2} u^* \left(\frac{2}{\kappa} \ln \frac{Ru^*}{\nu} + 2B - \frac{3}{\kappa} \right)
\end{aligned}
\tag{6.33}
$$

Introducing $\kappa = 0.41$ and $B = 5.0$, we obtain, numerically,

$$\frac{V}{u^*} \approx 2.44 \ln \frac{Ru^*}{\nu} + 1.34 \tag{6.34}$$

This looks only marginally interesting until we realize that V/u^* is directly related to the Darcy friction factor:

$$\frac{V}{u^*} = \left(\frac{\rho V^2}{\tau_w} \right)^{1/2} = \left(\frac{8}{f} \right)^{1/2} \tag{6.35}$$

Moreover, the argument of the logarithm in (6.34) is equivalent to

$$\frac{Ru^*}{\nu} = \frac{\frac{1}{2}Vd}{\nu} \frac{u^*}{V} = \frac{1}{2} \text{Re}_d \left(\frac{f}{8} \right)^{1/2} \tag{6.36}$$

Introducing (6.35) and (6.36) into Eq. (6.34), changing to a base-10 logarithm, and rearranging, we obtain

$$\frac{1}{f^{1/2}} \approx 1.99 \log (\text{Re}_d \, f^{1/2}) - 1.02 \tag{6.37}$$

In other words, by simply computing the mean velocity from the logarithmic law correlation, we obtain a relation between the friction factor and Reynolds number for turbulent pipe flow. Prandtl derived Eq. (6.37) in 1935 and then adjusted the constants slightly to fit friction data better:

$$\frac{1}{f^{1/2}} = 2.0 \log (\text{Re}_d \, f^{1/2}) - 0.8 \tag{6.38}$$

This is the accepted formula for a smooth-walled pipe. Some numerical values may be listed as follows:

Re_d	4000	10^4	10^5	10^6	10^7	10^8
f	0.0399	0.0309	0.0180	0.0116	0.0081	0.0059

Thus f drops by only a factor of 5 over a 10,000-fold increase in Reynolds number. Equation (6.38) is cumbersome to solve if Re_d is known and f is wanted. There are

many alternative approximations in the literature from which f can be computed explicitly from Re_d:

$$f = \begin{cases} 0.316\,\text{Re}_d^{-1/4} & 4000 < \text{Re}_d < 10^5 \quad \text{H. Blasius (1911)} \\ \left(1.8 \log \dfrac{\text{Re}_d}{6.9}\right)^{-2} & \qquad\qquad\qquad \text{Ref. 9, Colebrook} \end{cases} \qquad (6.39)$$

However, Eq. (6.38) the preferred formula, is easily solved by computer iteration.

Blasius, a student of Prandtl, presented his formula in the first correlation ever made of pipe friction versus Reynolds number. Although his formula has a limited range, it illustrates what was happening in Fig. 6.4 to Hagen's 1839 pressure-drop data. For a horizontal pipe, from Eq. (6.39),

$$h_f = \frac{\Delta p}{\rho g} = f \frac{L}{d} \frac{V^2}{2g} \approx 0.316 \left(\frac{\mu}{\rho V d}\right)^{1/4} \frac{L}{d} \frac{V^2}{2g}$$

or

$$\Delta p \approx 0.158\, L\rho^{3/4}\mu^{1/4}d^{-5/4}V^{7/4} \qquad (6.40)$$

at low turbulent Reynolds numbers. This explains why Hagen's data for pressure drop begin to increase as the 1.75 power of the velocity, in Fig. 6.4. Note that Δp varies only slightly with viscosity, which is characteristic of turbulent flow. Introducing $Q = \frac{1}{4}\pi d^2 V$ into Eq. (6.40), we obtain the alternative form

$$\Delta p \approx 0.241 L\rho^{3/4}\mu^{1/4}d^{-4.75}Q^{1.75} \qquad (6.41)$$

For a given flow rate Q, the turbulent pressure drop decreases with diameter even more sharply than the laminar formula (6.12). Thus the quickest way to reduce required pumping pressure is to increase the pipe size, although, of course, the larger pipe is more expensive. Doubling the pipe size decreases Δp by a factor of about 27 for a given Q. Compare Eq. (6.40) with Example 5.7 and Fig. 5.10.

The maximum velocity in turbulent pipe flow is given by Eq. (6.32), evaluated at $r = 0$:

$$\frac{u_{\max}}{u^*} \approx \frac{1}{\kappa} \ln \frac{Ru^*}{\nu} + B \qquad (6.42)$$

Combining this with Eq. (6.33), we obtain the formula relating mean velocity to maximum velocity:

$$\frac{V}{u_{\max}} \approx (1 + 1.3\sqrt{f})^{-1} \qquad (6.43)$$

Some numerical values are

Re_d	4000	10^4	10^5	10^6	10^7	10^8
$V/u_{\max}$	0.794	0.814	0.852	0.877	0.895	0.909

The ratio varies with the Reynolds number and is much larger than the value of 0.5 predicted for all laminar pipe flow in Eq. (6.12). Thus a turbulent velocity profile, as shown in Fig. 6.11b, is very flat in the center and drops off sharply to zero at the wall.
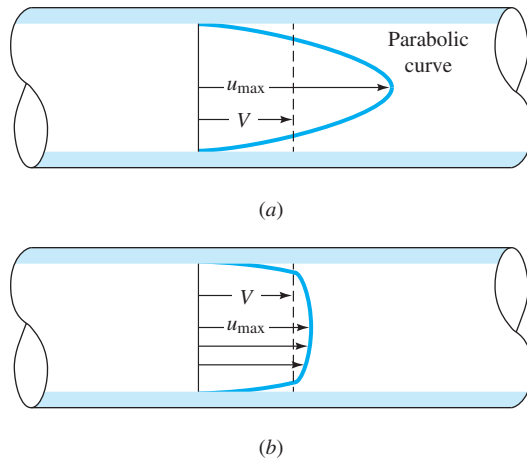
(a)

Fig. 6.11 Comparison of laminar and turbulent pipe flow velocity profiles for the same volume flow: (a) laminar flow; (b) turbulent flow.

(b)

Effect of Rough Walls

It was not known until experiments in 1800 by Coulomb [6] that surface roughness has an effect on friction resistance. It turns out that the effect is negligible for laminar pipe flow, and all the laminar formulas derived in this section are valid for rough walls also. But turbulent flow is strongly affected by roughness. In Fig. 6.10 the linear viscous sublayer extends out only to $y^+ = yu^*/\nu = 5$. Thus, compared with the diameter, the sublayer thickness y_s is only

$$\frac{y_s}{d} = \frac{5\nu/u^*}{d} = \frac{14.1}{\text{Re}_d f^{1/2}} \qquad (6.44)$$

For example, at $\text{Re}_d = 10^5$, $f = 0.0180$, and $y_s/d = 0.001$, a wall roughness of about $0.001d$ will break up the sublayer and profoundly change the wall law in Fig. 6.10.

Measurements of $u(y)$ in turbulent rough-wall flow by Prandtl's student Nikuradse [7] show, as in Fig. 6.12a, that a roughness height ε will force the logarithm law profile outward on the abscissa by an amount approximately equal to $\ln \varepsilon^+$, where $\varepsilon^+ = \varepsilon u^*/\nu$. The slope of the logarithm law remains the same, $1/\kappa$, but the shift outward causes the constant B to be less by an amount $\Delta B \approx (1/\kappa) \ln \varepsilon^+$.

Nikuradse [7] simulated roughness by gluing uniform sand grains onto the inner walls of the pipes. He then measured the pressure drops and flow rates and correlated friction factor versus Reynolds number in Fig. 6.12b. We see that laminar friction is unaffected, but turbulent friction, after an *onset* point, increases monotonically with the roughness ratio ε/d. For any given ε/d, the friction factor becomes constant (*fully rough*) at high Reynolds numbers. These points of change are certain values of $\varepsilon^+ = \varepsilon u^*/\nu$:

$\dfrac{\varepsilon u^*}{\nu} < 5$: *hydraulically smooth* walls, no effect of roughness on friction

$5 \leq \dfrac{\varepsilon u^*}{\nu} \leq 70$: *transitional* roughness, moderate Reynolds number effect

$\dfrac{\varepsilon u^*}{\nu} > 70$: *fully rough* flow, sublayer totally broken up and friction independent of Reynolds number
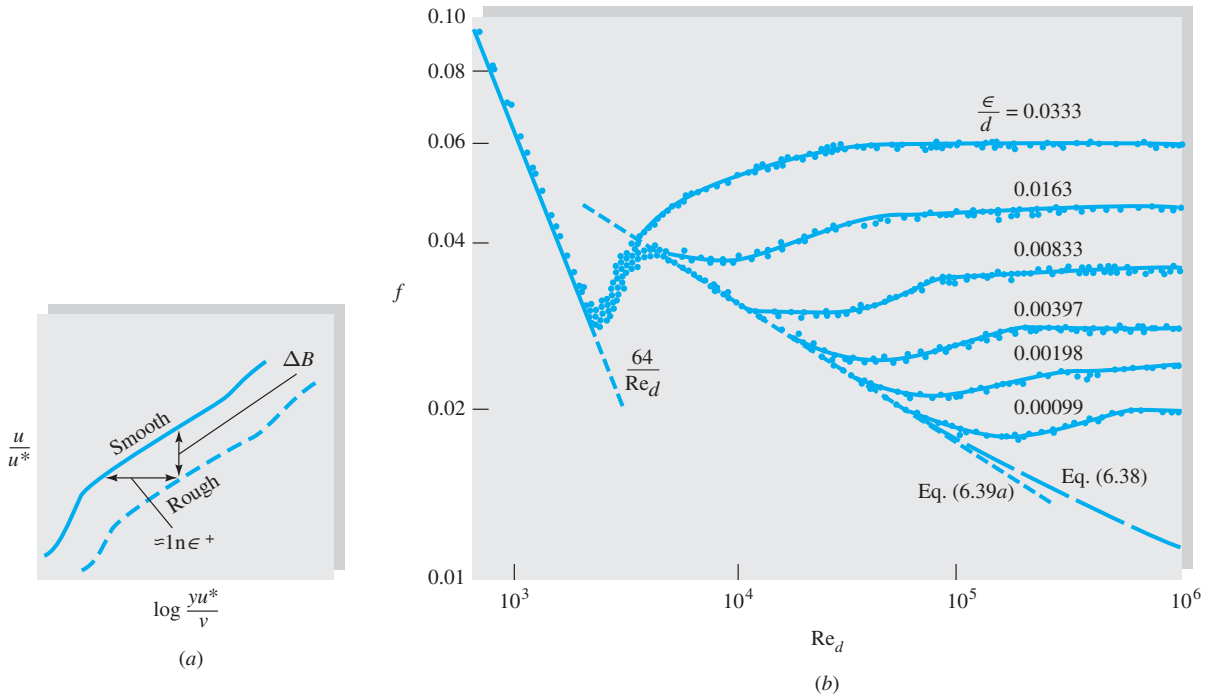
Fig. 6.12 Effect of wall roughness on turbulent pipe flow. (*a*) The logarithmic overlap velocity profile shifts down and to the right; (*b*) experiments with sand-grain roughness by Nikuradse [7] show a systematic increase of the turbulent friction factor with the roughness ratio.

For fully rough flow, $\varepsilon^+ > 70$, the log law downshift ΔB in Fig. 6.12*a* is

$$\Delta B \approx \frac{1}{\kappa} \ln \varepsilon^+ - 3.5 \tag{6.45}$$

and the logarithm law modified for roughness becomes

$$u^+ = \frac{1}{\kappa} \ln y^+ + B - \Delta B = \frac{1}{\kappa} \ln \frac{y}{\varepsilon} + 8.5 \tag{6.46}$$

The viscosity vanishes, and hence fully rough flow is independent of the Reynolds number. If we integrate Eq. (6.46) to obtain the average velocity in the pipe, we obtain

$$\frac{V}{u^*} = 2.44 \ln \frac{d}{\varepsilon} + 3.2$$

or $\qquad \dfrac{1}{f^{1/2}} = -2.0 \log \dfrac{\varepsilon/d}{3.7} \qquad$ fully rough flow $\qquad$ (6.47)

There is no Reynolds number effect; hence the head loss varies exactly as the square of the velocity in this case. Some numerical values of friction factor may be listed:

ε/d	0.00001	0.0001	0.001	0.01	0.05
f	0.00806	0.0120	0.0196	0.0379	0.0716

The friction factor increases by 9 times as the roughness increases by a factor of 5000. In the transitional roughness region, sand grains behave somewhat differently from commercially rough pipes, so Fig. 6.12b has now been replaced by the Moody chart.

The Moody Chart

In 1939 to cover the transitionally rough range, Colebrook [9] combined the smooth wall [Eq. (6.38)] and fully rough [Eq. (6.47)] relations into a clever interpolation formula:

$$\frac{1}{f^{1/2}} = -2.0 \log\left(\frac{\varepsilon/d}{3.7} + \frac{2.51}{\mathrm{Re}_d f^{1/2}}\right) \tag{6.48}$$

This is the accepted design formula for turbulent friction. It was plotted in 1944 by Moody [8] into what is now called the *Moody chart* for pipe friction (Fig. 6.13).
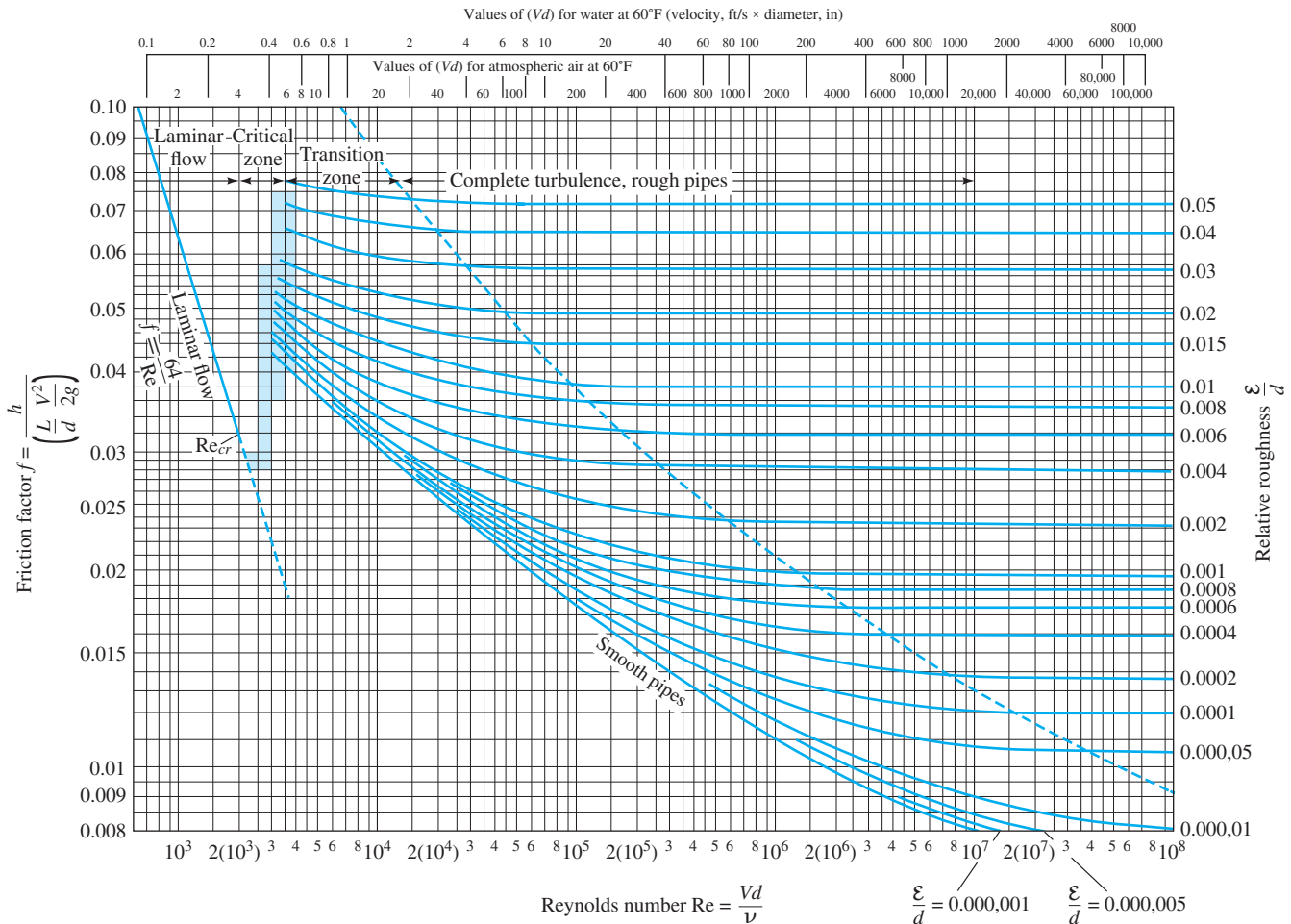
Fig. 6.13 The Moody chart for pipe friction with smooth and rough walls. This chart is identical to Eq. (6.48) for turbulent flow. *(From Ref. 8, Source: ASME.)*

Table 6.1 Recommended
Roughness Values for Commercial
Ducts

Material	Condition	ε ft	ε mm	Uncertainty, %
Steel	Sheet metal, new	0.00016	0.05	±60
	Stainless, new	0.000007	0.002	±50
	Commercial, new	0.00015	0.046	±30
	Riveted	0.01	3.0	±70
	Rusted	0.007	2.0	±50
Iron	Cast, new	0.00085	0.26	±50
	Wrought, new	0.00015	0.046	±20
	Galvanized, new	0.0005	0.15	±40
	Asphalted cast	0.0004	0.12	±50
Brass	Drawn, new	0.000007	0.002	±50
Plastic	Drawn tubing	0.000005	0.0015	±60
Glass	—	Smooth	Smooth	
Concrete	Smoothed	0.00013	0.04	±60
	Rough	0.007	2.0	±50
Rubber	Smoothed	0.000033	0.01	±60
Wood	Stave	0.0016	0.5	±40

The Moody chart is probably the most famous and useful figure in fluid mechanics. It is accurate to ±15 percent for design calculations over the full range shown in Fig. 6.13. It can be used for circular and noncircular (Sec. 6.6) pipe flows and for open-channel flows (Chap. 10). The data can even be adapted as an approximation to boundary layer flows (Chap. 7).

The Moody chart gives a good visual summary of laminar and turbulent pipe friction, including roughness effects. When the writer was in college, everyone solved problems by carefully reading this chart. Currently, though, Eq. (6.48), though implicit in f, is easily solved by iteration or a direct solver. If only a calculator is available, the clever explicit formula given by Haaland [33] as

$$\frac{1}{f^{1/2}} \approx -1.8 \log \left[\frac{6.9}{\text{Re}_d} + \left(\frac{\varepsilon/d}{3.7} \right)^{1.11} \right] \tag{6.49}$$

varies less than 2 percent from Eq. (6.48).

The shaded area in the Moody chart indicates the range where transition from laminar to turbulent flow occurs. There are no reliable friction factors in this range, $2000 < \text{Re}_{d,} < 4000$. Notice that the roughness curves are nearly horizontal in the fully rough regime to the right of the dashed line.

From tests with commercial pipes, recommended values for average pipe roughness are listed in Table 6.1.

EXAMPLE 6.6[2]

Compute the loss of head and pressure drop in 200 ft of horizontal 6-in-diameter asphalted cast iron pipe carrying water with a mean velocity of 6 ft/s.

---

[2]This example was given by Moody in his 1944 paper [8].

Solution

- *System sketch:* See Fig. 6.7 for a horizontal pipe, with $\Delta z = 0$ and h_f proportional to Δp.
- *Assumptions:* Turbulent flow, asphalted horizontal cast iron pipe, $d = 0.5$ ft, $L = 200$ ft.
- *Approach:* Find Re_d and ε/d; enter the Moody chart, Fig. 6.13; find f, then h_f and Δp.
- *Property values:* From Table A.3 for water, converting to BG units, $\rho = 998/515.38 = 1.94$ slug/ft^3, $\mu = 0.001/47.88 = 2.09$ E-5 slug/(ft-s).
- *Solution step 1:* Calculate Re_d and the roughness ratio. As a crutch, Moody provided water and air values of "Vd" at the top of Fig. 6.13 to find Re_d. Instead, let's calculate it ourselves:

$$\text{Re}_d = \frac{\rho V d}{\mu} = \frac{(1.94 \text{ slug/ft}^3)(6 \text{ ft/s})(0.5 \text{ ft})}{2.09 \text{ E-5 slug/(ft} \cdot \text{s)}} \approx 279{,}000 \quad \text{(turbulent)}$$

From Table 6.1, for asphalted cast iron, $\varepsilon = 0.0004$ ft. Then calculate

$$\varepsilon/d = (0.0004 \text{ ft})/(0.5 \text{ ft}) = 0.0008$$

- *Solution step 2:* Find the friction factor from the Moody chart or from Eq. (6.48). If you use the Moody chart, Fig. 6.13, you need practice. Find the line on the right side for $\varepsilon/d = 0.0008$ and follow it back to the left until it hits the vertical line for $\text{Re}_d \approx 2.79$ E5. Read, approximately, $f \approx 0.02$ [or compute $f = 0.0198$ from Eq. (6.48).]
- *Solution step 3:* Calculate h_f from Eq. (6.10) and Δp from Eq. (6.8) for a horizontal pipe:

$$h_f = f\frac{L}{d}\frac{V^2}{2g} = (0.02)\left(\frac{200 \text{ ft}}{0.5 \text{ ft}}\right)\frac{(6 \text{ ft/s})^2}{2(32.2 \text{ ft/s}^2)} \approx 4.5 \text{ ft} \qquad \qquad Ans.$$

$$\Delta p = \rho g h_f = (1.94 \text{ slug/ft}^3)(32.2 \text{ ft/s}^2)(4.5 \text{ ft}) \approx 280 \text{ lbf/ft}^2 \qquad \qquad Ans.$$

- *Comments:* In giving this example, Moody [8] stated that this estimate, even for clean new pipe, can be considered accurate only to about ± 10 percent.

EXAMPLE 6.7

Oil, with $\rho = 900$ kg/m^3 and $\nu = 0.00001$ m^2/s, flows at 0.2 m^3/s through 500 m of 200-mm-diameter cast iron pipe. Determine (*a*) the head loss and (*b*) the pressure drop if the pipe slopes down at $10°$ in the flow direction.

Solution

First compute the velocity from the known flow rate:

$$V = \frac{Q}{\pi R^2} = \frac{0.2 \text{ m}^3/\text{s}}{\pi(0.1 \text{ m})^2} = 6.4 \text{ m/s}$$

Then the Reynolds number is

$$\text{Re}_d = \frac{Vd}{\nu} = \frac{(6.4 \text{ m/s})(0.2 \text{ m})}{0.00001 \text{ m}^2/\text{s}} = 128{,}000$$

From Table 6.1, $\varepsilon = 0.26$ mm for cast iron pipe. Then

$$\frac{\varepsilon}{d} = \frac{0.26 \text{ mm}}{200 \text{ mm}} = 0.0013$$

Enter the Moody chart on the right at $\varepsilon/d = 0.0013$ (you will have to interpolate), and move to the left to intersect with Re $= 128,000$. Read $f \approx 0.0225$ [from Eq. (6.48) for these values we could compute $f = 0.0227$]. Then the head loss is

$$h_f = f\frac{L}{d}\frac{V^2}{2g} = (0.0225)\frac{500 \text{ m}}{0.2 \text{ m}}\frac{(6.4 \text{ m/s})^2}{2(9.81 \text{ m/s}^2)} = 117 \text{ m} \qquad\qquad Ans. \; (a)$$

From Eq. (6.9) for the inclined pipe,

$$h_f = \frac{\Delta p}{\rho g} + z_1 - z_2 = \frac{\Delta p}{\rho g} + L \sin 10°$$

or $\Delta p = \rho g[h_f - (500 \text{ m}) \sin 10°] = \rho g(117 \text{ m} - 87 \text{ m})$

$$= (900 \text{ kg/m}^3)(9.81 \text{ m/s}^2)(30 \text{ m}) = 265,000 \text{ kg/(m} \cdot \text{s}^2) = 265,000 \text{ Pa} \quad Ans. \; (b)$$

EXAMPLE 6.8

Repeat Example 6.4 to see whether there is any possible turbulent flow solution for a smooth-walled pipe.

Solution

In Example 6.4 we estimated a head loss $h_f \approx 1.66$ ft, assuming laminar exit flow ($\alpha \approx 2.0$). For this condition the friction factor is

$$f = h_f\frac{d}{L}\frac{2g}{V^2} = (1.66 \text{ ft})\frac{(0.004 \text{ ft})(2)(32.2 \text{ ft/s}^2)}{(1.0 \text{ ft})(3.32 \text{ ft/s})^2} \approx 0.0388$$

For laminar flow, $\text{Re}_d = 64/f = 64/0.0388 \approx 1650$, as we showed in Example 6.4. However, from the Moody chart (Fig. 6.13), we see that $f = 0.0388$ also corresponds to a *turbulent* smooth-wall condition, at $\text{Re}_d \approx 4500$. If the flow actually were turbulent, we should change our kinetic energy factor to $\alpha \approx 1.06$ [Eq. (3.77)], whence the corrected $h_f \approx 1.82$ ft and $f \approx 0.0425$. With f known, we can estimate the Reynolds number from our formulas:

$$\text{Re}_d \approx 3250 \; [\text{Eq. (6.38)}] \qquad \text{or} \qquad \text{Re}_d \approx 3400 \; [\text{Eq. (6.39}b)]$$

So the flow *might* have been turbulent, in which case the viscosity of the fluid would have been

$$\mu = \frac{\rho V d}{\text{Re}_d} = \frac{1.80(3.32)(0.004)}{3300} = 7.2 \times 10^{-6} \text{ slug/(ft} \cdot \text{s)} \qquad\qquad Ans.$$

This is about 55 percent less than our laminar estimate in Example 6.4. The moral is to keep the capillary-flow Reynolds number below about 1000 to avoid such duplicate solutions.

6.7 Four Types of Pipe Flow Problems

The Moody chart (Fig. 6.13) can be used to solve almost any problem involving friction losses in long pipe flows. However, many such problems involve considerable iteration and repeated calculations using the chart because the standard Moody chart is essentially a *head loss chart*. One is supposed to know all other variables, compute Re_d, enter the chart, find f, and hence compute h_f. This is one of four fundamental problems which are commonly encountered in pipe flow calculations:

1. Given d, L, and V or Q, ρ, μ, and g, compute the head loss h_f (head loss problem).
2. Given d, L, h_f, ρ, μ, and g, compute the velocity V or flow rate Q (flow rate problem).
3. Given Q, L, h_f, ρ, μ, and g, compute the diameter d of the pipe (sizing problem).
4. Given Q, d, h_f, ρ, μ, and g, compute the pipe length L.

Problems 1 and 4 are well suited to the Moody chart. We have to iterate to compute velocity or diameter because both d and V are contained in the ordinate *and* the abscissa of the chart.

There are two alternatives to iteration for problems of type 2 and type 3: (*a*) preparation of a suitable new Moody-type formula (see Probs. P6.68 and P6.73); or (*b*) the use of *solver* software, like Excel. Examples 6.9 and 6.11 include the Excel approach to these problems.

Type 2 Problem: Find the Flow Rate

Even though velocity (or flow rate) appears in both the ordinate and the abscissa on the Moody chart, iteration for turbulent flow is nevertheless quite fast because f varies so slowly with Re_d. In earlier editions, the writer rescaled the Colebrook formula (6.48) into a relation where Q could be calculated directly. That idea is now downsized to Problem P6.68. Example 6.9, which follows, is illustrated both by iteration and by an Excel solution.

EXAMPLE 6.9

Oil, with $\rho = 950$ kg/m^3 and $\nu = 2$ E-5 m^2/s, flows through a 30-cm-diameter pipe 100 m long with a head loss of 8 m. The roughness ratio is $\varepsilon/d = 0.0002$. Find the average velocity and flow rate.

Iterative Solution

By definition, the friction factor is known except for V:

$$f = h_f \frac{d}{L} \frac{2g}{V^2} = (8\text{ m})\left(\frac{0.3\text{ m}}{100\text{ m}}\right)\left[\frac{2(9.81\text{ m/s}^2)}{V^2}\right] \quad \text{or} \quad fV^2 \approx 0.471 \quad \text{(SI units)}$$

To get started, we only need to guess f, compute $V = \sqrt{0.471/f}$, then get Re_d, compute a better f from the Moody chart, and repeat. The process converges fairly rapidly. A good first guess is the "fully rough" value for $\varepsilon/d = 0.0002$, or $f \approx 0.014$ from Fig. 6.13. The iteration would be as follows:

Guess $f \approx 0.014$, then $V = \sqrt{0.471/0.014} = 5.80$ m/s and $Re_d = Vd/\nu \approx 87,000$.
At $Re_d = 87,000$ and $\varepsilon/d = 0.0002$, compute $f_{new} \approx 0.0195$ [Eq. (6.48)].

New $f \approx 0.0195$, $V = \sqrt{0.471/0.0195} = 4.91$ m/s and $\text{Re}_d = Vd/\nu = 73{,}700$. At $\text{Re}_d = 73{,}700$ and $\varepsilon/d = 0.0002$, compute $f_{\text{new}} \approx 0.0201$ [Eq. (6.48)].

Better $f \approx 0.0201$, $V = \sqrt{0.471/0.0201} = 4.84$ m/s and $\text{Re}_d \approx 72{,}600$. At $\text{Re}_d = 72{,}600$ and $\varepsilon/d = 0.0002$, compute $f_{\text{new}} \approx 0.0201$ [Eq. (6.48)].

We have converged to three significant figures. Thus our iterative solution is

$$V = 4.84 \text{ m/s}$$

$$Q = V\left(\frac{\pi}{4}\right)d^2 = (4.84)\left(\frac{\pi}{4}\right)(0.3)^2 \approx 0.342 \text{ m}^3/\text{s} \qquad\qquad Ans.$$

The iterative approach is straightforward and not too onerous, so it is routinely used by engineers. Obviously this repetitive procedure is ideal for a personal computer.

Solution by Iteration with Excel

To iterate by repeated copying in Excel, we need five columns: velocity, flow rate, Reynolds number, an initial guess for f, and a calculation of f from $(\varepsilon/d) = 0.0002$ and the current value of Re_d. We modify our guess for f, in the next row, with the new value of f and calculate again, as shown in the following table. Since f is a slowly varying function, the process converges rapidly.

	V(m/s) = $(0.471/\text{E1})\text{^}0.5$	Q(m^3/s) = $(\pi/4)\text{A1}*0.3\text{^}2$	Re_d = $\text{A1}*0.3/0.00002$	f(Eq. 6.48)	f-guess
	A	B	C	D	E
1	5.8002	0.4100	87004	0.02011	0.01400
2	4.8397	0.3421	72596	0.02011	0.02011
3	**4.8397**	**0.3421**	72596	0.02011	0.02011

As shown in the hand-iterated method, the proper solution is $V = 4.84$ m/s and $Q = 0.342$ m^2/s.

Type 3 Problem:
Find the Pipe Diameter

The Moody chart is especially awkward for finding the pipe size, since d occurs in all three parameters f, Re_d, and ε/d. Further, it depends on whether we know the velocity or the flow rate. We cannot know both, or else we could immediately compute $d = \sqrt{4Q/(\pi V)}$.

Let us assume that we know the flow rate Q. Note that this requires us to redefine the Reynolds number in terms of Q:

$$\text{Re}_d = \frac{Vd}{\nu} = \frac{4Q}{\pi d\nu} \tag{6.50}$$

If, instead, we knew the velocity V, we could use the first form for the Reynolds number. The writer finds it convenient to solve the Darcy friction factor correlation, Eq. (6.10), by solving for f:

$$f = h_f \frac{d}{L}\frac{2g}{V^2} = \frac{\pi^2}{8}\frac{gh_f\, d^5}{LQ^2} \tag{6.51}$$

The following two examples illustrate the iteration.

EXAMPLE 6.10

Work Example 6.9 backward, assuming that $Q = 0.342$ m^3/s and $\varepsilon = 0.06$ mm are known but that d (30 cm) is unknown. Recall $L = 100$ m, $\rho = 950$ kg/m^3, $\nu = 2$ E-5 m^2/s, and $h_f = 8$ m.

Iterative Solution

First write the diameter in terms of the friction factor:

$$f = \frac{\pi^2}{8} \frac{(9.81 \text{ m/s}^2)(8 \text{ m})d^5}{(100 \text{ m})(0.342 \text{ m}^3/\text{s})^2} = 8.28d^5 \qquad \text{or} \qquad d \approx 0.655f^{1/5} \qquad (1)$$

in SI units. Also write the Reynolds number and roughness ratio in terms of the diameter:

$$\text{Re}_d = \frac{4(0.342 \text{ m}^3/\text{s})}{\pi(2 \text{ E-5 m}^2/\text{s})d} = \frac{21{,}800}{d} \qquad (2)$$

$$\frac{\varepsilon}{d} = \frac{6 \text{ E-5 m}}{d} \qquad (3)$$

Guess f, compute d from (1), then compute Re_d from (2) and ε/d from (3), and compute a better f from the Moody chart or Eq. (6.48). Repeat until (fairly rapid) convergence. Having no initial estimate for f, the writer guesses $f \approx 0.03$ (about in the middle of the turbulent portion of the Moody chart). The following calculations result:

$$f \approx 0.03 \qquad d \approx 0.655(0.03)^{1/5} \approx 0.325 \text{ m}$$

$$\text{Re}_d \approx \frac{21{,}800}{0.325} \approx 67{,}000 \qquad \frac{\varepsilon}{d} \approx 1.85 \text{ E-4}$$

Eq. (6.48): $f_{\text{new}} \approx 0.0203$ then $d_{\text{new}} \approx 0.301 \text{ m}$

$$\text{Re}_{d,\text{new}} \approx 72{,}500 \qquad \frac{\varepsilon}{d} \approx 2.0 \text{ E-4}$$

Eq. (6.48): $f_{\text{better}} \approx 0.0201$ and $d = 0.300 \text{ m}$ *Ans.*

The procedure has converged to the correct diameter of 30 cm given in Example 6.9.

Solution by Iteration with Excel

To iterate by repeated copying in Excel, we need five columns: ε/d, friction factor, Reynolds number, diameter d, and an initial guess for f. With the guess for f, we calculate $d \approx 0.655f^{1/5}$, $\text{Re}_d \approx 21{,}800/d$, and $\varepsilon/d = (0.00006 \text{ m})/d$. Replace the guessed f with the new f. Thus Excel is doing the work of our previous hand calculation:

$\varepsilon/d =$ 0.00006/d	$f -$ Eq. (6.48)	Re$_d =$ 21,800/d	d(meters) = 0.655f^0.2	f-guess
A	B	C	D	E
1 0.000185	0.0196	67111	0.325	0.0300
2 0.000201	0.0201	73106	0.298	0.0196
3 0.000200	0.0201	72677	0.300	0.0201
4 0.000200	0.0201	72706	**0.300**	0.0201

As shown in our hand-iterated method, the proper solution is $d = 0.300$ m.

EXAMPLE 6.11

A smooth plastic pipe is to be designed to carry 8 ft^3/s of water at 20°C through 1000 ft of horizontal pipe with an exit at 15 lbf/in^2. The pressure drop is to be approximately 250 lbf/in^2. Determine (*a*) the proper diameter for this pipe and (*b*) whether a Schedule 40 is suitable if the pipe material has an allowable stress of 8000 lbf/in^2.

Solution by Excel Iteration

Assumptions: Steady turbulent flow, smooth walls. For water, take $\rho = 1.94$ slug/ft^3 and $\mu = 2.09$ E-5 slug/(ft · s). With d unknown, use Eq. (6.51):

$$f = \frac{\pi^2}{8}\frac{gh_f d^5}{LQ^2} = \frac{\pi^2}{8}\frac{\Delta p d^5}{\rho LQ^2} = \frac{\pi^2}{8}\frac{(250 \times 144 \text{ lbf/ft}^2)d^5}{(1.94 \text{ slug/ft}^3)(1000 \text{ ft})(8 \text{ ft}^3/\text{s})^2} = 0.358\, d^5 \quad (1)$$

We know neither d nor f, but they are related by the Prandtl formula, Eq. (6.38):

$$\frac{1}{f^{1/2}} \approx 2.0 \log(\text{Re}_d f^{1/2}) - 0.8, \text{ Re}_d = \frac{\rho Vd}{\mu} = \frac{4\rho Q}{\pi \mu d} = \frac{4(1.94)(8)}{\pi(2.09\,E - 5)d} = \frac{945,500}{d} \quad (2)$$

Part (a)   Equations (1) and (2) can be solved simultaneously for f and d. Using Excel iteration, we have four columns: a guessed $f = 0.02$, d from Eq. (1), Re$_d$ from Eq. (2), and a better f from Eq. (6.38). The pipe is smooth, so we don't need roughness:

$f -$ Eq. (6.38)	Re$_d =$ 945500/C2	$d =$ (D2/0.358)^0.2	f-guess
A	B	C	D
1 0.01009	1683574	0.562	0.02000
2 0.01047	1930316	0.490	0.01009
3 0.01044	1916418	0.493	0.01047
4 **0.01045**	**1917156**	**0.493**	0.01044

The process converges rapidly to:

$$\text{Re}_d \approx 1.92\,E6; \quad f \approx 0.01045; \quad d \approx 0.493 \text{ ft}$$

Take the next highest Schedule 40 diameter in Table 6.2: $d \approx 0.5$ ft = **6 in**   *Ans. (a)*

Part (b)   Check to see if Schedule 40 is strong enough. The maximum pressure occurs at the pipe entrance: $p_{max} = p_{exit} + \Delta p = 15 + 250 = 265$ lb/in². The schedule number is thus

$$\text{Schedule number} = (1000)\frac{(\text{maximum pressure})}{(\text{allowable stress})} = (1000)\left(\frac{265 \text{ psi}}{8000 \text{ psi}}\right) \approx 33$$

Schedule 30 is too weak for this pressure, so choose a **Schedule 40 pipe**.   *Ans.* (*b*)

Commercial Pipe Sizes

In solving a problem to find the pipe diameter, we should note that commercial pipes are made only in certain sizes. Table 6.2 gives nominal and actual sizes of pipes in the United States. The term *Schedule 40* is a measure of the pipe thickness and its resistance to stress caused by internal fluid pressure. If P is the internal fluid pressure and S is the allowable stress of the pipe material, then the schedule number = (1000) (*P/S*). Commercial schedules vary from 5 to 160, but 40 and 80 are by far the most popular. Example 6.11 is a typical application.

Type 4 Problem: Find the Pipe Length

In designing piping systems, it is desirable to estimate the appropriate pipe length for a given pipe diameter, pump power, and flow rate. The pump head will match the piping head loss. If minor losses, Sec. 6.9, are neglected, the (horizontal) pipe length follows from Darcy's formula (6.10):

$$h_{\text{pump}} = \frac{\text{Power}}{\rho g Q} = h_f = f\frac{L}{d}\frac{V^2}{2g} \tag{6.52}$$

With Q, d, and ε known, we may compute Re_d and f, after which L is obtained from the formula. Note that pump efficiency varies strongly with flow rate (Chap. 11). Thus, it is important to match pipe length to the pump's region of maximum efficiency.

Table 6.2 Nominal and Actual Sizes of Schedule 40 Pipe

Nominal size, in	Actual ID, in	Wall thickness, in
1/8	0.269	0.068
1/4	0.364	0.088
3/8	0.493	0.091
1/2	0.622	0.109
3/4	0.824	0.113
1	1.049	0.133
1-1/2	1.610	0.145
2	2.067	0.154
2-1/2	2.469	0.203
3	3.068	0.216
4	4.026	0.237
5	5.047	0.258
6	6.065	0.280

EXAMPLE 6.12

A pump delivers 0.6 hp to water at 68°F, flowing in a 6-in-diameter asphalted cast iron horizontal pipe at $V = 6$ ft/s. What is the proper pipe length to match these conditions?

Solution

- *Approach:*   Find h_f from the known power and find f from Re_d and ε/d. Then find L.
- *Water properties:*   For water at 68°F, Table A.3, converting to BG units, $\rho = 1.94$ slug/ft^3 and $\mu = 2.09$ E−5 slug/(ft − s).
- *Pipe roughness:*   From Table 6.1 for asphalted cast iron, $\varepsilon = 0.0004$ ft.
- *Solution step 1:*   Find the pump head from the flow rate and the pump power:

$$Q = AV = \frac{\pi}{4}(0.5 \text{ ft})^2 \left(6 \frac{\text{ft}}{\text{s}} \right) = 1.18 \frac{\text{ft}^3}{\text{s}}$$

$$h_{\text{pump}} = \frac{\text{Power}}{\rho g Q} = \frac{(0.6 \text{ hp})\left[550(\text{ft} \cdot \text{lbf})/(\text{s} \cdot \text{hp}) \right]}{(1.94 \text{ slug/ft}^3)\,(32.2 \text{ ft/s}^2)\,(1.18 \text{ ft}^3/\text{s})} = 4.48 \text{ ft}$$

- *Solution step 2:*   Compute the friction factor from the Colebrook formula, Eq. (6.48):

$$\mathrm{Re}_d = \frac{\rho V d}{\mu} = \frac{(1.94)(6)(0.5)}{2.09 \text{ E}-5} = 278{,}500 \qquad \frac{\varepsilon}{d} = \frac{0.0004 \text{ ft}}{0.5 \text{ ft}} = 0.0008$$

$$\frac{1}{\sqrt{f}} \approx -2.0 \log_{10}\left(\frac{\varepsilon/d}{3.7} + \frac{2.51}{\mathrm{Re}_d \sqrt{f}} \right) \quad \text{yields} \quad f = 0.0198$$

- *Solution step 3:*   Find the pipe length from the Darcy formula (6.10):

$$h_p = h_f = 4.48 \text{ ft} = f\frac{L}{d}\frac{V^2}{2g} = (0.0198)\left(\frac{L}{0.5 \text{ ft}} \right)\frac{(6 \text{ ft/s})^2}{2(32.2 \text{ ft/s}^2)}$$

$$\text{Solve for } L \approx 203 \text{ ft} \qquad\qquad Ans.$$

- *Comment:*   This is Moody's problem (Example 6.6) turned around so that the length is unknown.

6.8 Flow in Noncircular Ducts[3]

If the duct is noncircular, the analysis of fully developed flow follows that of the circular pipe but is more complicated algebraically. For laminar flow, one can solve the exact equations of continuity and momentum. For turbulent flow, the logarithm law velocity profile can be used, or (better and simpler) the hydraulic diameter is an excellent approximation.

The Hydraulic Diameter

For a noncircular duct, the control volume concept of Fig. 6.7 is still valid, but the cross-sectional area A does not equal πR^2 and the cross-sectional perimeter wetted by the shear stress $\mathcal{P}$ does not equal $2\pi R$. The momentum equation (6.9a) thus becomes

$$\Delta p\, A + \rho g A\, \Delta L \sin\phi - \bar{\tau}_w \mathcal{P} \Delta L = 0$$

or
$$h_f = \frac{\Delta p}{\rho g} + \Delta z = \frac{\bar{\tau}_w}{\rho g}\frac{\Delta L}{A/\mathcal{P}} \qquad (6.53)$$

[3]This section may be omitted without loss of continuity.

Comparing this to Eq. (6.9b), we see that $A/\mathcal{P}$ takes the place of one-fourth of the pipe diameter for a circular cross section. We define the friction factor in terms of average shear stress:

$$f_{\text{NCD}} = \frac{8\overline{\tau}_w}{\rho V^2} \tag{6.54}$$

where NCD stands for noncircular duct and $V = Q/A$ as usual, Eq. (6.53) becomes

$$h_f = f\frac{L}{D_h}\frac{V^2}{2g} \tag{6.55}$$

This is equivalent to Eq. (6.10) for pipe flow except that d is replaced by D_h. Therefore, we customarily define the *hydraulic diameter* as

$$\boxed{D_h = \frac{4A}{\mathcal{P}} = \frac{4 \times \text{area}}{\text{wetted perimeter}}} \tag{6.56}$$

We should stress that the wetted perimeter includes all surfaces acted upon by the shear stress. For example, in a circular annulus, both the outer and the inner perimeter should be added.

We would therefore expect by dimensional analysis that this friction factor f, based on hydraulic diameter as in Eq. (6.55), would correlate with the Reynolds number and roughness ratio based on the hydraulic diameter

$$f = F\left(\frac{VD_h}{\nu}, \frac{\varepsilon}{D_h}\right) \tag{6.57}$$

and this is the way the data are correlated. But we should not necessarily expect the Moody chart (Fig. 6.13) to hold exactly in terms of this new length scale. And it does not, but it is surprisingly accurate:

$$f \approx \begin{cases} \dfrac{64}{\text{Re}_{D_h}} & \pm 40\% \quad \text{laminar flow} \\[2ex] f_{\text{Moody}}\left(\text{Re}_{D_h}, \dfrac{\varepsilon}{D_h}\right) & \pm 15\% \quad \text{turbulent flow} \end{cases} \tag{6.58}$$

Now let us look at some particular cases.

Flow between Parallel Plates

Probably the simplest noncircular duct flow is fully developed flow between parallel plates a distance $2h$ apart, as in Fig. 6.14. As noted in the figure, the width $b \gg h$, so the flow is essentially two-dimensional; that is, $u = u(y)$ only. The hydraulic diameter is

$$D_h = \frac{4A}{\mathcal{P}} = \lim_{b \to \infty} \frac{4(2bh)}{2b + 4h} = 4h \tag{6.59}$$

that is, twice the distance between the plates. The pressure gradient is constant, $(-dp/dx) = \Delta p/L$, where L is the length of the channel along the x axis.
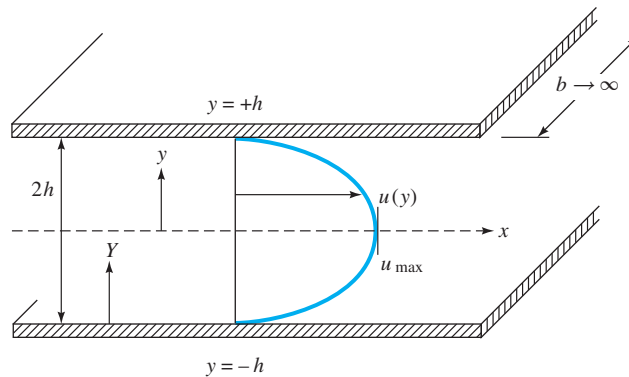
Fig. 6.14 Fully developed flow between parallel plates.

Laminar Flow Solution

The laminar solution was given in Sec. 4.10, in connection with Fig. 4.16b. Let us review those results here:

$$u = u_{max}\left(1 - \frac{y^2}{h^2}\right) \quad \text{where} \quad u_{max} = \frac{h^2}{2\mu}\frac{\Delta p}{L}$$

$$Q = \frac{2bh^3}{3\mu}\frac{\Delta p}{L}$$

$$V = \frac{Q}{A} = \frac{h^2}{3\mu}\frac{\Delta p}{L} = \frac{2}{3}u_{max} \tag{6.60}$$

$$\tau_w = \mu\left|\frac{du}{dy}\right|_{y=h} = h\frac{\Delta p}{L} = \frac{3\mu V}{h}$$

$$h_f = \frac{\Delta p}{\rho g} = \frac{3\mu L V}{\rho g h^2}$$

Now use the head loss to establish the laminar friction factor:

$$f_{lam} = \frac{h_f}{(L/D_h)(V^2/2g)} = \frac{96\mu}{\rho V(4h)} = \frac{96}{Re_{D_h}} \tag{6.61}$$

Thus, if we could not work out the laminar theory and chose to use the approximation $f \approx 64/Re_{D_h}$, we would be 33 percent low. The hydraulic-diameter approximation is relatively crude in laminar flow, as Eq. (6.58) states.

Just as in circular-pipe flow, the laminar solution above becomes unstable at about $Re_{D_h} \approx 2000$; transition occurs and turbulent flow results.

Turbulent Flow Solution

For turbulent flow between parallel plates, we can again use the logarithm law, Eq. (6.28), as an approximation across the entire channel, using not y but a wall coordinate Y, as shown in Fig. 6.14:

$$\frac{u(Y)}{u^*} \approx \frac{1}{\kappa}\ln\frac{Yu^*}{\nu} + B \qquad 0 < Y < h \tag{6.62}$$

This distribution looks very much like the flat turbulent profile for pipe flow in Fig. 6.11b, and the mean velocity is

$$V = \frac{1}{h}\int_0^h u\,dY = u^*\left(\frac{1}{\kappa}\ln\frac{hu^*}{\nu} + B - \frac{1}{\kappa}\right) \tag{6.63}$$

Recalling that $V/u* = (8/f)^{1/2}$, we see that Eq. (6.63) is equivalent to a parallel-plate friction law. Rearranging and cleaning up the constant terms, we obtain

$$\frac{1}{f^{1/2}} \approx 2.0 \log (\text{Re}_{D_h} f^{1/2}) - 1.19 \tag{6.64}$$

where we have introduced the hydraulic diameter $D_h = 4h$. This is remarkably close to the smooth-wall pipe friction law, Eq. (6.38). Therefore we conclude that the use of the hydraulic diameter in this turbulent case is quite successful. That turns out to be true for other noncircular turbulent flows also.

Equation (6.64) can be brought into exact agreement with the pipe law by rewriting it in the form

$$\frac{1}{f^{1/2}} = 2.0 \log (0.64 \, \text{Re}_{D_h} f^{1/2}) - 0.8 \tag{6.65}$$

Thus the turbulent friction is predicted most accurately when we use an effective diameter D_{eff} equal to 0.64 times the hydraulic diameter. The effect on f itself is much less, about 10 percent at most. We can compare with Eq. (6.66) for laminar flow, which predicted

Parallel plates: $$D_{\text{eff}} = \frac{64}{96} D_h = \frac{2}{3} D_h \tag{6.66}$$

This close resemblance ($0.64D_h$ versus $0.667D_h$) occurs so often in noncircular duct flow that we take it to be a general rule for computing turbulent friction in ducts:

$$D_{\text{eff}} = D_h = \frac{4A}{\mathcal{P}} \quad \text{reasonable accuracy}$$

$$D_{\text{eff}} = D_h \frac{64}{(f \text{Re}_{D_h})\text{laminar theory}} \quad \text{better accuracy} \tag{6.67}$$

Jones [10] shows that the effective-laminar-diameter idea collapses all data for rectangular ducts of arbitrary height-to-width ratio onto the Moody chart for pipe flow. We recommend this idea for all noncircular ducts.

EXAMPLE 6.13

Fluid flows at an average velocity of 6 ft/s between horizontal parallel plates a distance of 2.4 in apart. Find the head loss and pressure drop for each 100 ft of length for $\rho = 1.9$ slugs/ft^3 and (a) $\nu = 0.00002$ ft^2/s and (b) $\nu = 0.002$ ft^2/s. Assume smooth walls.

Solution

Part (a)   The viscosity $\mu = \rho\nu = 3.8 \times 10^{-5}$ slug/(ft · s). The spacing is $2h = 2.4$ in $= 0.2$ ft, and $D_h = 4h = 0.4$ ft. The Reynolds number is

$$\text{Re}_{D_h} = \frac{VD_h}{\nu} = \frac{(6.0 \text{ ft/s})(0.4 \text{ ft})}{0.00002 \text{ ft}^2/\text{s}} = 120,000$$

The flow is therefore turbulent. For reasonable accuracy, simply look on the Moody chart (Fig. 6.13) for smooth walls:

$$f \approx 0.0173 \quad h_f \approx f \frac{L}{D_h} \frac{V^2}{2g} = 0.0173 \frac{100}{0.4} \frac{(6.0)^2}{2(32.2)} \approx 2.42 \text{ ft} \qquad \textit{Ans. (a)}$$

Since there is no change in elevation,

$$\Delta p = \rho g h_f = 1.9(32.2)(2.42) = 148 \text{ lbf/ft}^2 \qquad \textit{Ans. (a)}$$

This is the head loss and pressure drop per 100 ft of channel. For more accuracy, take $D_{\text{eff}} = \frac{64}{96} D_h$ from laminar theory; then

$$\text{Re}_{\text{eff}} = \frac{64}{96}(120{,}000) = 80{,}000$$

and from the Moody chart read $f \approx 0.0189$ for smooth walls. Thus a better estimate is

$$h_f = 0.0189 \frac{100}{0.4} \frac{(6.0)^2}{2(32.2)} = 2.64 \text{ ft}$$

and $\qquad\qquad \Delta p = 1.9(32.2)(2.64) = 161 \text{ lbf/ft}^2 \qquad\qquad \textit{Better ans. (a)}$

The more accurate formula predicts friction about 9 percent higher.

Part (a)   Compute $\mu = \rho \nu = 0.0038$ slug/(ft · s). The Reynolds number is $6.0(0.4)/0.002 = 1200$; therefore the flow is laminar, since Re is less than 2300.
   You could use the laminar flow friction factor, Eq. (6.61)

$$f_{\text{lam}} = \frac{96}{\text{Re}_{D_h}} = \frac{96}{1200} = 0.08$$

from which $\qquad\qquad h_f = 0.08 \frac{100}{0.4} \frac{(6.0)^2}{2(32.2)} = 11.2 \text{ ft}$

and $\qquad\qquad \Delta p = 1.9(32.2)(11.2) = 684 \text{ lbf/ft}^2 \qquad\qquad \textit{Ans. (b)}$

Alternately you can finesse the Reynolds number and go directly to the appropriate laminar flow formula, Eq. (6.60):

$$V = \frac{h^2}{3\mu} \frac{\Delta p}{L}$$

or $\qquad \Delta p = \dfrac{3(6.0 \text{ ft/s})[0.0038 \text{ slug/(ft} \cdot \text{s)}](100 \text{ ft})}{(0.1 \text{ ft})^2} = 684 \text{ slugs/(ft} \cdot \text{s}^2) = 684 \text{ lbf/ft}^2$

and $\qquad\qquad h_f = \dfrac{\Delta p}{\rho g} = \dfrac{684}{1.9(32.2)} = 11.2 \text{ ft}$

Flow through a Concentric Annulus

Consider steady axial laminar flow in the annular space between two concentric cylinders, as in Fig. 6.15. There is no slip at the inner $(r = b)$ and outer radius $(r = a)$. For $u = u(r)$ only, the governing relation is Eq. (D.7) in Appendix D:

$$\frac{d}{dr}\left(r\mu \frac{du}{dr}\right) = Kr \qquad K = \frac{d}{dx}(p + \rho g z) \qquad (6.68)$$
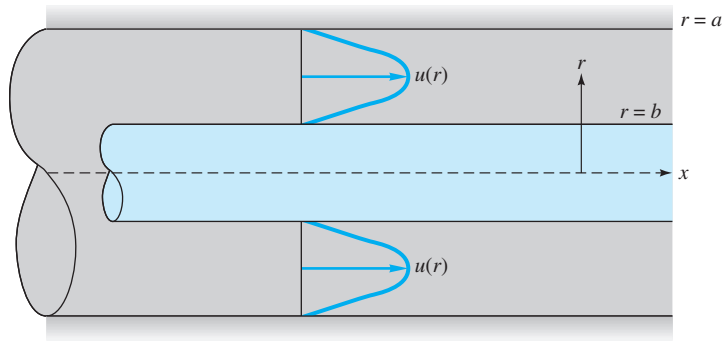
Fig. 6.15 Fully developed flow through a concentric annulus.

Integrate this twice:

$$u = \frac{1}{4} r^2 \frac{K}{\mu} + C_1 \ln r + C_2$$

The constants are found from the two no-slip conditions:

$$u(r = a) = 0 = \frac{1}{4} a^2 \frac{K}{\mu} + C_1 \ln a + C_2$$

$$u(r = b) = 0 = \frac{1}{4} b^2 \frac{K}{\mu} + C_1 \ln b + C_2$$

The final solution for the velocity profile is

$$u = \frac{1}{4\mu}\left[-\frac{d}{dx}(p + \rho g z) \right]\left[a^2 - r^2 + \frac{a^2 - b^2}{\ln (b/a)} \ln \frac{a}{r} \right] \qquad (6.69)$$

The volume flow is given by

$$Q = \int_b^a u\, 2\pi r\, dr = \frac{\pi}{8\mu}\left[-\frac{d}{dx}(p + \rho g z) \right]\left[a^4 - b^4 - \frac{(a^2 - b^2)^2}{\ln (a/b)} \right] \qquad (6.70)$$

The velocity profile $u(r)$ resembles a parabola wrapped around in a circle to form a split doughnut, as in Fig. 6.15.

It is confusing to base the friction factor on the wall shear because there are two shear stresses, the inner stress being greater than the outer. It is better to define f with respect to the head loss, as in Eq. (6.55),

$$f = h_f \frac{D_h}{L} \frac{2g}{V^2} \qquad \text{where } V = \frac{Q}{\pi(a^2 - b^2)} \qquad (6.71)$$

The hydraulic diameter for an annulus is

$$D_h = \frac{4\pi(a^2 - b^2)}{2\pi(a + b)} = 2(a - b) \qquad (6.72)$$

It is twice the clearance, rather like the parallel-plate result of twice the distance between plates [Eq. (6.59)].

Substituting h_f, D_h, and V into Eq. (6.71), we find that the friction factor for laminar flow in a concentric annulus is of the form

$$f = \frac{64\zeta}{\text{Re}_{D_h}} \qquad \zeta = \frac{(a - b)^2(a^2 - b^2)}{a^4 - b^4 - (a^2 - b^2)^2/\ln{(a/b)}} \tag{6.73}$$

The dimensionless term ζ is a sort of correction factor for the hydraulic diameter. We could rewrite Eq. (6.73) as

Table 6.3 Laminar Friction Factors for a Concentric Annulus

Concentric annulus: $\qquad f = \dfrac{64}{\text{Re}_{\text{eff}}} \qquad \text{Re}_{\text{eff}} = \dfrac{1}{\zeta}\text{Re}_{D_h}$ (6.74)

b/a	$f\ \text{Re}_{D_h}$	$D_{\text{eff}}/D_h = 1/\zeta$
0.0	64.0	1.000
0.00001	70.09	0.913
0.0001	71.78	0.892
0.001	74.68	0.857
0.01	80.11	0.799
0.05	86.27	0.742
0.1	89.37	0.716
0.2	92.35	0.693
0.4	94.71	0.676
0.6	95.59	0.670
0.8	95.92	0.667
1.0	96.0	0.667

Some numerical values of $f\ \text{Re}_{D_h}$ and $D_{\text{eff}}/D_h = 1/\zeta$ are given in Table 6.3. Again, laminar annular flow becomes unstable at $\text{Re}_{D_h} \approx 2000$.

For turbulent flow through a concentric annulus, the analysis might proceed by patching together two logarithmic law profiles, one going out from the inner wall to meet the other coming in from the outer wall. We omit such a scheme here and proceed directly to the friction factor. According to the general rule proposed in Eq. (6.58), turbulent friction is predicted with excellent accuracy by replacing d in the Moody chart with $D_{\text{eff}} = 2(a - b)/\zeta$, with values listed in Table 6.3.[4] This idea includes roughness also (replace ε/d in the chart with $\varepsilon/D_{\text{eff}}$). For a quick design number with about 10 percent accuracy, one can simply use the hydraulic diameter $D_h = 2(a - b)$.

EXAMPLE 6.14

What should the reservoir level h be to maintain a flow of 0.01 m³/s through the commercial steel annulus 30 m long shown in Fig. E6.14? Neglect entrance effects and take $\rho = 1000$ kg/m³ and $\nu = 1.02 \times 10^{-6}$ m²/s for water.

E6.14
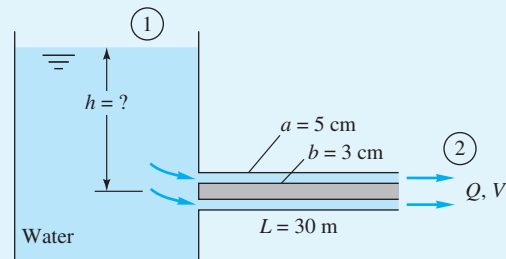
Solution

- *Assumptions:* Fully developed annulus flow, minor losses neglected.
- *Approach:* Determine the Reynolds number, then find f and h_f and thence h.

---

[4]Jones and Leung [44] show that data for annular flow also satisfy the effective-laminar-diameter idea.

- *Property values:* Given $\rho = 1000$ kg/m^3 and $\nu = 1.02$ E-6 m^2/s.
- *Solution step 1:* Calculate the velocity, hydraulic diameter, and Reynolds number:

$$V = \frac{Q}{A} = \frac{0.01 \text{ m}^3/\text{s}}{\pi\left[(0.05 \text{ m})^2 - (0.03 \text{ m})^2\right]} = 1.99 \frac{\text{m}}{\text{s}}$$

$$D_h = 2(a - b) = 2(0.05 \text{ m} - 0.03 \text{ m}) = 0.04 \text{ m}$$

$$\text{Re}_{D_h} = \frac{VD_h}{\nu} = \frac{(1.99 \text{ m/s})(0.04 \text{ m})}{1.02 \text{ E-6 m}^2/\text{s}} = 78{,}000 \quad (\text{turbulent flow})$$

- *Solution step 2:* Apply the steady flow energy equation between sections 1 and 2:

$$\frac{p_1}{\rho g} + \frac{\alpha_1 V_1^2}{2g} + z_1 = \frac{p_2}{\rho g} + \frac{\alpha_2 V_2^2}{2g} + z_2 + h_f$$

or

$$h = \frac{\alpha_2 V_2^2}{2g} + h_f = \frac{V_2^2}{2g}\left(\alpha_2 + f\frac{L}{D_h}\right) \tag{1}$$

Note that $z_1 = h$. For turbulent flow, from Eq. (3.43c), we estimate $\alpha_2 \approx 1.03$

- *Solution step 3:* Determine the roughness ratio and the friction factor. From Table 6.1, for (new) commercial steel pipe, $\varepsilon = 0.046$ mm. Then

$$\frac{\varepsilon}{D_h} = \frac{0.046 \text{ mm}}{40 \text{ mm}} = 0.00115$$

For a reasonable estimate, use Re_{D_h} to estimate the friction factor from Eq. (6.48):

$$\frac{1}{\sqrt{f}} \approx -2.0 \log_{10}\left(\frac{0.00115}{3.7} + \frac{2.51}{78{,}000\sqrt{f}}\right) \quad \text{solve for } f \approx 0.0232$$

For slightly better accuracy, we could use $D_{\text{eff}} = D_h/\zeta$. From Table 6.3, for $b/a = 3/5$, $1/\zeta = 0.67$. Then $D_{\text{eff}} = 0.67(40 \text{ mm}) = 26.8$ mm, whence $\text{Re}_{D_{\text{eff}}} = 52{,}300$, $\varepsilon/D_{\text{eff}} = 0.00172$, and $f_{\text{eff}} \approx 0.0257$. Using the latter estimate, we find the required reservoir level from Eq. (1):

$$h = \frac{V_2^2}{2g}\left(\alpha_2 + f_{\text{eff}}\frac{L}{D_h}\right) = \frac{(1.99 \text{ m/s})^2}{2(9.81 \text{ m/s})^2}\left[1.03 + 0.0257\frac{30 \text{ m}}{0.04 \text{ m}}\right] \approx 4.1 \text{ m} \qquad Ans.$$

- *Comments:* Note that we do *not* replace D_h with D_{eff} in the head loss term fL/D_h, which comes from a momentum balance and *requires* hydraulic diameter. If we used the simpler friction estimate, $f \approx 0.0232$, we would obtain $h \approx 3.72$ m, or about 9 percent lower.

Other Noncircular Cross Sections

In principle, any duct cross section can be solved analytically for the laminar flow velocity distribution, volume flow, and friction factor. This is because any cross section can be mapped onto a circle by the methods of complex variables, and other powerful analytical techniques are also available. Many examples are given by White [3, pp. 112–115], Berker [11], and Olson [12]. Reference 34 is devoted entirely to laminar duct flow.

In general, however, most unusual duct sections have strictly academic and not commercial value. We list here only the rectangular and isosceles-triangular sections, in Table 6.4, leaving other cross sections for you to find in the references.
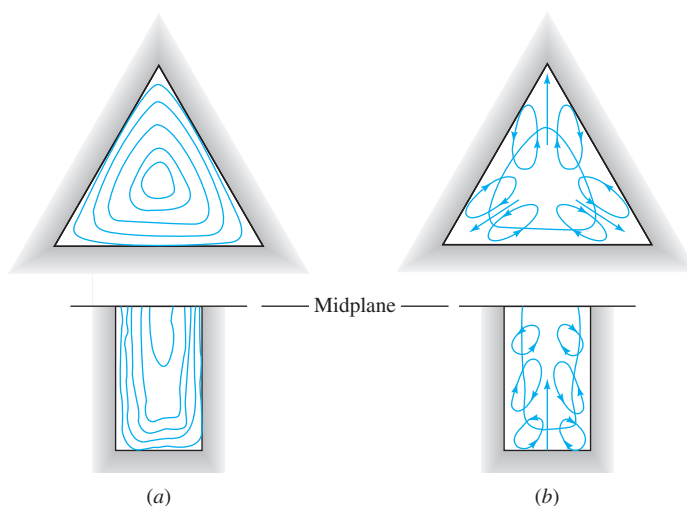
Fig. 6.16 Illustration of secondary turbulent flow in noncircular ducts: (*a*) axial mean velocity contours; (*b*) secondary flow in-plane cellular motions. *(After J. Nikuradse, dissertation, Göttingen, 1926.)*

Table 6.4 Laminar Friction Constants fRe for Rectangular and Triangular Ducts

Rectangular		Isosceles triangle	
b/a	$f\,\mathrm{Re}_{D_h}$	θ, deg	$f\,\mathrm{Re}_{D_h}$
0.0	96.00	0	48.0
0.05	89.91	10	51.6
0.1	84.68	20	52.9
0.125	82.34	30	53.3
0.167	78.81	40	52.9
0.25	72.93	50	52.0
0.4	65.47	60	51.1
0.5	62.19	70	49.5
0.75	57.89	80	48.3
1.0	56.91	90	48.0

For turbulent flow in a duct of unusual cross section, one should replace d with D_h on the Moody chart if no laminar theory is available. If laminar results are known, such as Table 6.4, replace d with $D_{\mathrm{eff}} = [64/(f\mathrm{Re})]D_h$ for the particular geometry of the duct.

For laminar flow in rectangles and triangles, the wall friction varies greatly, being largest near the midpoints of the sides and zero in the corners. In turbulent flow through the same sections, the shear is nearly constant along the sides, dropping off sharply to zero in the corners. This is because of the phenomenon of turbulent *secondary flow,* in which there are nonzero mean velocities v and w in the plane of the cross section. Some measurements of axial velocity and secondary flow patterns are shown in Fig. 6.16, as sketched by Nikuradse in his 1926 dissertation. The secondary flow "cells" drive the mean flow toward the corners, so that the axial velocity contours are similar to the cross section and the wall shear is nearly constant. This is why the hydraulic-diameter concept is so successful for turbulent flow. Laminar flow in a straight noncircular duct has no secondary flow. An accurate theoretical prediction of turbulent secondary flow has yet to be achieved, although numerical models are often successful [36].

EXAMPLE 6.15

Air, with $\rho = 0.00237$ slug/ft^3 and $\nu = 0.000157$ ft^2/s, is forced through a horizontal square 9-by-9-in duct 100 ft long at 25 ft^3/s. Find the pressure drop if $\varepsilon = 0.0003$ ft.

Solution

Compute the mean velocity and hydraulic diameter:

$$V = \frac{25 \text{ ft}^3/\text{s}}{(0.75 \text{ ft})^2} = 44.4 \text{ ft/s}$$

$$D_h = \frac{4A}{\mathcal{P}} = \frac{4(81 \text{ in}^2)}{36 \text{ in}} = 9 \text{ in} = 0.75 \text{ ft}$$

From Table 6.4, for $b/a = 1.0$, the effective diameter is

$$D_{\text{eff}} = \frac{64}{56.91} D_h = 0.843 \text{ ft}$$

whence

$$\text{Re}_{\text{eff}} = \frac{V D_{\text{eff}}}{\nu} = \frac{44.4(0.843)}{0.000157} = 239,000$$

$$\frac{\varepsilon}{D_{\text{eff}}} = \frac{0.0003}{0.843} = 0.000356$$

From the Moody chart, read $f = 0.0177$. Then the pressure drop is

$$\Delta p = \rho g h_f = \rho g \left(f \frac{L}{D_h} \frac{V^2}{2g} \right) = 0.00237(32.2) \left[0.0177 \frac{100}{0.75} \frac{44.4^2}{2(32.2)} \right]$$

or

$$\Delta p = 5.5 \text{ lbf/ft}^2 \qquad\qquad Ans.$$

Pressure drop in air ducts is usually small because of the low density.

6.9 Minor or Local Losses in Pipe Systems

For any pipe system, in addition to the Moody-type friction loss computed for the length of pipe, there are additional so-called *minor losses* or *local losses* due to

1. Pipe entrance or exit.
2. Sudden expansion or contraction.
3. Bends, elbows, tees, and other fittings.
4. Valves, open or partially closed.
5. Gradual expansions or contractions.

The losses may not be so minor; for example, a partially closed valve can cause a greater pressure drop than a long pipe.

Since the flow pattern in fittings and valves is quite complex, the theory is very weak. The losses are commonly measured experimentally and correlated with the pipe flow parameters. The data, especially for valves, are somewhat dependent on the particular manufacturer's design, so that the values listed here must be taken as average design estimates [15, 16, 35, 43, 46].

The measured minor loss is usually given as a ratio of the head loss $h_m = \Delta p/(\rho g)$ through the device to the velocity head $V^2/(2g)$ of the associated piping system:

$$\text{Loss coefficient } K = \frac{h_m}{V^2/(2g)} = \frac{\Delta p}{\frac{1}{2}\rho V^2} \qquad\qquad (6.75)$$

Although K is dimensionless, it often is not correlated in the literature with the Reynolds number and roughness ratio but rather simply with the raw size of the pipe in, say, inches. Almost all data are reported for turbulent flow conditions.

A single pipe system may have many minor losses. Since all are correlated with $V^2/(2g)$, they can be summed into a single total system loss if the pipe has constant diameter:

$$\Delta h_{\text{tot}} = h_f + \sum h_m = \frac{V^2}{2g} \left(\frac{fL}{d} + \sum K \right) \qquad\qquad (6.76)$$
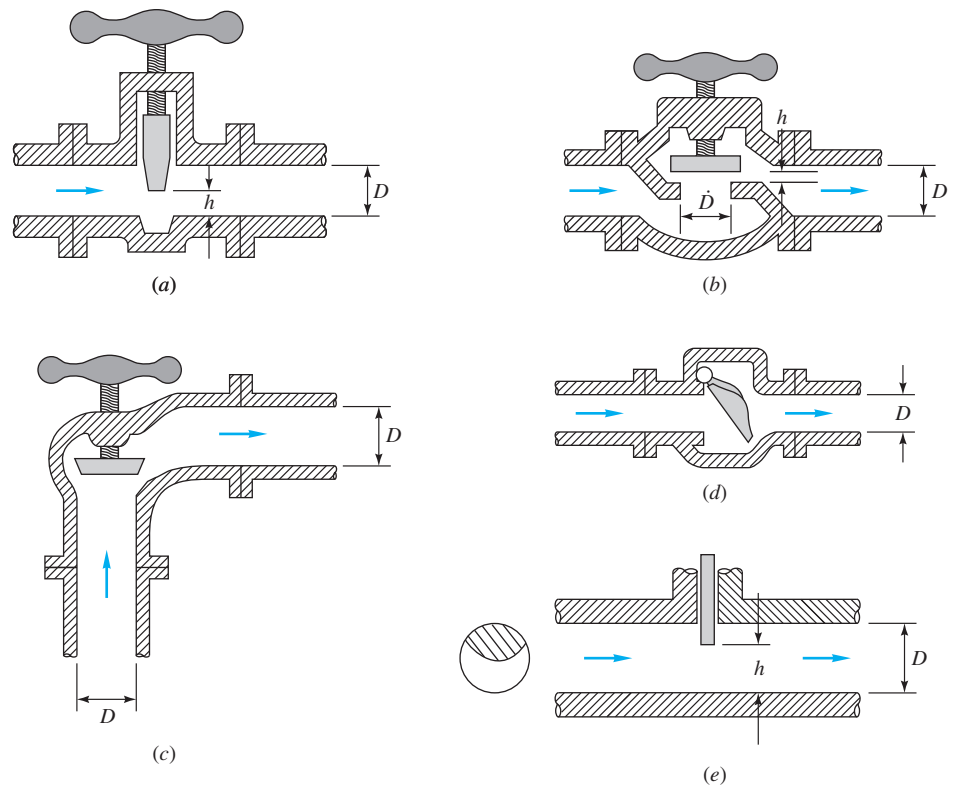
Fig. 6.17 Typical commercial valve geometries: (*a*) gate valve; (*b*) globe valve; (*c*) angle valve; (*d*) swing-check valve; (*e*) disk-type gate valve.

Note, however, that we must sum the losses separately if the pipe size changes so that V^2 changes. The length L in Eq. (6.76) is the total length of the pipe axis.

There are many different valve designs in commercial use. Figure 6.17 shows five typical designs: (*a*) the *gate,* which slides down across the section; (*b*) the *globe,* which closes a hole in a special insert; (*c*) the *angle,* similar to a globe but with a 90° turn; (*d*) the *swing-check* valve, which allows only one-way flow; and (*e*) the *disk,* which closes the section with a circular gate. The globe, with its tortuous flow path, has the highest losses when fully open. Many excellent details about these and other valves are given in the handbooks by Skousen [35] and Crane Co. [52].

Table 6.5 lists loss coefficients K for four types of valve, three angles of elbow fitting, and two tee connections. Fittings may be connected by either internal screws or flanges, hence the two listings. We see that K generally decreases with pipe size, which is consistent with the higher Reynolds number and decreased roughness ratio of large pipes. We stress that Table 6.5 represents losses *averaged among various manufacturers,* so there is an uncertainty as high as ±50 percent.

In addition, most of the data in Table 6.5 are relatively old [15, 16] and therefore based on fittings manufactured in the 1950s. Modern forged and molded fittings may yield somewhat different loss factors, often less than those listed in Table 6.5. An example, shown in Fig. 6.18*a*, gives recent data [48] for fairly short (bend-radius/elbow-diameter = 1.2) flanged 90° elbows. The elbow diameter was 1.69 in. Notice first that K is plotted versus Reynolds number, rather than versus the raw (dimensional) pipe

Table 6.5 Resistance Coefficients $K = h_m/[V^2/(2g)]$ for Open Valves, Elbows, and Tees

	Nominal diameter, in								
	Screwed				Flanged				
	$\frac{1}{2}$	1	2	4	1	2	4	8	20
Valves (fully open):									
Globe	14	8.2	6.9	5.7	13	8.5	6.0	5.8	5.5
Gate	0.30	0.24	0.16	0.11	0.80	0.35	0.16	0.07	0.03
Swing check	5.1	2.9	2.1	2.0	2.0	2.0	2.0	2.0	2.0
Angle	9.0	4.7	2.0	1.0	4.5	2.4	2.0	2.0	2.0
Elbows:									
45° regular	0.39	0.32	0.30	0.29					
45° long radius					0.21	0.20	0.19	0.16	0.14
90° regular	2.0	1.5	0.95	0.64	0.50	0.39	0.30	0.26	0.21
90° long radius	1.0	0.72	0.41	0.23	0.40	0.30	0.19	0.15	0.10
180° regular	2.0	1.5	0.95	0.64	0.41	0.35	0.30	0.25	0.20
180° long radius					0.40	0.30	0.21	0.15	0.10
Tees:									
Line flow	0.90	0.90	0.90	0.90	0.24	0.19	0.14	0.10	0.07
Branch flow	2.4	1.8	1.4	1.1	1.0	0.80	0.64	0.58	0.41

diameters in Table 6.5, and therefore Fig. 6.18a has more generality. Then notice that the K values of 0.23 ± 0.05 are significantly less than the values for 90° elbows in Table 6.5, indicating smoother walls and/or better design. One may conclude that (1) Table 6.5 data are probably conservative and (2) loss factors are highly dependent on actual design and manufacturing factors, with Table 6.5 serving only as a rough guide.

The valve losses in Table 6.5 are for the fully open condition. Losses can be much higher for a partially open valve. Figure 6.18b gives average losses for three valves
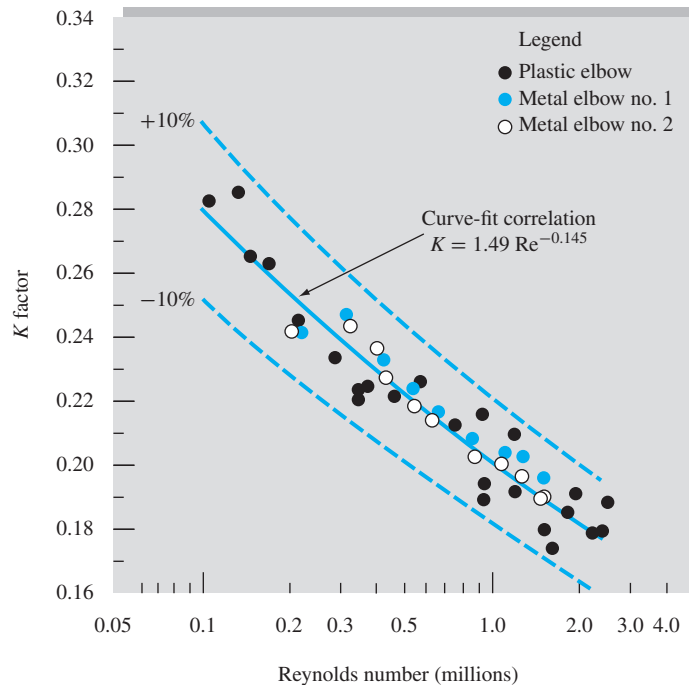
Fig. 6.18a Recent measured loss coefficients for 90° elbows. These values are less than those reported in Table 6.5. *(From Ref. 48, Source of Data R. D. Coffield.)*
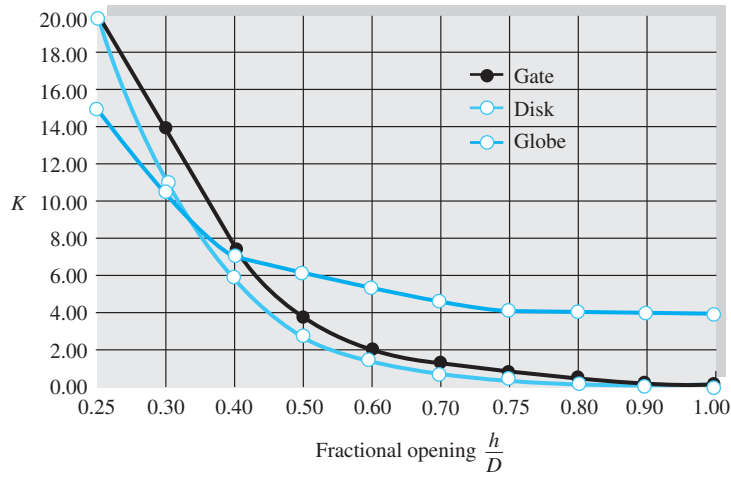
Fig. 6.18b Average loss coefficients for partially open valves (see sketches in Fig. 6.17).
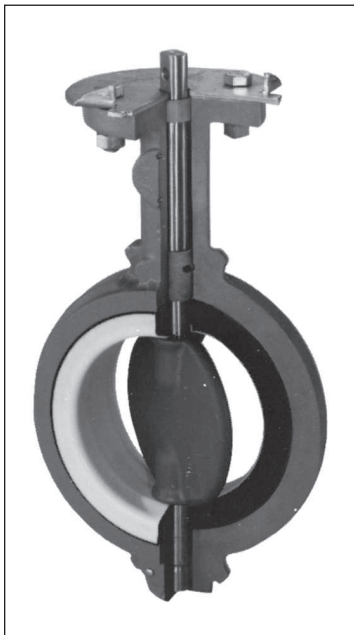
(a)

Fig. 6.19 Performance of butterfly valves: (a) typical geometry (*Courtesy of Tyco Engineered Products and Services*); (b) loss coefficients for three different manufacturers.
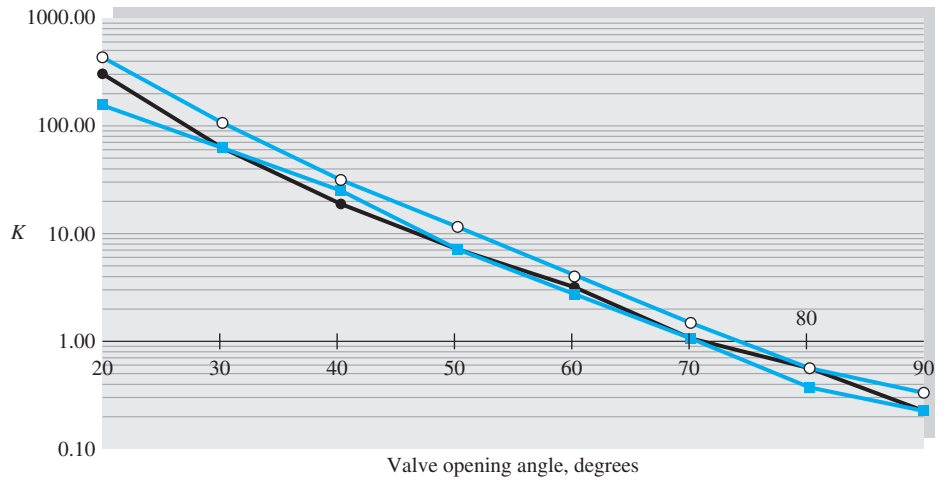
(b)

as a function of "percentage open," as defined by the opening-distance ratio h/D (see Fig. 6.17 for the geometries). Again we should warn of a possible uncertainty of ± 50 percent. Of all minor losses, valves, because of their complex geometry, are most sensitive to manufacturers' design details. For more accuracy, the particular design and manufacturer should be consulted [35].

The *butterfly* valve of Fig. 6.19a is a stem-mounted disk that, when closed, seats against an O-ring or compliant seal near the pipe surface. A single 90° turn opens the valve completely, hence the design is ideal for controllable quick-opening and quick-closing situations such as occur in fire protection and the electric power industry. However, considerable dynamic torque is needed to close these valves, and losses are high when the valves are nearly closed.

Figure 6.19b shows butterfly-valve loss coefficients as a function of the opening angle θ for turbulent flow conditions ($\theta = 0$ is closed). The losses are huge when the
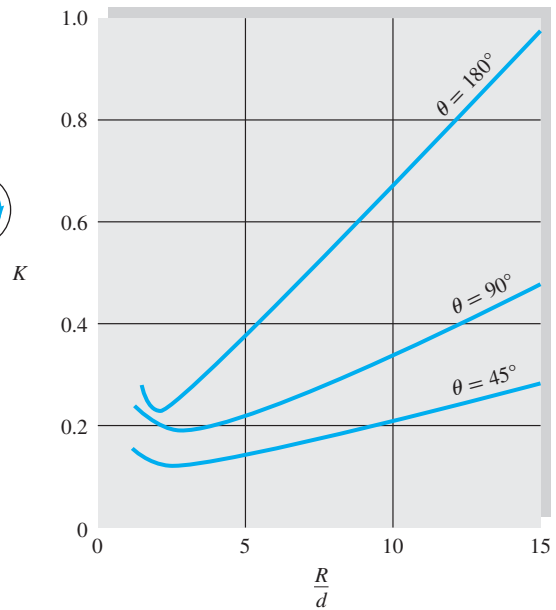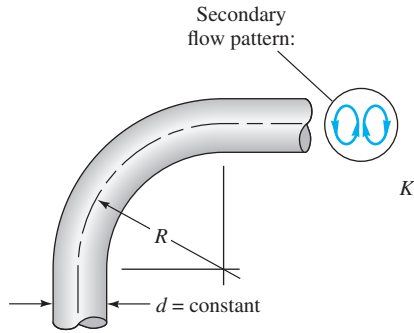
Fig. 6.20 Resistance coefficients for smooth-walled 45°, 90°, and 180° bends, at $\text{Re}_d = 200{,}000$, after Ito [49].
Source: After H. Ito, "Pressure Losses in Smooth Pipe Bends," Journal of Basic Engineering, March 1960, pp. 131–143.

opening is small, and K drops off nearly exponentially with the opening angle. There is a factor of 2 spread among the various manufacturers. Note that K in Fig. 6.19b is, as usual, based on the average *pipe* velocity $V = Q/A$, not on the increased velocity of the flow as it passes through the narrow valve passage.

A bend or curve in a pipe, as in Fig. 6.20, always induces a loss larger than the simple straight-pipe Moody friction loss, due to flow separation on the curved walls and a swirling secondary flow arising from the centripetal acceleration. The smooth-wall loss coefficients K in Fig. 6.20, from the data of Ito [49], are for *total* loss, including Moody friction effects. The separation and secondary flow losses decrease with R/d, while the Moody losses increase because the bend length increases. The curves in Fig. 6.20 thus show a minimum where the two effects cross. Ito [49] gives a curve-fit formula for the 90° bend in turbulent flow:

$$90° \text{ bend: } K \approx 0.388\alpha \left(\frac{R}{d}\right)^{0.84} \text{Re}_D^{-0.17} \text{ where } \alpha = 0.95 + 4.42 \left(\frac{R}{d}\right)^{-1.96} \geq 1 \qquad (6.80a)$$

The formula accounts for Reynolds number, which equals 200,000 in Fig. 6.20. Comprehensive reviews of curved-pipe flow, for both laminar and turbulent flow, are given by Berger et al. [53] and for 90° bends by Spedding et al. [54].

As shown in Fig. 6.21, entrance losses are highly dependent on entrance geometry, but exit losses are not. Sharp edges or protrusions in the entrance cause large zones of flow separation and large losses. A little rounding goes a long way, and a well-rounded entrance ($r = 0.2d$) has a nearly negligible loss $K = 0.05$. At a submerged exit, on the other hand, the flow simply passes out of the pipe into the large downstream reservoir and loses all its velocity head due to viscous dissipation. Therefore $K = 1.0$ for all *submerged exits,* no matter how well rounded.

If the entrance is from a finite reservoir, it is termed a *sudden contraction* (SC) between two sizes of pipe. If the exit is to finite-sized pipe, it is termed a *sudden expansion* (SE). The losses for both are graphed in Fig. 6.22. For the sudden expansion,
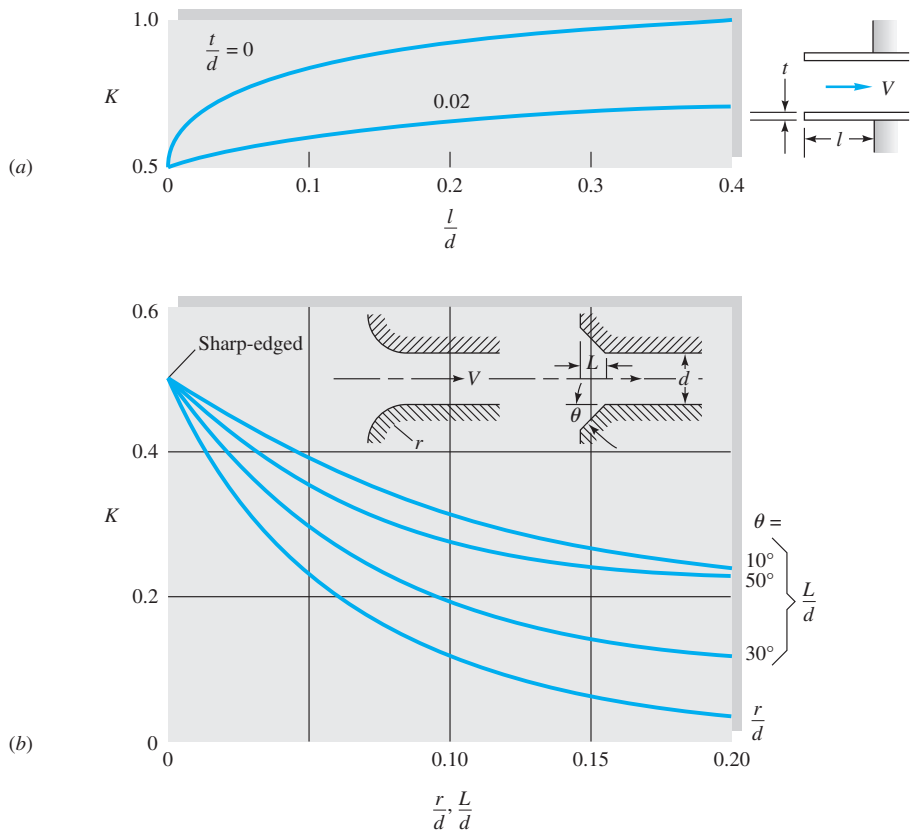
Fig. 6.21 Entrance and exit loss coefficients: (*a*) reentrant inlets; (*b*) rounded and beveled inlets. Exit losses are $K \approx 1.0$ for all shapes of exit (reentrant, sharp, beveled, or rounded).

Source: From ASHRAE Handbook-2012 Fundamentals, ASHRAE, Atlanta, GA, 2012.
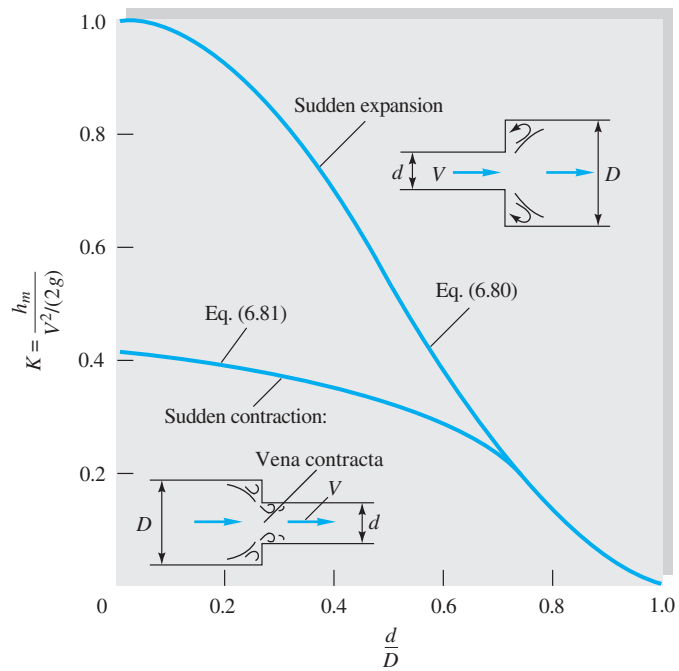
Fig. 6.22 Sudden expansion and contraction losses. Note that the loss is based on velocity head in the small pipe.

the shear stress in the corner separated flow, or deadwater region, is negligible, so that a control volume analysis between the expansion section and the end of the separation zone gives a theoretical loss:

$$K_{SE} = \left(1 - \frac{d^2}{D^2}\right)^2 = \frac{h_m}{V^2/(2g)} \tag{6.77}$$

Note that K is based on the velocity head in the small pipe. Equation (6.77) is in excellent agreement with experiment.

For the sudden contraction, however, flow separation in the downstream pipe causes the main stream to contract through a minimum diameter d_{min}, called the *vena contracta*, as sketched in Fig. 6.22. Because the theory of the vena contracta is not well developed, the loss coefficient in the figure for sudden contraction is experimental. It fits the empirical formula

$$K_{SC} \approx 0.42\left(1 - \frac{d^2}{D^2}\right) \tag{6.78}$$

up to the value $d/D = 0.76$, above which it merges into the sudden-expansion prediction, Eq. (6.77).

Gradual Expansion—The Diffuser   As flow enters a gradual expansion or *diffuser*, such as the conical geometry of Fig. 6.23, the velocity drops and the pressure rises. An efficient diffuser reduces the pumping power required. Head loss can be large, due to flow separation on the walls, if the cone angle is too great. A thinner entrance boundary layer, as in Fig. 6.6, causes
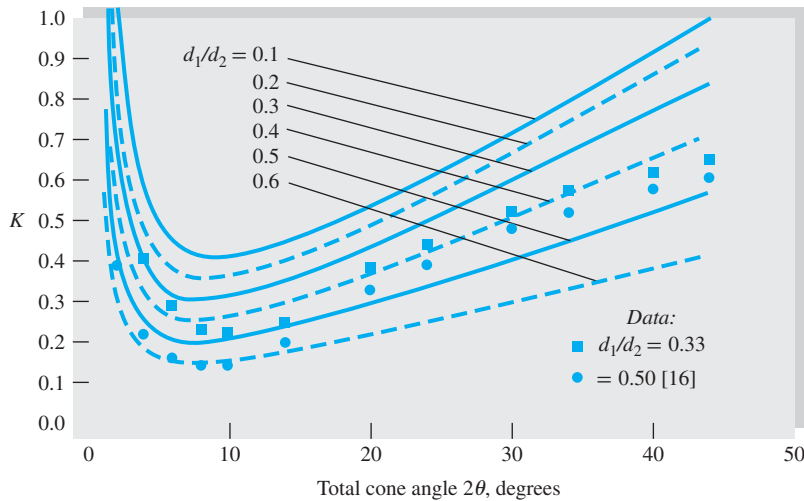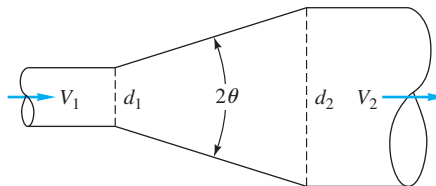
Fig. 6.23 Flow losses in a gradual conical expansion region, as calculated from Gibson's suggestion [15, 50], Eq. (6.79), for a smooth wall.

a slightly smaller loss than a fully developed inlet flow. The flow loss is a combination of nonideal pressure recovery plus wall friction. Some correlating curves are shown in Fig. 6.23. The loss coefficient K is based on the velocity head in the inlet (small) pipe and depends upon cone angle 2θ and the diffuser diameter ratio d_1/d_2. There is scatter in the reported data [15, 16]. The curves in Fig. 6.23 are based on a correlation by A. H. Gibson [50], cited in Ref. 15:

$$K_{\text{diffuser}} = \frac{h_m}{V_1^2/(2\,g)} \approx 2.61 \sin\theta \left(1 - \frac{d^2}{D^2}\right)^2 + f_{\text{avg}}\frac{L}{d_{\text{avg}}} \qquad \text{for} \quad 2\theta \le 45° \quad (6.79)$$

For large angles, $2\theta > 45°$, drop the coefficient $(2.61 \sin\theta)$, which leaves us with a loss equivalent to the sudden expansion of Eq. (6.77). As seen, the formula is in reasonable agreement with the data from Ref. 16. The minimum loss lies in the region $5° < 2\theta < 15°$, which is the best geometry for an efficient diffuser. For angles less than 5°, the diffuser is too long and has too much friction. Angles greater than 15° cause flow separation, resulting in poor pressure recovery. Professor Gordon Holloway provided the writer a recent example, where an improved diffuser design reduced the power requirement of a wind tunnel by 40 percent (100 hp decrease!). We shall look again at diffusers in Sec. 6.11, using the data of Ref. 14.

For a gradual *contraction,* the loss is very small, as seen from the following experimental values [15]:

Contraction cone angle 2θ, deg	30	45	60
K for gradual contraction	0.02	0.04	0.07

References 15, 16, 43, and 46 contain additional data on minor losses.

EXAMPLE 6.16

Water, $\rho = 1.94$ slugs/ft^3 and $\nu = 0.000011$ ft^2/s, is pumped between two reservoirs at 0.2 ft^3/s through 400 ft of 2-in-diameter pipe and several minor losses, as shown in Fig. E6.16. The roughness ratio is $\varepsilon/d = 0.001$. Compute the pump horsepower required.
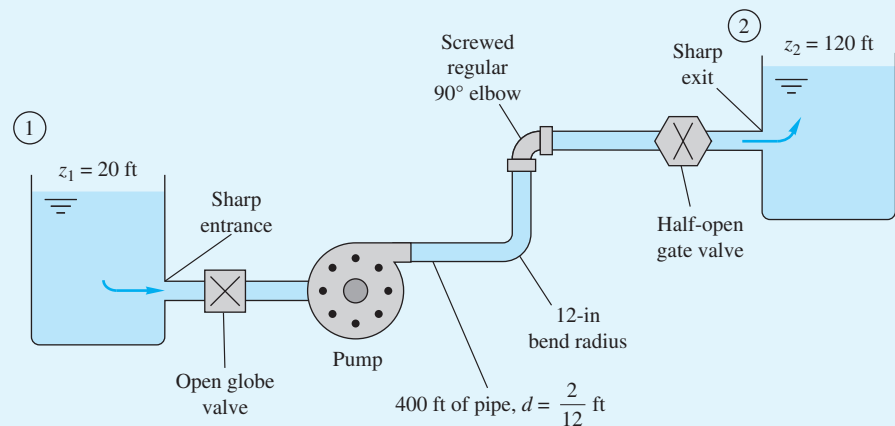
E6.16

Solution

Write the steady flow energy equation between sections 1 and 2, the two reservoir surfaces:

$$\frac{p_1}{\rho g} + \frac{V_1^2}{2g} + z_1 = \left(\frac{p_2}{\rho g} + \frac{V_2^2}{2g} + z_2\right) + h_f + \sum h_m - h_p$$

where h_p is the head increase across the pump. But since $p_1 = p_2$ and $V_1 = V_2 \approx 0$, solve for the pump head:

$$h_p = z_2 - z_1 + h_f + \sum h_m = 120 \text{ ft} - 20 \text{ ft} + \frac{V^2}{2g}\left(\frac{fL}{d} + \sum K\right) \tag{1}$$

Now with the flow rate known, calculate

$$V = \frac{Q}{A} = \frac{0.2 \text{ ft}^3/\text{s}}{\frac{1}{4}\pi(\frac{2}{12} \text{ ft})^2} = 9.17 \text{ ft/s}$$

Now list and sum the minor loss coefficients:

Loss	K
Sharp entrance (Fig. 6.21)	0.5
Open globe valve (2 in, Table 6.5)	6.9
12-in bend (Fig. 6.20)	0.25
Regular 90° elbow (Table 6.5)	0.95
Half-closed gate valve (from Fig. 6.18b)	3.8
Sharp exit (Fig. 6.21)	1.0
	$\Sigma K = 13.4$

Calculate the Reynolds number and pipe friction factor:

$$\text{Re}_d = \frac{Vd}{\nu} = \frac{9.17(\frac{2}{12})}{0.000011} = 139{,}000$$

For $\varepsilon/d = 0.001$, from the Moody chart read $f = 0.0216$. Substitute into Eq. (1):

$$h_p = 100 \text{ ft} + \frac{(9.17 \text{ ft/s})^2}{2(32.2 \text{ ft/s}^2)}\left[\frac{0.0216(400)}{\frac{2}{12}} + 13.4\right]$$

$$= 100 \text{ ft} + 85 \text{ ft} = 185 \text{ ft pump head}$$

The pump must provide a power to the water of

$$P = \rho g Q h_p = \left[1.94(32.2) \text{ lbf/ft}^3\right](0.2 \text{ ft}^3/\text{s})(185 \text{ ft}) \approx 2300 \text{ ft} \cdot \text{lbf/s}$$

The conversion factor is 1 hp $= 550$ ft $\cdot$ lbf/s. Therefore

$$P = \frac{2300}{550} = 4.2 \text{ hp} \qquad\qquad Ans.$$

Allowing for an efficiency of 70 to 80 percent, a pump is needed with an input of about 6 hp.

Laminar Flow Minor Losses

The data in Table 6.5 are for *turbulent* flow in fittings. If the flow is laminar, a different form of loss occurs, which is proportional to V, not V^2. By analogy with Eqs. (6.12) for Poiseuille flow, the laminar minor loss takes the form

$$K_{\text{lam}} = \frac{\Delta p_{\text{loss}} d}{\mu V}$$

Laminar minor losses are just beginning to be studied, due to increased interest in micro- and nano-flows in tubes. They can be substantial, comparable to the Poiseuille loss. Professor Bruce Finlayson, of the University of Washington, kindly provided the writer with new data in the following table:

Laminar Minor Loss Coefficients K_{lam} in Tube Fittings for $1 \leq \text{Re}_d \leq 10$ [60]

Type of fitting	K_{lam}
45° bend, long radius	0.2
90° bend, short radius	0.5
90° bend, long radius	0.36
2:1 pipe contraction	7.3
3:1 pipe contraction	8.6
4:1 pipe contraction	9.0
2:1 pipe expansion	3.1
3:1 pipe expansion	4.1
4:1 pipe expansion	4.5

For the bends in the table, K_{lam} is the excess loss after calculating Poiseuille flow around the centerline of the bend. For the contractions and expansion, K_{lam} is based upon the velocity in the smaller section.

6.10 Multiple-Pipe Systems[5]

If you can solve the equations for one-pipe systems, you can solve them all; but when systems contain two or more pipes, certain basic rules make the calculations very smooth. Any resemblance between these rules and the rules for handling electric circuits is not coincidental.

Figure 6.24 shows three examples of multiple-pipe systems.

Pipes in Series

The first is a set of three (or more) pipes in series. Rule 1 is that the flow rate is the same in all pipes:

$$Q_1 = Q_2 = Q_3 = \text{const} \tag{6.80}$$

or
$$V_1 d_1^2 = V_2 d_2^2 = V_3 d_3^2 \tag{6.81}$$

Rule 2 is that the total head loss through the system equals the sum of the head loss in each pipe:

$$\Delta h_{A \to B} = \Delta h_1 + \Delta h_2 + \Delta h_3 \tag{6.82}$$

In terms of the friction and minor losses in each pipe, we could rewrite this as

$$\Delta h_{A \to B} = \frac{V_1^2}{2g}\left(\frac{f_1 L_1}{d_1} + \sum K_1\right) + \frac{V_2^2}{2g}\left(\frac{f_2 L_2}{d_2} + \sum K_2\right)$$
$$+ \frac{V_3^2}{2g}\left(\frac{f_3 L_3}{d_3} + \sum K_3\right) \tag{6.83}$$

and so on for any number of pipes in the series. Since V_2 and V_3 are proportional to V_1 from Eq. (6.81), Eq. (6.83) is of the form

$$\Delta h_{A \to B} = \frac{V_1^2}{2g}(\alpha_0 + \alpha_1 f_1 + \alpha_2 f_2 + \alpha_3 f_3) \tag{6.84}$$

[5]This section may be omitted without loss of continuity.
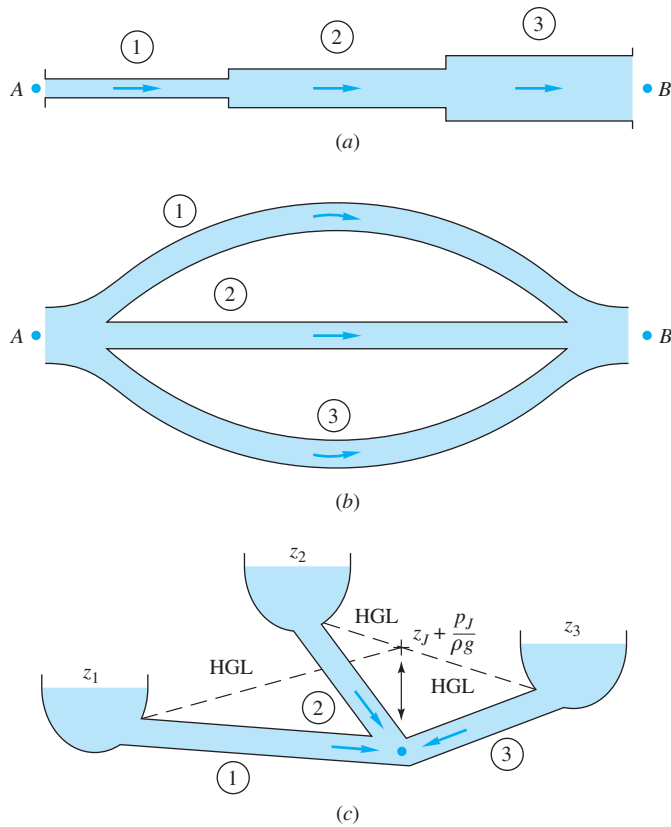
Fig. 6.24 Examples of multiple-pipe systems: (*a*) pipes in series; (*b*) pipes in parallel; (*c*) the three-reservoir junction problem.

where the α_i are dimensionless constants. If the flow rate is given, we can evaluate the right-hand side and hence the total head loss. If the head loss is given, a little iteration is needed, since f_1, f_2, and f_3 all depend on V_1 through the Reynolds number. Begin by calculating f_1, f_2, and f_3, assuming fully rough flow, and the solution for V_1 will converge with one or two iterations.

EXAMPLE 6.17

Given is a three-pipe series system, as in Fig. 6.24a. The total pressure drop is $p_A - p_B = 150{,}000$ Pa, and the elevation drop is $z_A - z_B = 5$ m. The pipe data are

Pipe	L, m	d, cm	ε, mm	ε/d
1	100	8	0.24	0.003
2	150	6	0.12	0.002
3	80	4	0.20	0.005

The fluid is water, $\rho = 1000$ kg/m³ and $\nu = 1.02 \times 10^{-6}$ m²/s. Calculate the flow rate Q in m³/h through the system.

Solution

The total head loss across the system is

$$\Delta h_{A \to B} = \frac{p_A - p_B}{\rho g} + z_A - z_B = \frac{150,000}{1000(9.81)} + 5 \text{ m} = 20.3 \text{ m}$$

From the continuity relation (6.84) the velocities are

$$V_2 = \frac{d_1^2}{d_2^2} V_1 = \frac{16}{9} V_1 \qquad V_3 = \frac{d_1^2}{d_3^2} V_1 = 4V_1$$

and $\qquad\qquad \text{Re}_2 = \frac{V_2 d_2}{V_1 d_1} \text{Re}_1 = \frac{4}{3} \text{Re}_1 \qquad \text{Re}_3 = 2\text{Re}_1$

Neglecting minor losses and substituting into Eq. (6.83), we obtain

$$\Delta h_{A \to B} = \frac{V_1^2}{2g} \left[1250 f_1 + 2500 \left(\frac{16}{9} \right)^2 f_2 + 2000(4)^2 f_3 \right]$$

or $\qquad\qquad 20.3 \text{ m} = \frac{V_1^2}{2g} (1250 f_1 + 7900 f_2 + 32,000 f_3) \qquad\qquad (1)$

This is the form that was hinted at in Eq. (6.84). It seems to be dominated by the third pipe loss $32,000 f_3$. Begin by estimating f_1, f_2, and f_3 from the Moody-chart fully rough regime:

$$f_1 = 0.0262 \qquad f_2 = 0.0234 \qquad f_3 = 0.0304$$

Substitute in Eq. (1) to find $V_1^2 \approx 2g(20.3)/(33 + 185 + 973)$. The first estimate thus is $V_1 = 0.58$ m/s, from which

$$\text{Re}_1 \approx 45,400 \qquad \text{Re}_2 = 60,500 \qquad \text{Re}_3 = 90,800$$

Hence, from the Moody chart,

$$f_1 = 0.0288 \qquad f_2 = 0.0260 \qquad f_3 = 0.0314$$

Substitution into Eq. (1) gives the better estimate

$$V_1 = 0.565 \text{ m/s} \qquad Q = \tfrac{1}{4} \pi d_1^2 V_1 = 2.84 \times 10^{-3} \text{ m}^3/\text{s}$$

or $\qquad\qquad\qquad\qquad Q = 10.2 \text{ m}^3/\text{h} \qquad\qquad\qquad\qquad\qquad Ans.$

A second iteration gives $Q = 10.22$ m³/h, a negligible change.

Pipes in Parallel

The second multiple-pipe system is the *parallel* flow case shown in Fig. 6.24b. Here the pressure drop is the same in each pipe, and the total flow is the sum of the individual flows:

$$\Delta h_{A \to B} = \Delta h_1 = \Delta h_2 = \Delta h_3 \qquad\qquad (6.85a)$$
$$Q = Q_1 + Q_2 + Q_3 \qquad\qquad (6.85b)$$

If the total head loss is known, it is straightforward to solve for Q_i in each pipe and sum them, as will be seen in Example 6.18. The reverse problem, of determining ΣQ_i when h_f is known, requires iteration. Each pipe is related to h_f by the Moody relation $h_f = f(L/d)(V^2/2g) = fQ^2/C$, where $C = \pi^2 g d^5/8L$. Thus each pipe has nearly quadratic nonlinear parallel resistance, and head loss is related to total flow rate by

$$h_f = \frac{Q^2}{(\Sigma \sqrt{C_i/f_i})^2} \qquad \text{where } C_i = \frac{\pi^2 g d_i^5}{8 L_i} \qquad\qquad (6.86)$$

Since the f_i vary with Reynolds number and roughness ratio, one begins Eq. (6.86) by guessing values of f_i (fully rough values are recommended) and calculating a first estimate of h_f. Then each pipe yields a flow-rate estimate $Q_i \approx (C_i h_f/f_i)^{1/2}$ and hence a new Reynolds number and a better estimate of f_i. Then repeat Eq. (6.86) to convergence.

It should be noted that both of these parallel-pipe cases—finding either ΣQ or h_f—are easily solved by Excel if reasonable guesses are given.

EXAMPLE 6.18

Assume that the same three pipes in Example 6.17 are now in parallel with the same total head loss of 20.3 m. Compute the total flow rate Q, neglecting minor losses.

Solution

From Eq. (6.85a) we can solve for each V separately:

$$20.3 \text{ m} = \frac{V_1^2}{2g} 1250 f_1 = \frac{V_2^2}{2g} 2500 f_2 = \frac{V_3^2}{2g} 2000 f_3 \tag{1}$$

Guess fully rough flow in pipe 1: $f_1 = 0.0262$, $V_1 = 3.49$ m/s; hence $\text{Re}_1 = V_1 d_1/\nu = 273{,}000$. From the Moody chart read $f_1 = 0.0267$; recompute $V_1 = 3.46$ m/s, $Q_1 = 62.5$ m³/h.

Next guess for pipe 2: $f_2 \approx 0.0234$, $V_2 \approx 2.61$ m/s; then $\text{Re}_2 = 153{,}000$, and hence $f_2 = 0.0246$, $V_2 = 2.55$ m/s, $Q_2 = 25.9$ m³/h.

Finally guess for pipe 3: $f_3 \approx 0.0304$, $V_3 \approx 2.56$ m/s; then $\text{Re}_3 = 100{,}000$, and hence $f_3 = 0.0313$, $V_3 = 2.52$ m/s, $Q_3 = 11.4$ m³/h.

This is satisfactory convergence. The total flow rate is

$$Q = Q_1 + Q_2 + Q_3 = 62.5 + 25.9 + 11.4 = 99.8 \text{ m}^3/\text{h} \qquad Ans.$$

These three pipes carry 10 times more flow in parallel than they do in series.

This example may be solved by Excel iteration using the Colebrook-formula procedure outlined in Ex. 6.9. Each pipe is a separate iteration of friction factor, Reynolds number, and flow rate. The pipes are rough, so only one iteration is needed. Here are the Excel results:

	A	B	C	D	E	F
			Ex. 6.18 – Pipe 1			
	Re_1	$(\varepsilon/d)_1$	V_1 – m/s	Q_1 – m³/h	f_1	f_1-guess
1	313053	0.003	3.991	72.2	0.0267	0.0200
2	271100	0.003	3.457	**62.5**	0.0267	0.0267
			Ex. 6.18 – Pipe 2			
	Re_2	$(\varepsilon/d)_2$	V_2 – m/s	Q_2 – m³/h	f_2	f_2-guess
1	166021	0.002	2.822	28.7	0.0246	0.0200
2	149739	0.002	2.546	**25.9**	0.0246	0.0246
			Ex. 6.18 – Pipe 3			
	Re_3	$(\varepsilon/d)_3$	V_3 – m/s	Q_3 – m³/h	f_3	f_3-guess
1	123745	0.005	3.155	14.3	0.0313	0.0200
2	98891	0.005	2.522	**11.4**	0.0313	0.0313

Thus, as in the hand calculations, the total flow rate $= 62.5 + 25.9 + 11.4 = $ **99.8** m³/h. *Ans.*

Three-Reservoir Junction

Consider the third example of a *three-reservoir pipe junction,* as in Fig. 6.24c. If all flows are considered positive toward the junction, then

$$Q_1 + Q_2 + Q_3 = 0 \tag{6.87}$$

which obviously implies that one or two of the flows must be away from the junction. The pressure must change through each pipe so as to give the same static pressure p_J at the junction. In other words, let the HGL at the junction have the elevation

$$h_J = z_J + \frac{p_J}{\rho g}$$

where p_J is in gage pressure for simplicity. Then the head loss through each, assuming $p_1 = p_2 = p_3 = 0$ (gage) at each reservoir surface, must be such that

$$\Delta h_1 = \frac{V_1^2}{2g} \frac{f_1 L_1}{d_1} = z_1 - h_J$$

$$\Delta h_2 = \frac{V_2^2}{2g} \frac{f_2 L_2}{d_2} = z_2 - h_J \tag{6.88}$$

$$\Delta h_3 = \frac{V_3^2}{2g} \frac{f_3 L_3}{d_3} = z_3 - h_J$$

We guess the position h_J and solve Eqs. (6.88) for V_1, V_2, and V_3 and hence Q_1, Q_2, and Q_3, iterating until the flow rates balance at the junction according to Eq. (6.87). If we guess h_J too *high*, the sum $Q_1 + Q_2 + Q_3$ will be *negative* and the remedy is to reduce h_J, and vice versa.

EXAMPLE 6.19

Take the same three pipes as in Example 6.17, and assume that they connect three reservoirs at these surface elevations

$$z_1 = 20 \text{ m} \quad z_2 = 100 \text{ m} \quad z_3 = 40 \text{ m}$$

Find the resulting flow rates in each pipe, neglecting minor losses.

Solution

As a first guess, take h_J equal to the middle reservoir height, $z_3 = h_J = 40$ m. This saves one calculation ($Q_3 = 0$) and enables us to get the lay of the land:

Reservoir	h_J, m	$z_i - h_J$, m	f_i	V_i, m/s	Q_i, m³/h	L_i/d_i
1	40	−20	0.0267	−3.43	−62.1	1250
2	40	60	0.0241	4.42	45.0	2500
3	40	0		0	0	2000
					$\Sigma Q = -17.1$	

Since the sum of the flow rates toward the junction is negative, we guessed h_J too high. Reduce h_J to 30 m and repeat:

Reservoir	h_J, m	$z_i - h_J$, m	f_i	V_i, m/s	Q_i, m³/h
1	30	-10	0.0269	-2.42	-43.7
2	30	70	0.0241	4.78	48.6
3	30	10	0.0317	1.76	8.0
					$\Sigma Q = 12.9$

This is positive ΣQ, and so we can linearly interpolate to get an accurate guess: $h_J \approx 34.3$ m. Make one final list:

Reservoir	h_J, m	$z_i - h_J$, m	f_i	V_i, m/s	Q_i, m³/h
1	34.3	-14.3	0.0268	-2.90	-52.4
2	34.3	65.7	0.0241	4.63	47.1
3	34.3	5.7	0.0321	1.32	6.0
					$\Sigma Q = 0.7$

This is close enough; hence we calculate that the flow rate is 52.4 m³/h toward reservoir 3, balanced by 47.1 m³/h away from reservoir 1 and 6.0 m³/h away from reservoir 3.

One further iteration with this problem would give $h_J = 34.53$ m, resulting in $Q_1 = -52.8$, $Q_2 = 47.0$, and $Q_3 = 5.8$ m³/h, so that $\Sigma Q = 0$ to three-place accuracy. Pedagogically speaking, we would then be exhausted.

Pipe Networks

The ultimate case of a multipipe system is the *piping network* illustrated in Fig. 6.25. This might represent a water supply system for an apartment or subdivision
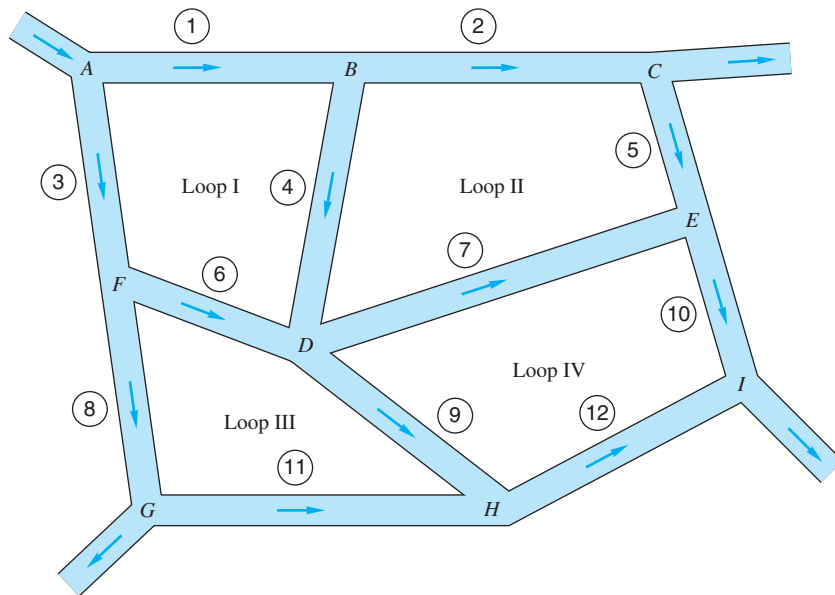
Fig. 6.25 Schematic of a piping network.

or even a city. This network is quite complex algebraically but follows the same basic rules:

1. The net flow into any junction must be zero.
2. The net pressure change around any closed loop must be zero. In other words, the HGL at each junction must have one and only one elevation.
3. All pressure changes must satisfy the Moody and minor-loss friction correlations.

By supplying these rules to each junction and independent loop in the network, one obtains a set of simultaneous equations for the flow rates in each pipe leg and the HGL (or pressure) at each junction. Solution may then be obtained by numerical iteration, as first developed in a hand calculation technique by Prof. Hardy Cross in 1936 [17]. Computer solution of pipe network problems is now quite common and is covered in at least one specialized text [18]. Network analysis is quite useful for real water distribution systems if well calibrated with the actual system head loss data.

6.11 Experimental Duct Flows: Diffuser Performance[6]

The Moody chart is such a great correlation for tubes of any cross section with any roughness or flow rate that we may be deluded into thinking that the world of internal flow prediction is at our feet. Not so. The theory is reliable only for ducts of constant cross section. As soon as the section varies, we must rely principally on experiment to determine the flow properties. As mentioned many times before, experimentation is a vital part of fluid mechanics.

Literally thousands of papers in the literature report experimental data for specific internal and external viscous flows. We have already seen several examples:

1. Vortex shedding from a cylinder (Fig. 5.2).
2. Drag of a sphere and a cylinder (Fig. 5.3).
3. Hydraulic model of a dam spillway (Fig. 5.9).
4. Rough-wall pipe flows (Fig. 6.12).
5. Secondary flow in ducts (Fig. 6.16).
6. Minor duct loss coefficients (Sec. 6.9).

Chapter 7 will treat a great many more external flow experiments, especially in Sec. 7.6. Here we shall show data for one type of internal flow, the diffuser.

Diffuser Performance

A diffuser, shown in Fig. 6.26*a* and *b*, is an expansion or area increase intended to reduce velocity in order to recover the pressure head of the flow. Rouse and Ince [6] relate that it may have been invented by customers of the early Roman (about 100 A.D.) water supply system, where water flowed continuously and was billed according to pipe size. The ingenious customers discovered that they could increase the flow rate at no extra cost by flaring the outlet section of the pipe.

Engineers have always designed diffusers to increase pressure and reduce kinetic energy of ducted flows, but until about 1950, diffuser design was a combination of art, luck, and vast amounts of empiricism. Small changes in design parameters caused large changes in performance. The Bernoulli equation seemed highly suspect as a useful tool.

[6]This section may be omitted without loss of continuity.

(a)

(b)

Throat

Exit

(c)
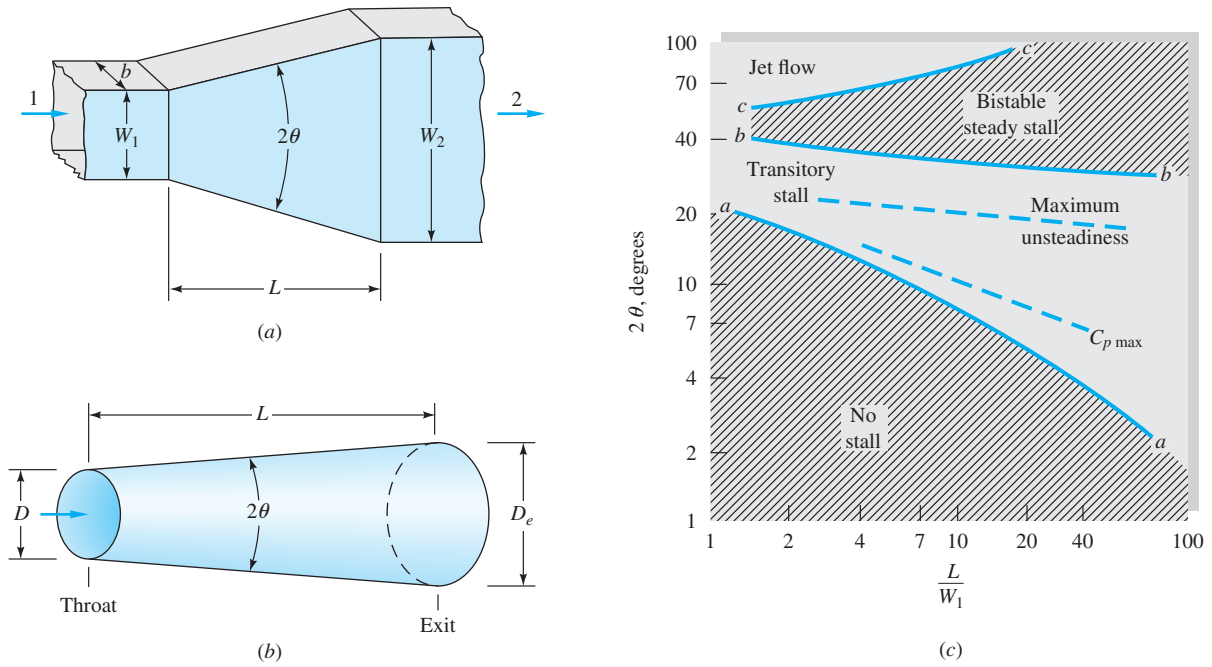
Fig. 6.26 Diffuser geometry and typical flow regimes: (*a*) geometry of a flat-walled diffuser; (*b*) geometry of a conical diffuser; (*c*) flat diffuser stability map. *(From Ref. 14, by permission of Creare, Inc.)*

Neglecting losses and gravity effects, the incompressible Bernoulli equation predicts that

$$p + \tfrac{1}{2}\rho V^2 = p_0 = \text{const} \qquad (6.89)$$

where p_0 is the stagnation pressure the fluid would achieve if the fluid were slowed to rest ($V = 0$) without losses.

The basic output of a diffuser is the *pressure-recovery coefficient* C_p, defined as

$$C_p = \frac{p_e - p_t}{p_{0t} - p_t} \qquad (6.90)$$

where subscripts e and t mean the exit and the throat (or inlet), respectively. Higher C_p means better performance.

Consider the flat-walled diffuser in Fig. 6.26*a*, where section 1 is the inlet and section 2 the exit. Application of Bernoulli's equation (6.89) to this diffuser predicts that

$$p_{01} = p_1 + \tfrac{1}{2}\rho V_1^2 = p_2 + \tfrac{1}{2}\rho V_2^2 = p_{02}$$

or

$$C_{p,\text{frictionless}} = 1 - \left(\frac{V_2}{V_1}\right)^2 \qquad (6.91)$$
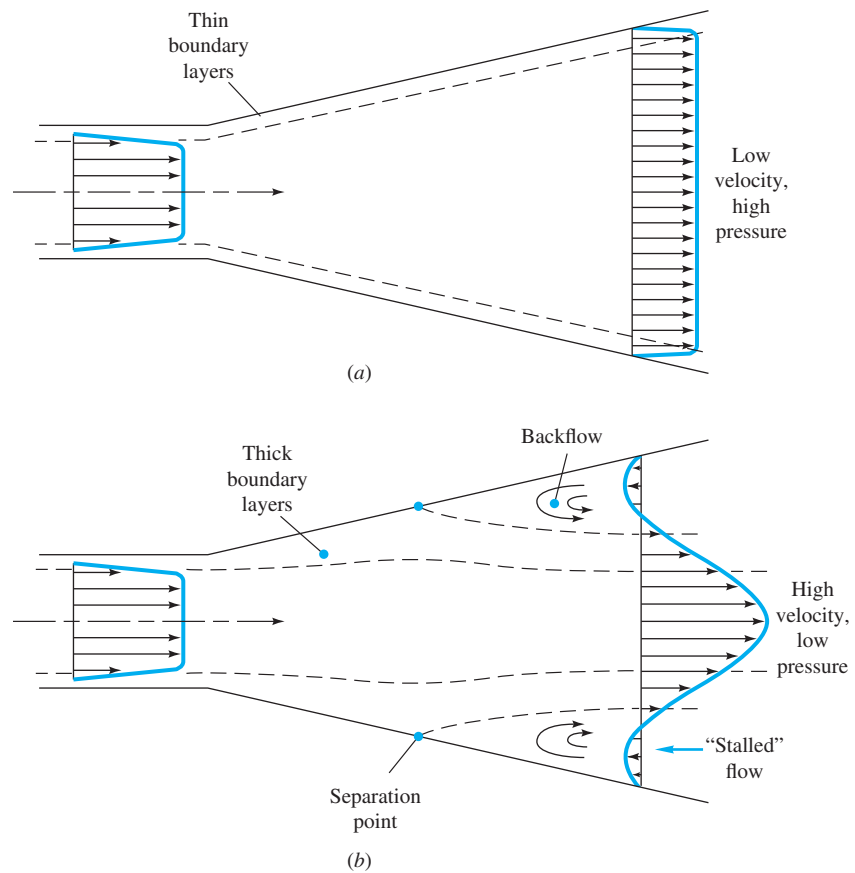
Fig. 6.27 Diffuser performance:
(*a*) ideal pattern with good
performance; (*b*) actual measured
pattern with boundary layer
separation and resultant poor
performance.

Meanwhile, steady one-dimensional continuity would require that

$$Q = V_1 A_1 = V_2 A_2 \tag{6.92}$$

Combining (6.91) and (6.92), we can write the performance in terms of the *area ratio*
AR $= A_2/A_1$, which is a basic parameter in diffuser design:

$$C_{p,\text{frictionless}} = 1 - (\text{AR})^{-2} \tag{6.93}$$

A typical design would have AR = 5:1, for which Eq. (6.93) predicts $C_p = 0.96$, or
nearly full recovery. But, in fact, measured values of C_p for this area ratio [14] are
only as high as 0.86 and can be as low as 0.24.

The basic reason for the discrepancy is flow separation, as sketched in Fig. 6.27*b*.
The increasing pressure in the diffuser is an unfavorable gradient (Sec. 7.5), which
causes the viscous boundary layers to break away from the walls and greatly reduces
the performance. Computational fluid dynamics (CFD) can now predict this
behavior.

As an added complication to boundary layer separation, the flow patterns in a diffuser are highly variable and were considered mysterious and erratic until 1955, when Kline revealed the structure of these patterns with flow visualization techniques in a simple water channel.

A complete *stability map* of diffuser flow patterns was published in 1962 by Fox and Kline [21], as shown in Fig. 6.26c. There are four basic regions. Below line *aa* there is steady viscous flow, no separation, and moderately good performance. Note that even a very short diffuser will separate, or stall, if its half-angle is greater than 10°.

Between lines *aa* and *bb* is a transitory stall pattern with strongly unsteady flow. Best performance (highest C_p) occurs in this region. The third pattern, between *bb* and *cc*, is steady bistable stall from one wall only. The stall pattern may flip-flop from one wall to the other, and performance is poor.

The fourth pattern, above line *cc*, is *jet flow,* where the wall separation is so gross and pervasive that the mainstream ignores the walls and simply passes on through at nearly constant area. Performance is extremely poor in this region.

Dimensional analysis of a flat-walled or conical diffuser shows that C_p should depend on the following parameters:

1. Any two of the following geometric parameters:
    a. Area ratio AR $= A_2/A_1$ or $(D_e/D)^2$
    b. Divergence angle 2θ
    c. Slenderness L/W_1 or L/D
2. Inlet Reynolds number $Re_t = V_1 W_1/\nu$ or $Re_t = V_1 D/\nu$
3. Inlet Mach number $Ma_t = V_1/a_1$
4. Inlet boundary layer *blockage factor* $B_t = A_{BL}/A_1$, where A_{BL} is the wall area blocked, or displaced, by the retarded boundary layer flow in the inlet (typically B_t varies from 0.03 to 0.12)

A flat-walled diffuser would require an additional shape parameter to describe its cross section:

5. Aspect ratio AS $= b/W_1$

Even with this formidable list, we have omitted five possible important effects: inlet turbulence, inlet swirl, inlet profile vorticity, superimposed pulsations, and downstream obstruction, all of which occur in practical machinery applications.

The three most important parameters are AR, θ, and B. Typical performance maps for diffusers are shown in Fig. 6.28. For this case of 8 to 9 percent blockage, both the flat-walled and conical types give about the same maximum performance, $C_p = 0.70$, but at different divergence angles (9° flat versus 4.5° conical). Both types fall far short of the Bernoulli estimates of $C_p = 0.93$ (flat) and 0.99 (conical), primarily because of the blockage effect.

From the data of Ref. 14 we can determine that, in general, performance decreases with blockage and is approximately the same for both flat-walled and conical diffusers, as shown in Table 6.6. In all cases, the best conical diffuser is 10 to 80 percent longer than the best flat-walled design. Therefore, if length is limited in the design, the flat-walled design will give the better performance depending on duct cross section.
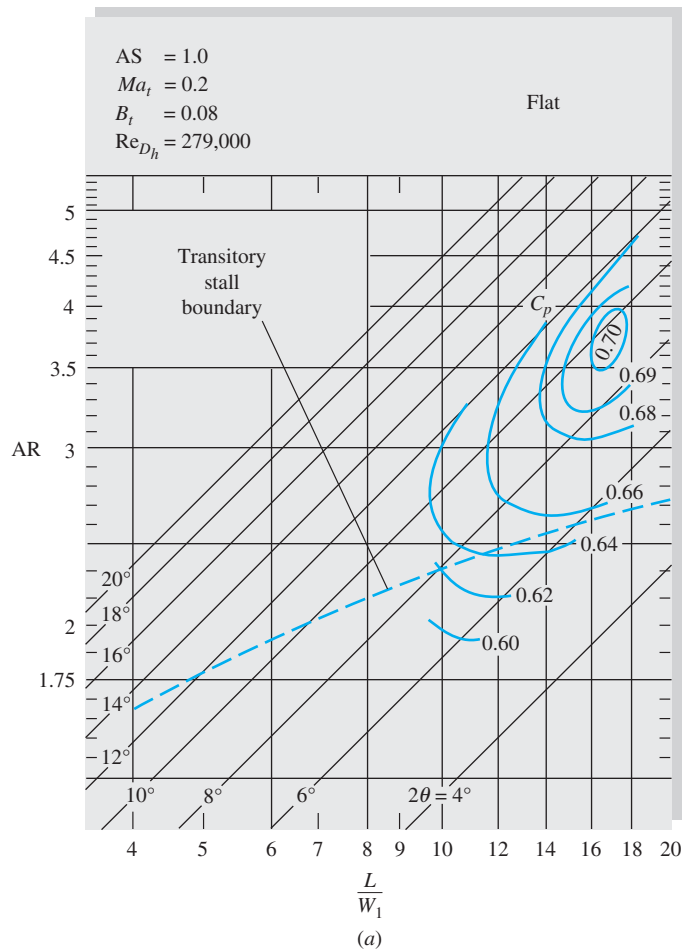
Fig. 6.28a Typical performance maps for flat-wall and conical diffusers at similar operating conditions: flat wall.

Source: From P. W. Runstadler, Jr., et al., "Diffuser Data Book," Crème Inc. Tech. Note 186, Hanover, NH, 1975., by permission of Creare, Inc.

The experimental design of a diffuser is an excellent example of a successful attempt to minimize the undesirable effects of adverse pressure gradient and flow separation.

Table 6.6 Maximum Diffuser Performance Data [14]

Source: From P. W. Runstadler, Jr., et al., "Diffuser Data Book," Crème Inc. Tech. Note 186, Hanover, NH, 1975.

Inlet blockage B_t	Flat-walled		Conical	
	C_p,max	L/W_1	C_p,max	L/d
0.02	0.86	18	0.83	20
0.04	0.80	18	0.78	22
0.06	0.75	19	0.74	24
0.08	0.70	20	0.71	26
0.10	0.66	18	0.68	28
0.12	0.63	16	0.65	30
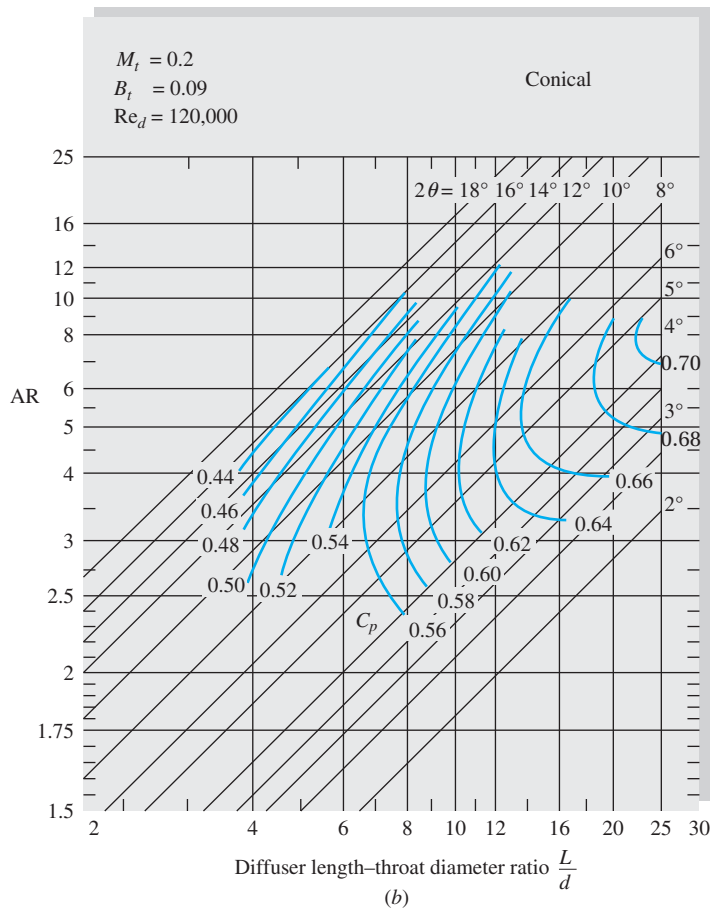
Fig. 6.28b Typical performance maps for flat-wall and conical diffusers at similar operating conditions: conical wall. *(From Ref. 14, by permission of Creare, Inc.)*

6.12 Fluid Meters

Almost all practical fluid engineering problems are associated with the need for an accurate flow measurement. There is a need to measure *local* properties (velocity, pressure, temperature, density, viscosity, turbulent intensity), *integrated* properties (mass flow and volume flow), and *global* properties (visualization of the entire flow field). We shall concentrate in this section on velocity and volume flow measurements.

We have discussed pressure measurement in Sec. 2.10. Measurement of other thermodynamic properties, such as density, temperature, and viscosity, is beyond the scope of this text and is treated in specialized books such as Refs. 22 and 23. Global visualization techniques were discussed in Sec. 1.11 for low-speed flows, and the special optical techniques used in high-speed flows are treated in Ref. 34 of Chap. 1. Flow measurement schemes suitable for open-channel and other free-surface flows are treated in Chap. 10.

Local Velocity Measurements

Velocity averaged over a small region, or point, can be measured by several different physical principles, listed in order of increasing complexity and sophistication:

1. Trajectory of floats or neutrally buoyant particles.
2. Rotating mechanical devices:
   a. Cup anemometer.
   b. Savonius rotor.
   c. Propeller meter.
   d. Turbine meter.
3. Pitot-static tube (Fig. 6.30).
4. Electromagnetic current meter.
5. Hot wires and hot films.
6. Laser-doppler anemometer (LDA).
7. Particle image velocimetry (PIV).

Some of these meters are sketched in Fig. 6.29.
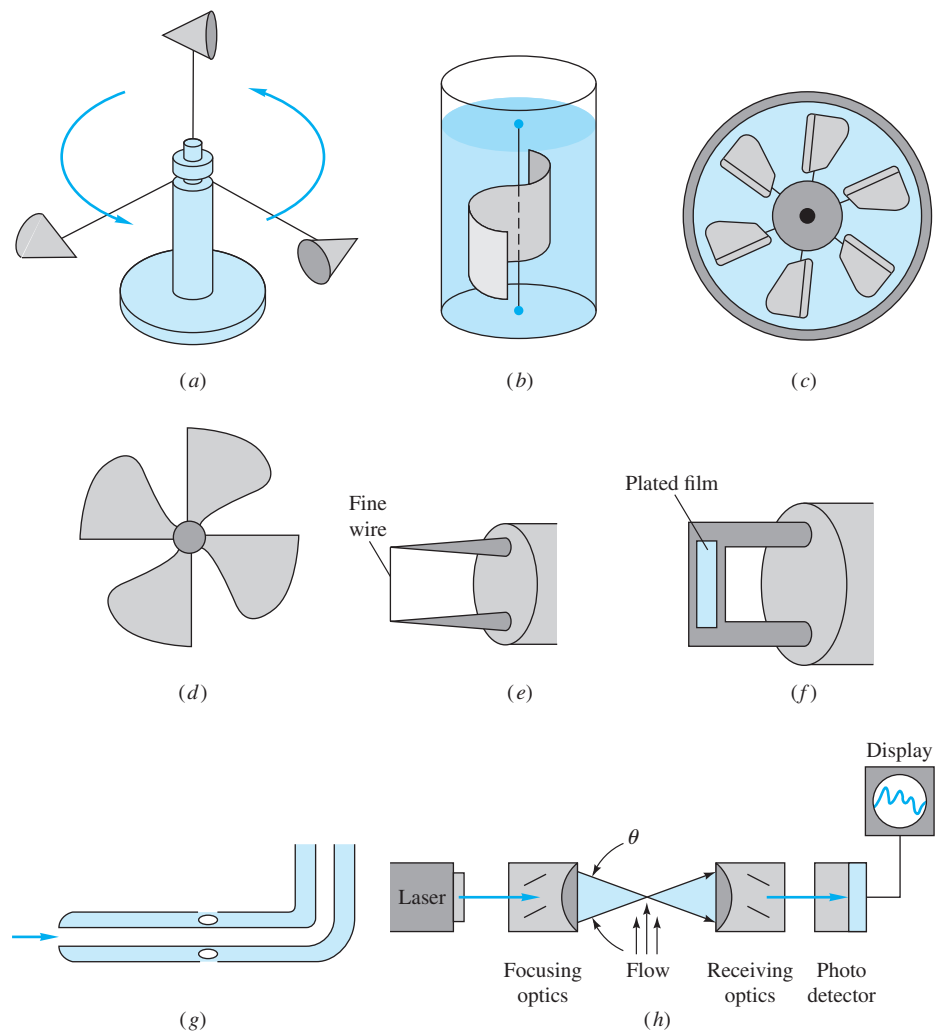
Fig. 6.29 Eight common velocity meters: (*a*) three-cup anemometer; (*b*) Savonius rotor; (*c*) turbine mounted in a duct; (*d*) free-propeller meter; (*e*) hot-wire anemometer; (*f*) hot-film anemometer; (*g*) pitot-static tube; (*h*) laser-doppler anemometer.
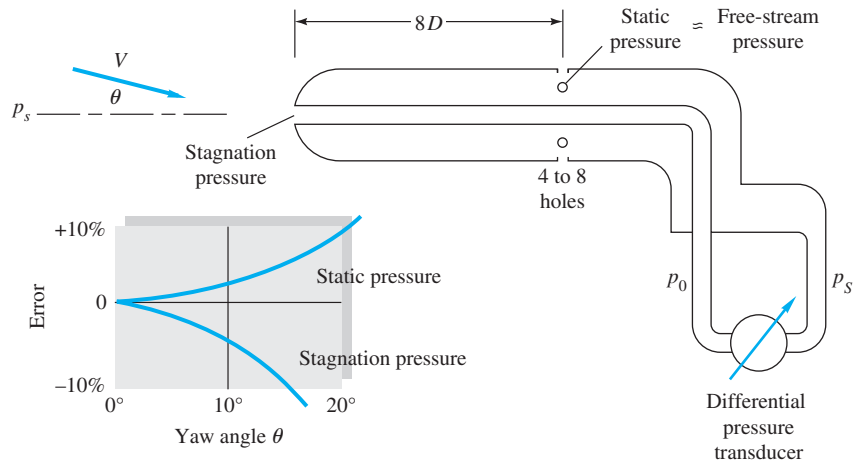
Fig. 6.30 Pitot-static tube for combined measurement of static and stagnation pressure in a moving stream.

Floats or Buoyant Particles. A simple but effective estimate of flow velocity can be found from visible particles entrained in the flow. Examples include flakes on the surface of a channel flow, small neutrally buoyant spheres mixed with a liquid, or hydrogen bubbles. Sometimes gas flows can be estimated from the motion of entrained dust particles. One must establish whether the particle motion truly simulates the fluid motion. Floats are commonly used to track the movement of ocean waters and can be designed to move at the surface, along the bottom, or at any given depth [24]. Many official tidal current charts [25] were obtained by releasing and timing a floating spar attached to a length of string. One can release whole groups of spars to determine a flow pattern.

Rotating Sensors. The rotating devices of Fig. 6.29a to d can be used in either gases or liquids, and their rotation rate is approximately proportional to the flow velocity. The cup anemometer (Fig. 6.29a) and Savonius rotor (Fig. 6.29b) always rotate the same way, regardless of flow direction. They are popular in atmospheric and oceanographic applications and can be fitted with a direction vane to align themselves with the flow. The ducted-propeller (Fig. 6.29c) and free-propeller (Fig. 6.29d) meters must be aligned with the flow parallel to their axis of rotation. They can sense reverse flow because they will then rotate in the opposite direction. All these rotating sensors can be attached to counters or sensed by electromagnetic or slip-ring devices for either a continuous or a digital reading of flow velocity. All have the disadvantage of being relatively large and thus not representing a "point."

Pitot-Static Tube. A slender tube aligned with the flow (Figs. 6.29g and 6.30) can measure local velocity by means of a pressure difference. It has sidewall holes to measure the static pressure p_s in the moving stream and a hole in the front to measure the *stagnation* pressure p_0, where the stream is decelerated to zero velocity. Instead of measuring p_0 or p_s separately, it is customary to measure their difference with, say, a transducer, as in Fig. 6.30.

If $\mathrm{Re}_D > 1000$, where D is the probe diameter, the flow around the probe is nearly frictionless and Bernoulli's relation, Eq. (3.54), applies with good accuracy. For incompressible flow

$$p_s + \tfrac{1}{2}\rho V^2 + \rho g z_s \approx p_0 + \tfrac{1}{2}\rho(0)^2 + \rho g z_0$$

Assuming that the elevation pressure difference $\rho g(z_s - z_0)$ is negligible, this reduces to

$$V \approx \left[2\frac{(p_0 - p_s)}{\rho} \right]^{1/2} \qquad (6.94)$$

This is the *Pitot formula,* named after the French engineer, Henri de Pitot, who designed the device in 1732.

The primary disadvantage of the pitot tube is that it must be aligned with the flow direction, which may be unknown. For yaw angles greater than 5°, there are substantial errors in both the p_0 and p_s measurements, as shown in Fig. 6.30. The pitot-static tube is useful in liquids and gases; for gases a compressibility correction is necessary if the stream Mach number is high (Chap. 9). Because of the slow response of the fluid-filled tubes leading to the pressure sensors, it is not useful for unsteady flow measurements. It does resemble a point and can be made small enough to measure, for example, blood flow in arteries and veins. It is not suitable for low-velocity measurement in gases because of the small pressure differences developed. For example, if $V = 1$ ft/s in standard air, from Eq. (6.94) we compute $p_0 - p$ equal to only 0.001 lbf/ft^2 (0.048 Pa). This is beyond the resolution of most pressure gages.

Electromagnetic Meter. If a magnetic field is applied across a conducting fluid, the fluid motion will induce a voltage across two electrodes placed in or near the flow. The electrodes can be streamlined or built into the wall, and they cause little or no flow resistance. The output is very strong for highly conducting fluids such as liquid metals. Seawater also gives good output, and electromagnetic current meters are in common use in oceanography. Even low-conductivity fresh water can be measured by amplifying the output and insulating the electrodes. Commercial instruments are available for most liquid flows but are relatively costly. Electromagnetic flowmeters are treated in Ref. 26.

Hot-Wire Anemometer. A very fine wire ($d = 0.01$ mm or less) heated between two small probes, as in Fig. 6.29e, is ideally suited to measure rapidly fluctuating flows such as the turbulent boundary layer. The idea dates back to work by L. V. King in 1914 on heat loss from long, thin cylinders. If electric power is supplied to heat the cylinder, the loss varies with flow velocity across the cylinder according to *King's law*

$$q = I^2 R \approx a + b(\rho V)^n \qquad (6.95)$$

where $n \approx \frac{1}{3}$ at very low Reynolds numbers and equals $\frac{1}{2}$ at high Reynolds numbers. The hot wire normally operates in the high-Reynolds-number range but should be calibrated in each situation to find the best-fit a, b, and n. The wire can be operated either at constant current I, so that resistance R is a measure of V, or at constant resistance R (constant temperature), with I a measure of velocity. In either case, the output is a nonlinear function of V, and the equipment should contain a *linearizer* to produce convenient velocity data. Many varieties of commercial hot-wire equipment are available, as are do-it-yourself designs [27]. Excellent detailed discussions of the hot wire are given in Ref. 28.

Because of its frailty, the hot wire is not suited to liquid flows, whose high density and entrained sediment will knock the wire right off. A more stable yet quite sensitive alternative for liquid flow measurement is the hot-film anemometer (Fig. 6.29f). A thin metallic film, usually platinum, is plated onto a relatively thick support, which

can be a wedge, a cone, or a cylinder. The operation is similar to the hot wire. The cone gives best response but is liable to error when the flow is yawed to its axis.

Hot wires can easily be arranged in groups to measure two- and three-dimensional velocity components.

Laser-Doppler Anemometer. In the LDA a laser beam provides highly focused, coherent monochromatic light that is passed through the flow. When this light is scattered from a moving particle in the flow, a stationary observer can detect a change, or *doppler shift,* in the frequency of the scattered light. The shift Δf is proportional to the velocity of the particle. There is essentially zero disturbance of the flow by the laser.

Figure 6.29*h* shows the popular dual-beam mode of the LDA. A focusing device splits the laser into two beams, which cross the flow at an angle θ. Their intersection, which is the measuring volume or resolution of the measurement, resembles an ellipsoid about 0.5 mm wide and 0.1 mm in diameter. Particles passing through this measuring volume scatter the beams; they then pass through receiving optics to a photodetector, which converts the light to an electric signal. A signal processor then converts electric frequency to a voltage that can be either displayed or stored. If λ is the wavelength of the laser light, the measured velocity is given by

$$V = \frac{\lambda \, \Delta f}{2 \sin (\theta/2)} \tag{6.96}$$

Multiple components of velocity can be detected by using more than one photodetector and other operating modes. Either liquids or gases can be measured as long as scattering particles are present. In liquids, normal impurities serve as scatterers, but gases may have to be seeded. The particles may be as small as the wavelength of the light. Although the measuring volume is not as small as with a hot wire, the LDA is capable of measuring turbulent fluctuations.

The advantages of the LDA are as follows:

1. No disturbance of the flow.
2. High spatial resolution of the flow field.
3. Velocity data that are independent of the fluid thermodynamic properties.
4. An output voltage that is linear with velocity.
5. No need for calibration.

The disadvantages are that both the apparatus and the fluid must be transparent to light and that the cost is high (a basic system shown in Fig. 6.29*h* begins at about $50,000).

Once installed, an LDA can map the entire flow field in minutest detail. To truly appreciate the power of the LDA, one should examine, for instance, the amazingly detailed three-dimensional flow profiles measured by Eckardt [29] in a high-speed centrifugal compressor impeller. Extensive discussions of laser velocimetry are given in Refs. 38 and 39.

Particle Image Velocimetry. This popular new idea, called PIV for short, measures not just a single point but instead maps the entire field of flow. An illustration was shown in Fig. 1.18*b*. The flow is seeded with neutrally buoyant particles. A planar laser light sheet across the flow is pulsed twice and photographed twice. If $\Delta \mathbf{r}$ is the particle displacement vector over a short time Δt, an estimate of its velocity is $\mathbf{V} \approx \Delta \mathbf{r}/\Delta t$.

A dedicated computer applies this formula to a whole cloud of particles and thus maps the flow field. One can also use the data to calculate velocity gradient and vorticity fields. Since the particles all look alike, other cameras may be needed to identify them. Three-dimensional velocities can be measured by two cameras in a stereoscopic arrangement. The PIV method is not limited to stop-action. New high-speed cameras (up to 10,000 frames per second) can record movies of unsteady flow fields. For further details, see the monograph by M. Raffel [51].

EXAMPLE 6.20

The pitot-static tube of Fig. 6.30 uses mercury as a manometer fluid. When it is placed in a water flow, the manometer height reading is $h = 8.4$ in. Neglecting yaw and other errors, what is the flow velocity V in ft/s?

Solution

From the two-fluid manometer relation (2.23b), with $z_A = z_2$, the pressure difference is related to h by

$$p_0 - p_s = (\gamma_M - \gamma_w)h$$

Taking the specific weights of mercury and water from Table 2.1, we have

$$p_0 - p_s = (846 - 62.4 \text{ lbf/ft}^3)\,\frac{8.4}{12}\text{ft} = 549 \text{ lbf/ft}^2$$

The density of water is $62.4/32.2 = 1.94$ slugs/ft^3. Introducing these values into the pitot-static formula (6.97), we obtain

$$V = \left[\frac{2(549 \text{ lbf/ft}^2)}{1.94 \text{ slugs/ft}^3}\right]^{1/2} = 23.8 \text{ ft/s} \qquad\qquad Ans.$$

Since this is a low-speed flow, no compressibility correction is needed.

Volume Flow Measurements

It is often desirable to measure the integrated mass, or volume flow, passing through a duct. Accurate measurement of flow is vital in billing customers for a given amount of liquid or gas passing through a duct. The different devices available to make these measurements are discussed in great detail in the ASME text on fluid meters [30]. These devices split into two classes: mechanical instruments and head loss instruments.

The mechanical instruments measure actual mass or volume of fluid by trapping it and counting it. The various types of measurement are

1. Mass measurement
    a.   Weighing tanks
    b.   Tilting traps
2. Volume measurement
    a.   Volume tanks
    b.   Reciprocating pistons

  c. Rotating slotted rings

  d. Nutating disc

  e. Sliding vanes

  f. Gear or lobed impellers

  g. Reciprocating bellows

  h. Sealed-drum compartments

The last three of these are suitable for gas flow measurement.

  The head loss devices obstruct the flow and cause a pressure drop, which is a measure of flux:

1. Bernoulli-type devices

  a. Thin-plate orifice

  b. Flow nozzle

  c. Venturi tube

2. Friction loss devices

  a. Capillary tube

  b. Porous plug

The friction loss meters cause a large nonrecoverable head loss and obstruct the flow too much to be generally useful.

  Six other widely used meters operate on different physical principles:

1. Turbine meter

2. Vortex meter

3. Ultrasonic flowmeter

4. Rotameter

5. Coriolis mass flowmeter

6. Laminar flow element

Nutating Disc Meter. For measuring liquid *volumes,* as opposed to volume rates, the most common devices are the nutating disc and the turbine meter. Figure 6.31 shows
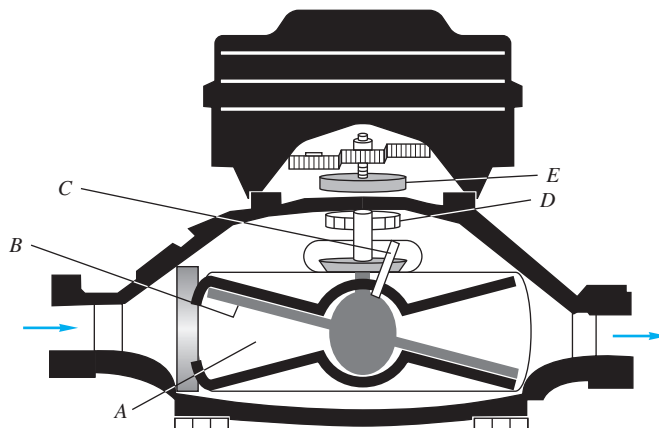
Fig. 6.31 Cutaway sketch of a nutating disc fluid meter. *A*: metered-volume chamber; *B*: nutating disc; *C*: rotating spindle; *D*: drive magnet; *E*: magnetic counter sensor.
Source: Courtesy of Badger Meter, Inc., Milwaukee, Wisconsin.

a cutaway sketch of *a nutating disc meter,* widely used in both water and gasoline delivery systems. The mechanism is clever and perhaps beyond the writer's capability to explain. The metering chamber is a slice of a sphere and contains a rotating disc set at an angle to the incoming flow. The fluid causes the disc to *nutate* (spin eccentrically), and one revolution corresponds to a certain fluid volume passing through. Total volume is obtained by counting the number of revolutions.

Turbine Meter.   The turbine meter, sometimes called a *propeller meter,* is a freely rotating propeller that can be installed in a pipeline. A typical design is shown in Fig. 6.32*a.* There are flow straighteners upstream of the rotor, and the rotation is
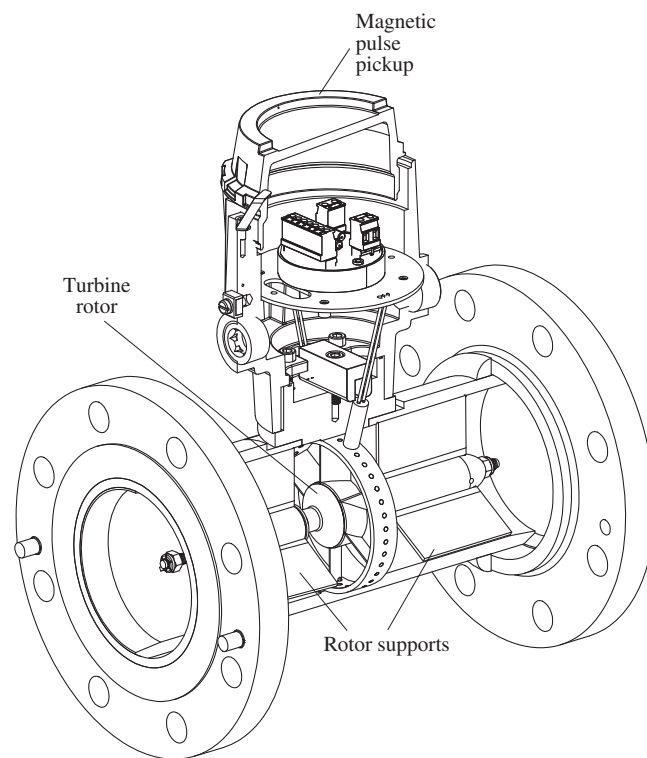
(*a*)

Fig. 6.32 The turbine meter widely used in the oil and gas industry: (*a*) basic design; (*b*) the linearity curve is the measure of variation in the signal output across the 10% to 100% nominal flow range of the meter. *(Daniel Measurement and Control, Houston, TX.)*
Source: (a) Daniel Industries of Fluke Calibration, Houston, TX.
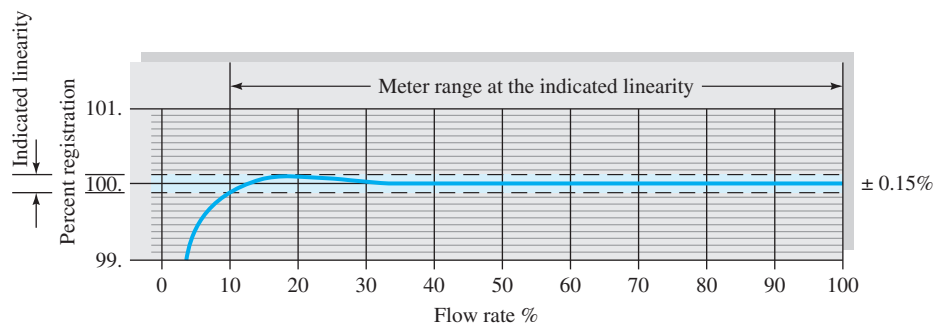
Fig. 6.33 A Commercial handheld wind velocity turbine meter. *(Courtesy of Nielsen-Kellerman Company.)*

measured by electric or magnetic pickup of pulses caused by passage of a point on the rotor. The rotor rotation is approximately proportional to the volume flow in the pipe.

Like the nutating disc, a major advantage of the turbine meter is that each pulse corresponds to a finite incremental volume of fluid, and the pulses are digital and can be summed easily. Liquid flow turbine meters have as few as two blades and produce a constant number of pulses per unit fluid volume over a 5:1 flow rate range with ±0.25 percent accuracy. Gas meters need many blades to produce sufficient torque and are accurate to ±1 percent.

Since turbine meters are very individualistic, flow calibration is an absolute necessity. A typical liquid meter calibration curve is shown in Fig. 6.32b. Researchers attempting to establish universal calibration curves have met with little practical success as a result of manufacturing variabilities.

Turbine meters can also be used in unconfined flow situations, such as winds or ocean currents. They can be compact, even microsize with two or three component directions. Figure 6.33 illustrates a handheld wind velocity meter that uses a seven-bladed turbine with a calibrated digital output. The accuracy of this device is quoted at ±2 percent.

Vortex Flowmeters. Recall from Fig. 5.2 that a bluff body placed in a uniform crossflow sheds alternating vortices at a nearly uniform Strouhal number St $= fL/U$, where U is the approach velocity and L is a characteristic body width. Since L and St are constant, this means that the shedding frequency is proportional to velocity:

$$f = (\text{const})(U) \tag{6.97}$$

The vortex meter introduces a shedding element across a pipe flow and picks up the shedding frequency downstream with a pressure, ultrasonic, or heat transfer type of sensor. A typical design is shown in Fig. 6.34.
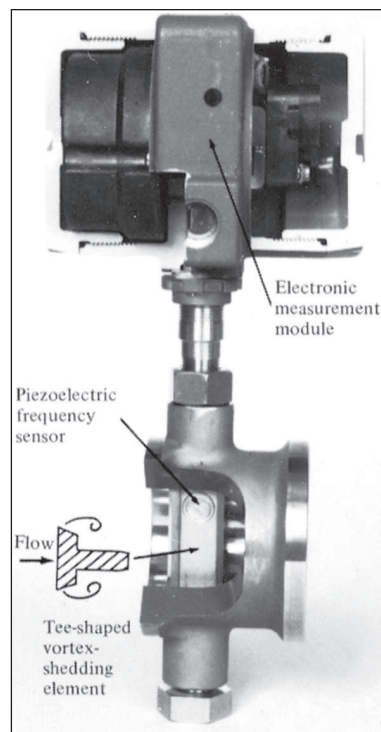
Fig. 6.34 A vortex flowmeter.
(Courtesy of Invensys p/c.)

The advantages of a vortex meter are as follows:

1. Absence of moving parts.
2. Accuracy to ± 1 percent over a wide flow rate range (up to 100:1).
3. Ability to handle very hot or very cold fluids.
4. Requirement of only a short pipe length.
5. Calibration insensitive to fluid density or viscosity.

For further details see Ref. 40.

Ultrasonic Flowmeters.   The sound-wave analog of the laser velocimeter of Fig. 6.29*h* is the ultrasonic flowmeter. Two examples are shown in Fig. 6.35. The pulse-type flowmeter is shown in Fig. 6.35*a*. Upstream piezoelectric transducer *A* is excited with a short sonic pulse that propagates across the flow to downstream transducer *B*. The arrival at *B* triggers another pulse to be created at *A*, resulting in a regular pulse frequency f_A. The same process is duplicated in the reverse direction from *B* to *A*, creating frequency f_B. The difference $f_A - f_B$ is proportional to the flow rate. Figure 6.35*b* shows a doppler-type arrangement, where sound waves from transmitter *T* are scattered by particles or contaminants in the flow to receiver *R*. Comparison of the two signals reveals a doppler frequency shift that is proportional to the flow rate. Ultrasonic meters are nonintrusive and can be directly attached to pipe flows in the
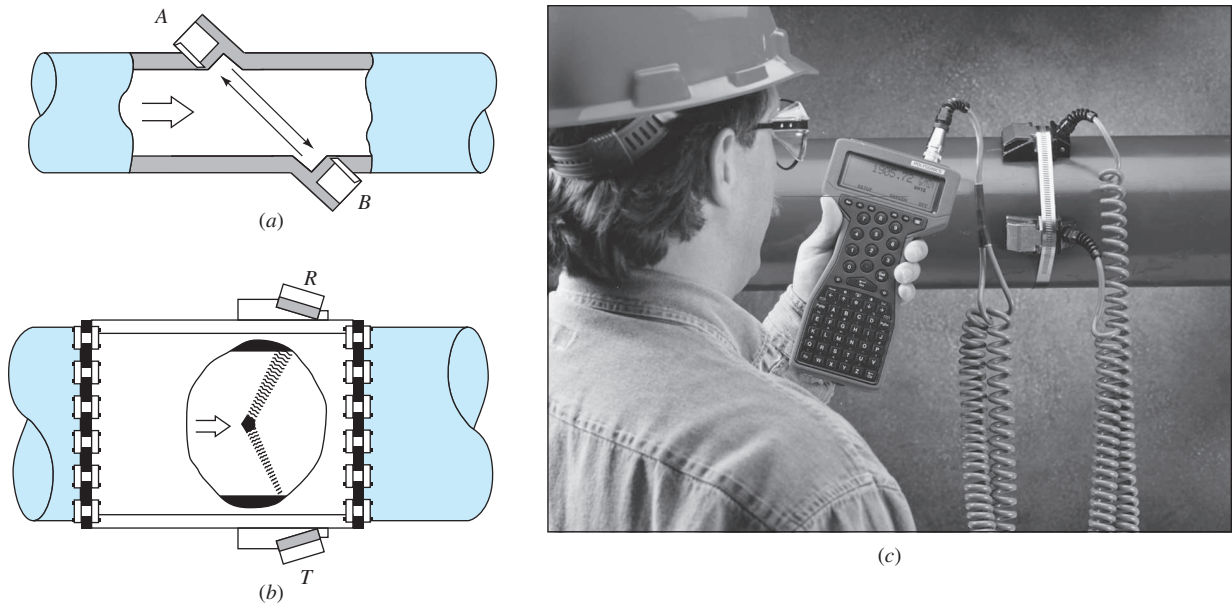
Fig. 6.35 Ultrasonic flowmeters: (*a*) pulse type; (*b*) doppler-shift type *(from Ref. 41)*; (*c*) a portable noninvasive installation *(Courtesy of Thermo Polysonics, Houston, TX.)*

field (Fig. 6.35*c*). Their quoted uncertainty of ± 1 to 2 percent can rise to ± 5 percent or more due to irregularities in velocity profile, fluid temperature, or Reynolds number. For further details see Ref. 41.

Rotameter.   The variable-area transparent *rotameter* of Fig. 6.36 has a float that, under the action of flow, rises in the vertical tapered tube and takes a certain equilibrium position for any given flow rate. A student exercise for the forces on the float would yield the approximate relation

$$Q = C_d A_a \left(\frac{2W_{\text{net}}}{A_{\text{float}} \rho_{\text{fluid}}} \right)^{1/2} \tag{6.98}$$

where W_{net} is the float's net weight in the fluid, $A_a = A_{\text{tube}} - A_{\text{float}}$ is the annular area between the float and the tube, and C_d is a dimensionless discharge coefficient of order unity, for the annular constricted flow. For slightly tapered tubes, A_a varies nearly linearly with the float position, and the tube may be calibrated and marked with a flow rate scale, as in Fig. 6.36. The rotameter thus provides a readily visible measure of the flow rate. Capacity may be changed by using different-sized floats. Obviously the tube must be vertical, and the device does not give accurate readings for fluids containing high concentrations of bubbles or particles.

Coriolis Mass Flowmeter.   Most commercial meters measure *volume* flow, with mass flow then computed by multiplying by the nominal fluid density. An attractive

modern alternative is a *mass* flowmeter, which operates on the principle of the Coriolis acceleration associated with noninertial coordinates [recall Fig. 3.11 and the Coriolis term $2\Omega \times V$ in Eq. (3.48)]. The output of the meter is directly proportional to mass flow.

Figure 6.37 is a schematic of a Coriolis device, to be inserted into a piping system. The flow enters a loop arrangement, which is electromagnetically vibrated at a high natural frequency (amplitude < 1 mm and frequency > 100 Hz). The Coriolis effect induces a downward force on the loop entrance and an upward force on the loop exit, as shown. The loop twists, and the twist angle can be measured and is proportional to the mass flow through the tube. Accuracy is typically less than 1 percent of full scale.

Laminar Flow Element.   In many, perhaps most, commercial flowmeters, the flow through the meter is turbulent and the variation of flow rate with pressure drop is nonlinear. In laminar duct flow, however, Q is linearly proportional to Δp, as in Eq. (6.12): $Q = [\pi R^4/(8\mu L)]\,\Delta p$. Thus a *laminar* flow sensing element is attractive, since its calibration will be linear. To ensure laminar flow for what otherwise would be a turbulent condition, all or part of the fluid is directed into small passages, each of which has a low (laminar) Reynolds number. A honeycomb is a popular design.

Figure 6.38 uses axial flow through a narrow annulus to create laminar flow. The theory again predicts $Q \propto \Delta p$, as in Eq. (6.70). However, the flow is very sensitive to passage size; for example, halving the annulus clearance increases Δp more than eight times. Careful calibration is thus necessary. In Fig. 6.38 the laminar flow concept has been synthesized into a complete mass flow system, with temperature control, differential pressure measurement, and a microprocessor all self-contained. The accuracy of this device is rated at ± 0.2 percent.

Fig. 6.36 A commercial rotameter. The float rises in the tapered tube to an equilibrium position, which is a measure of the fluid flow rate. *(Courtesy of Blue White Industries, Huntington Beach, CA.)*
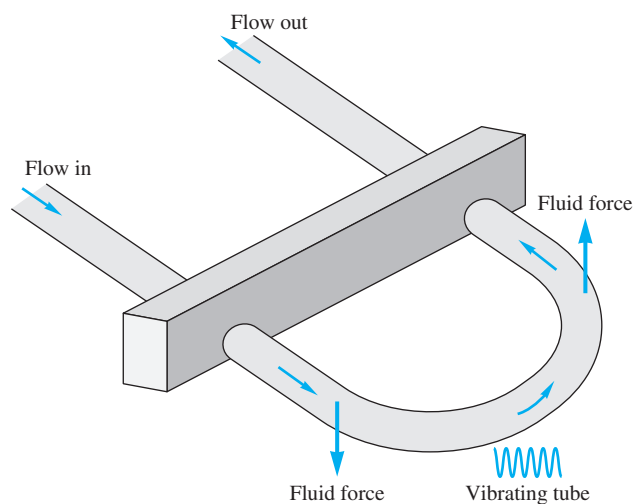
Fig. 6.37 Schematic of a Coriolis mass flowmeter.
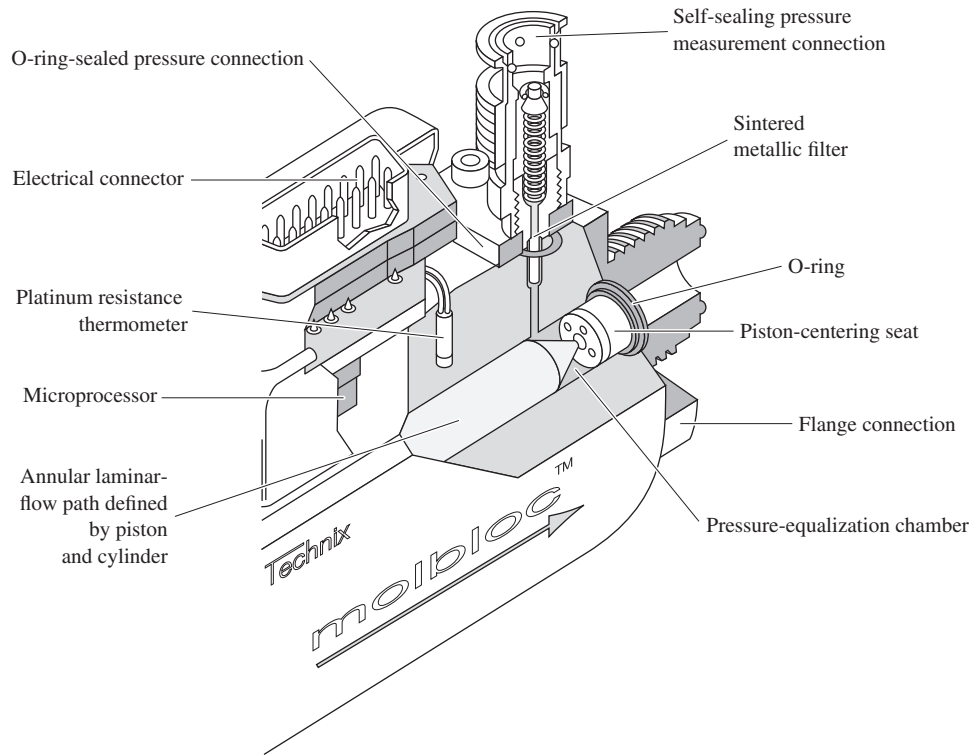
Fig. 6.38 A complete flowmeter system using a laminar flow element (in this case a narrow annulus). The flow rate is linearly proportional to the pressure drop.
Source: Courtesy of Martin Girard, DH Instruments, Inc.

Bernoulli Obstruction Theory. Consider the generalized flow obstruction shown in Fig. 6.39. The flow in the basic duct of diameter D is forced through an obstruction of diameter d; the β ratio of the device is a key parameter:

$$\beta = \frac{d}{D} \tag{6.99}$$

After leaving the obstruction, the flow may neck down even more through a vena contracta of diameter $D_2 < d$, as shown. Apply the Bernoulli and continuity equations for incompressible steady frictionless flow to estimate the pressure change:

Continuity: $Q = \frac{\pi}{4}D^2 V_1 = \frac{\pi}{4}D_2^2 V_2$

Bernoulli: $p_0 = p_1 + \frac{1}{2}\rho V_1^2 = p_2 + \frac{1}{2}\rho V_2^2$

Eliminating V_1, we solve these for V_2 or Q in terms of the pressure change $p_1 - p_2$:

$$\frac{Q}{A_2} = V_2 \approx \left[\frac{2(p_1 - p_2)}{\rho(1 - D_2^4/D^4)}\right]^{1/2} \tag{6.100}$$

But this is surely inaccurate because we have neglected friction in a duct flow, where we know friction will be very important. Nor do we want to get into the business of measuring vena contracta ratios D_2/d for use in (6.100). Therefore we assume that
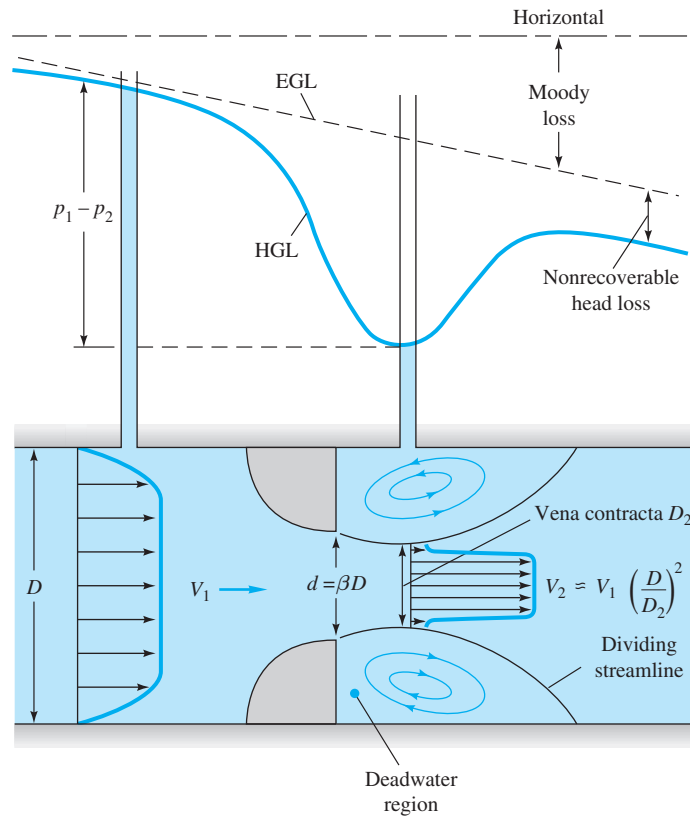
Fig. 6.39 Velocity and pressure change through a generalized Bernoulli obstruction meter.

$D_2/D \approx \beta$ and then calibrate the device to fit the relation

$$Q = A_t V_t = C_d A_t \left[\frac{2(p_1 - p_2)/\rho}{1 - \beta^4} \right]^{1/2} \qquad (6.101)$$

where subscript t denotes the throat of the obstruction. The dimensionless *discharge coefficient* C_d accounts for the discrepancies in the approximate analysis. By dimensional analysis for a given design we expect

$$C_d = f(\beta, \text{Re}_D) \quad \text{where} \quad \text{Re}_D = \frac{V_1 D}{\nu} \qquad (6.102)$$

The geometric factor involving β in (6.101) is called the *velocity-of-approach factor*:

$$E = (1 - \beta^4)^{-1/2} \qquad (6.103)$$

One can also group C_d and E in Eq. (6.101) to form the dimensionless *flow coefficient* α:

$$\alpha = C_d E = \frac{C_d}{(1 - \beta^4)^{1/2}} \qquad (6.104)$$

Thus Eq. (6.101) can be written in the equivalent form

$$Q = \alpha A_t \left[\frac{2(p_1 - p_2)}{\rho} \right]^{1/2} \tag{6.105}$$

Obviously the flow coefficient is correlated in the same manner:

$$\alpha = f(\beta, \text{Re}_D) \tag{6.106}$$

Occasionally one uses the throat Reynolds number instead of the approach Reynolds number:

$$\text{Re}_d = \frac{V_t d}{\nu} = \frac{\text{Re}_D}{\beta} \tag{6.107}$$

Since the design parameters are assumed known, the correlation of α from Eq. (6.106) or of C_d from Eq. (6.102) is the desired solution to the fluid metering problem.

The mass flow is related to Q by

$$\dot{m} = \rho Q \tag{6.108}$$

and is thus correlated by exactly the same formulas.

Figure 6.40 shows the three basic devices recommended for use by the International Organization for Standardization (ISO) [31]: the orifice, nozzle, and venturi tube.
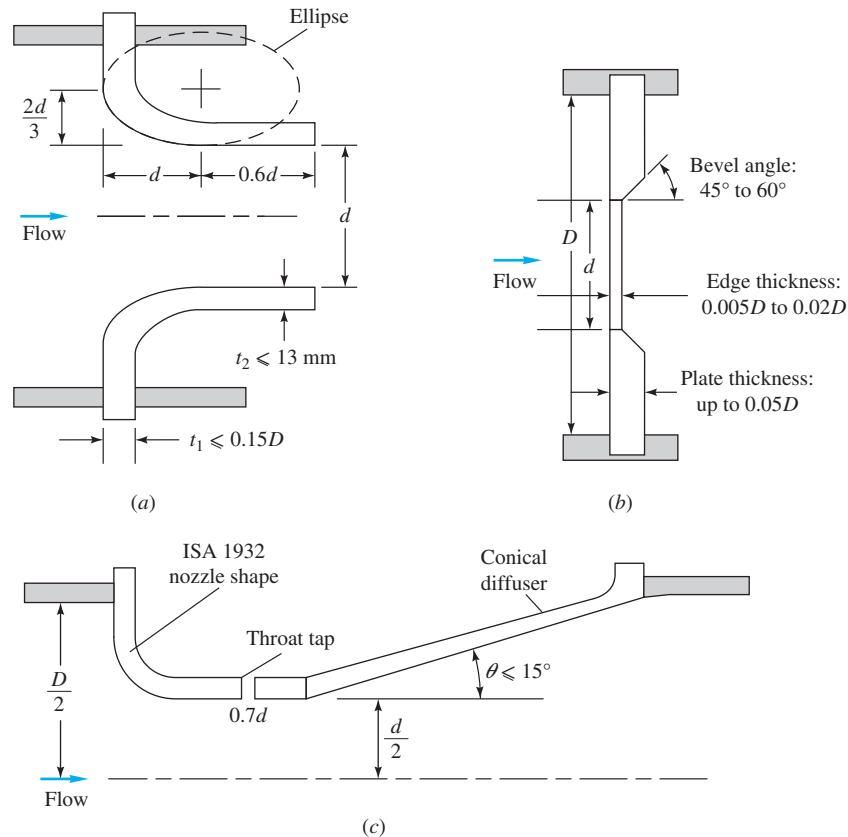
Fig. 6.40 Standard shapes for the three primary Bernoulli obstruction-type meters: (*a*) long-radius nozzle; (*b*) thin-plate orifice; (*c*) venturi nozzle. *(Based on data from the International Organization for Standardization.)*

Thin-Plate Orifice.   The thin-plate orifice, Fig. 6.40b, can be made with β in the range of 0.2 to 0.8, except that the hole diameter d should not be less than 12.5 mm. To measure p_1 and p_2, three types of tappings are commonly used:

1. Corner taps where the plate meets the pipe wall.
2. D: $\frac{1}{2}D$ taps: pipe-wall taps at D upstream and $\frac{1}{2}D$ downstream.
3. Flange taps: 1 in (25 mm) upstream and 1 in (25 mm) downstream of the plate, regardless of the size D.

Types 1 and 2 approximate geometric similarity, but since the flange taps 3 do not, they must be correlated separately for every single size of pipe in which a flange-tap plate is used [30, 31].

Figure 6.41 shows the discharge coefficient of an orifice with D: $\frac{1}{2}D$ or type 2 taps in the Reynolds number range $\mathrm{Re}_D = 10^4$ to 10^7 of normal use. Although detailed charts such as Fig. 6.41 are available for designers [30], the ASME recommends use of the curve-fit formulas developed by the ISO [31]. The basic form of the curve fit is [42]

$$C_d = f(\beta) + 91.71\beta^{2.5}\mathrm{Re}_D^{-0.75} + \frac{0.09\beta^4}{1 - \beta^4}F_1 - 0.0337\beta^3F_2 \qquad (6.109)$$

where

$$f(\beta) = 0.5959 + 0.0312\beta^{2.1} - 0.184\beta^8$$
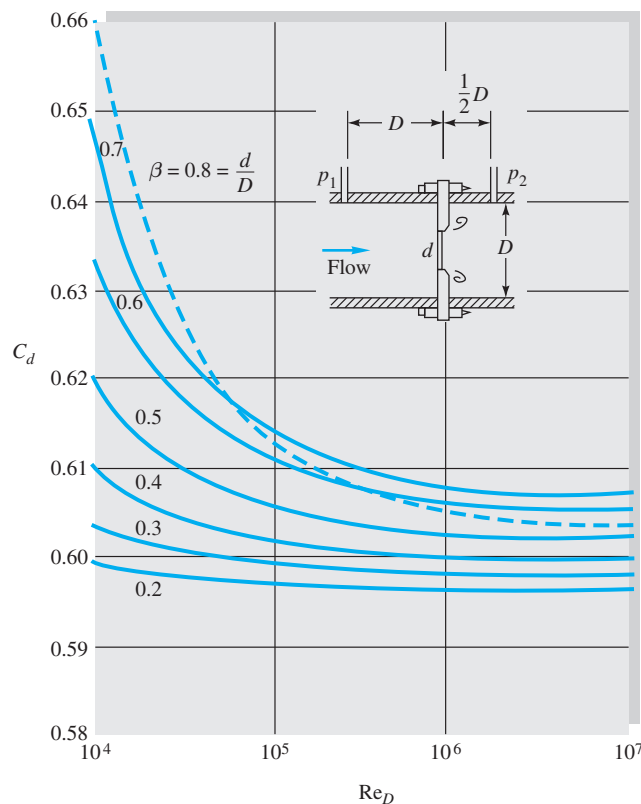
Fig. 6.41 Discharge coefficient for a thin-plate orifice with D: $\frac{1}{2}D$ taps, plotted from Eqs. (6.109) and (6.110b).

The correlation factors F_1 and F_2 vary with tap position:

Corner taps: $\qquad\qquad\qquad\qquad\qquad F_1 = 0 \quad F_2 = 0$ $\qquad\qquad\qquad\qquad\qquad$ (6.110a)

$D: \frac{1}{2}D$ taps: $\qquad\qquad\qquad\qquad\quad F_1 = 0.4333 \quad F_2 = 0.47$ $\qquad\qquad\qquad\quad$ (6.110b)

Flange taps: $\quad F_2 = \dfrac{1}{D \text{ (in)}} \quad F_1 = \begin{cases} \dfrac{1}{D \text{ (in)}} & D > 2.3 \text{ in} \\ 0.4333 & 2.0 \le D \le 2.3 \text{ in} \end{cases}$ $\qquad$ (6.110c)

Note that the flange taps (6.110c), not being geometrically similar, use raw diameter in inches in the formula. The constants will change if other diameter units are used. We cautioned against such dimensional formulas in Example 1.4 and Eq. (5.17) and give Eq. (6.110c) only because flange taps are widely used in the United States.

Flow Nozzle. The flow nozzle comes in two types, a long-radius type shown in Fig. 6.40a and a short-radius type (not shown) called the ISA 1932 nozzle [30, 31]. The flow nozzle, with its smooth, rounded entrance convergence, practically eliminates the vena contracta and gives discharge coefficients near unity. The nonrecoverable loss is still large because there is no diffuser provided for gradual expansion.

The ISO recommended correlation for long-radius-nozzle discharge coefficient is

$$C_d \approx 0.9965 - 0.00653\beta^{1/2}\left(\frac{10^6}{\text{Re}_D}\right)^{1/2} = 0.9965 - 0.00653\left(\frac{10^6}{\text{Re}_d}\right)^{1/2} \quad (6.111)$$

The second form is independent of the β ratio and is plotted in Fig. 6.42. A similar ISO correlation is recommended for the short-radius ISA 1932 flow nozzle:

$$C_d \approx 0.9900 - 0.2262\beta^{4.1}$$
$$+ (0.000215 - 0.001125\beta + 0.00249\beta^{4.7})\left(\frac{10^6}{\text{Re}_D}\right)^{1.15} \quad (6.112)$$

Flow nozzles may have β values between 0.2 and 0.8.
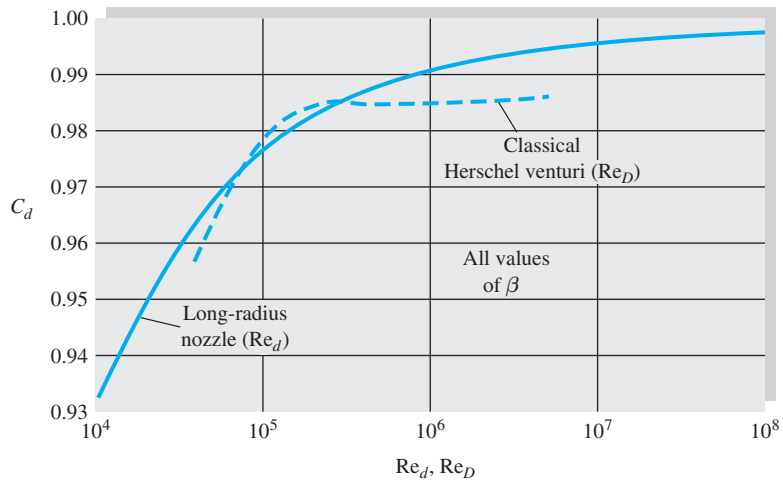
Fig. 6.42 Discharge coefficient for long-radius nozzle and classical Herschel-type venturi.
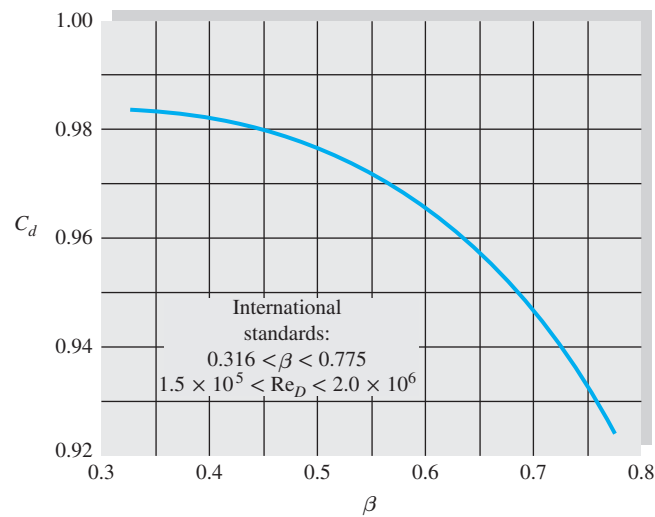
Fig. 6.43 Discharge coefficient for a venturi nozzle.

Venturi Meter. The third and final type of obstruction meter is the venturi, named in honor of Giovanni Venturi (1746–1822), an Italian physicist who first tested conical expansions and contractions. The original, or *classical,* venturi was invented by a U.S. engineer, Clemens Herschel, in 1898. It consisted of a 21° conical contraction, a straight throat of diameter d and length d, then a 7° to 15° conical expansion. The discharge coefficient is near unity, and the nonrecoverable loss is very small. Herschel venturis are seldom used now.

The modern venturi nozzle, Fig. 6.40c, consists of an ISA 1932 nozzle entrance and a conical expansion of half-angle no greater than 15°. It is intended to be operated in a narrow Reynolds number range of 1.5×10^5 to 2×10^6. Its discharge coefficient, shown in Fig. 6.43, is given by the ISO correlation formula

$$C_d \approx 0.9858 - 0.196\beta^{4.5} \tag{6.113}$$

It is independent of Re_D within the given range. The Herschel venturi discharge varies with Re_D but not with β, as shown in Fig. 6.42. Both have very low net losses.

The choice of meter depends on the loss and the cost and can be illustrated by the following table:

Type of meter	Net head loss	Cost
Orifice	Large	Small
Nozzle	Medium	Medium
Venturi	Small	Large

As so often happens, the product of inefficiency and initial cost is approximately constant.

The average nonrecoverable head losses for the three types of meters, expressed as a fraction of the throat velocity head $V_t^2/(2g)$, are shown in Fig. 6.44. The orifice has the greatest loss and the venturi the least, as discussed. The orifice and nozzle
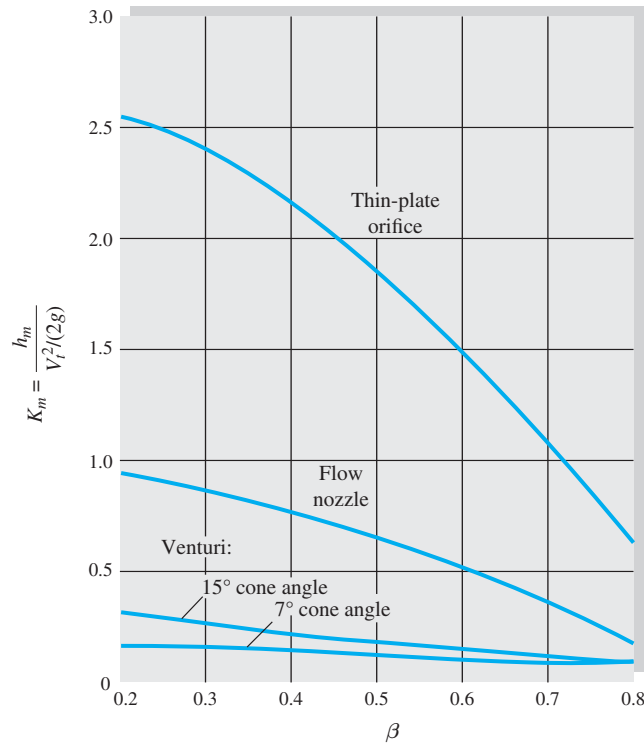
Fig. 6.44 Nonrecoverable head loss in Bernoulli obstruction meters. *(Adapted from Ref. 30.)*

simulate partially closed valves as in Fig. 6.18*b*, while the venturi is a very minor loss. When the loss is given as a fraction of the measured *pressure drop,* the orifice and nozzle have nearly equal losses, as Example 6.21 will illustrate.

The other types of instruments discussed earlier in this section can also serve as flowmeters if properly constructed. For example, a hot wire mounted in a tube can be calibrated to read volume flow rather than point velocity. Such hot-wire meters are commercially available, as are other meters modified to use velocity instruments. For further details see Ref. 30.

Compressible Gas Flow Correction Factor. The orifice/nozzle/venturi formulas in this section assume incompressible flow. If the fluid is a gas, and the pressure ratio (p_2/p_1) is not near unity, a compressibility correction is needed. Equation (6.101) is rewritten in terms of mass flow and the upstream density ρ_1:

$$\dot{m} = C_d\, Y A_t \sqrt{\frac{2\rho_1(p_1 - p_2)}{1 - \beta^4}} \quad \text{where} \quad \beta = \frac{d}{D} \tag{6.114}$$

The dimensionless *expansion factor Y* is a function of pressure ratio, β, and the type of meter. Some values are plotted in Fig. 6.45. The orifice, with its strong jet contraction, has a different factor from the venturi or the flow nozzle, which are designed to eliminate contraction.
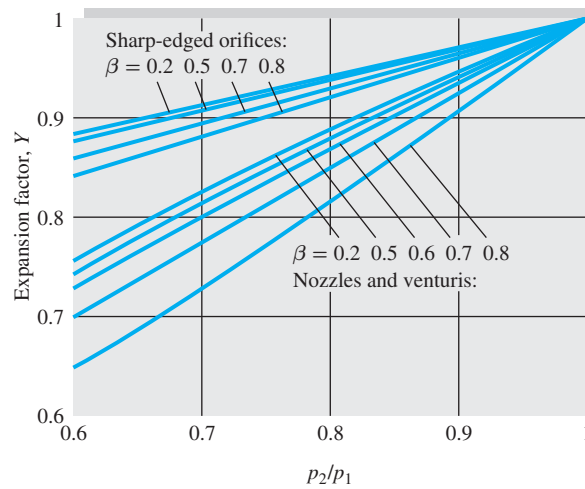
Fig. 6.45 Compressible flow expansion factor Y for flowmeters.

EXAMPLE 6.21

We want to meter the volume flow of water ($\rho = 1000$ kg/m³, $\nu = 1.02 \times 10^{-6}$ m²/s) moving through a 200-mm-diameter pipe at an average velocity of 2.0 m/s. If the differential pressure gage selected reads accurately at $p_1 - p_2 = 50{,}000$ Pa, what size meter should be selected for installing (a) an orifice with D: $\frac{1}{2}D$ taps, (b) a long-radius flow nozzle, or (c) a venturi nozzle? What would be the nonrecoverable head loss for each design?

Solution

Here the unknown is the β ratio of the meter. Since the discharge coefficient is a complicated function of β, iteration will be necessary. We are given $D = 0.2$ m and $V_1 = 2.0$ m/s. The pipe-approach Reynolds number is thus

$$\text{Re}_D = \frac{V_1 D}{\nu} = \frac{(2.0)(0.2)}{1.02 \times 10^{-6}} = 392{,}000$$

For all three cases [(a) to (c)] the generalized formula (6.105) holds:

$$V_t = \frac{V_1}{\beta^2} = \alpha \left[\frac{2(p_1 - p_2)}{\rho} \right]^{1/2} \qquad \alpha = \frac{C_d}{(1 - \beta^4)^{1/2}} \qquad (1)$$

where the given data are $V_1 = 2.0$ m/s, $\rho = 1000$ kg/m³, and $\Delta p = 50{,}000$ Pa. Inserting these known values into Eq. (1) gives a relation between β and α:

$$\frac{2.0}{\beta^2} = \alpha \left[\frac{2(50{,}000)}{1000} \right]^{1/2} \qquad \text{or} \qquad \beta^2 = \frac{0.2}{\alpha} \qquad (2)$$

The unknowns are β (or α) and C_d. Parts (a) to (c) depend on the particular chart or formula needed for $C_d = \text{fcn}(\text{Re}_D, \beta)$. We can make an initial guess $\beta \approx 0.5$ and iterate to convergence.

Part (a) For the orifice with D: $\frac{1}{2}D$ taps, use Eq. (6.109) or Fig. 6.41. The iterative sequence is

$$\beta_1 \approx 0.5, \ C_{d1} \approx 0.604, \ \alpha_1 \approx 0.624, \ \beta_2 \approx 0.566, \ C_{d2} \approx 0.606, \ \alpha_2 \approx 0.640, \ \beta_3 = 0.559$$

We have converged to three figures. The proper orifice diameter is

$$d = \beta D = 112 \text{ mm} \qquad \qquad \textit{Ans. (a)}$$

Part (b)   For the long-radius flow nozzle, use Eq. (6.111) or Fig. 6.42. The iterative sequence is

$$\beta_1 \approx 0.5, C_{d1} \approx 0.9891, \alpha_1 \approx 1.022, \beta_2 \approx 0.442, C_{d2} \approx 0.9896, \alpha_2 \approx 1.009, \beta_3 = 0.445$$

We have converged to three figures. The proper nozzle diameter is

$$d = \beta D = 89 \text{ mm} \qquad \qquad \textit{Ans. (b)}$$

Part (c)   For the venturi nozzle, use Eq. (6.113) or Fig. 6.43. The iterative sequence is

$$\beta_1 \approx 0.5, C_{d1} \approx 0.977, \alpha_1 \approx 1.009, \beta_2 \approx 0.445, C_{d2} \approx 0.9807, \alpha_2 \approx 1.0004, \beta_3 = 0.447$$

We have converged to three figures. The proper venturi diameter is

$$d = \beta D = 89 \text{ mm} \qquad \qquad \textit{Ans. (c)}$$

Comments: These meters are of similar size, but their head losses are not the same. From Fig. 6.44 for the three different shapes we may read the three K factors and compute

$$h_{m,\text{orifice}} \approx 3.5 \text{ m} \qquad h_{m,\text{nozzle}} \approx 3.6 \text{ m} \qquad h_{m,\text{venturi}} \approx 0.8 \text{ m}$$

The venturi loss is only about 22 percent of the orifice and nozzle losses.

Solution by Excel Iteration for the Flow Nozzle

Parts (*a, b, c*) were solved by hand, but Excel is ideal for these calculations. You may review this procedure from the instructions in Example 6.5. We need five columns: C_d, calculated from Eq. (6.111), throat velocity V_t calculated from Δp, α as calculated from Eq. (6.104), and β calculated from the velocity ratio (V/V_t). The fifth column is an initial guess for β, which is replaced in its next row by the newly computed β. Any initial $\beta < 1$ will do. Here we chose $\beta = 0.5$ as in part (*b*) for the flow nozzle. Remember to use *cell* names, not symbols: in row 1, $C_d = $ A1, $V_t = $ B1, $\alpha = $ C1, and $\beta = $ D1. The process converges rapidly, in only two or three iterations:

	C_d from Eq.(6.114)	$V_t = \alpha(2\Delta p/\rho)$	$\alpha = C_d/(1 - \beta^4)^\wedge 0.5$	$\beta = (V/V_t)^\wedge 0.5$	β-guess
	A	B	C	D	E
1	0.9891	10.216	1.0216	0.4425	0.5000
2	0.9896	10.091	1.0091	0.4452	0.4425
3	0.9895	10.096	1.0096	0.4451	0.4452
4	0.9895	10.096	1.0096	0.4451	0.4451

The final answers for the long-radius flow nozzle are:

$$\alpha = 1.0096 \qquad C_d = 0.9895 \qquad \beta = 0.4451 \qquad \qquad \textit{Ans. (b)}$$

EXAMPLE 6.22

A long-radius nozzle of diameter 6 cm is used to meter airflow in a 10-cm-diameter pipe. Upstream conditions are $p_1 = 200$ kPa and $T_1 = 100°C$. If the pressure drop through the nozzle is 60 kPa, estimate the flow rate in m^3/s.

Solution

- *Assumptions:* The pressure drops 30 percent, so we need the compressibility factor Y, and Eq. (6.114) is applicable to this problem.
- *Approach:* Find ρ_1 and C_d and apply Eq. (6.114) with $\beta = 6/10 = 0.6$.
- *Property values:* Given p_1 and T_1, $\rho_1 = p_1/RT_1 = (200{,}000)/[287(100 + 273)] = 1.87$ kg/m³. The downstream pressure is $p_2 = 200 - 60 = 140$ kPa, hence $p_2/p_1 = 0.7$. At 100°C, from Table A.2, the viscosity of air is 2.17 E-5 kg/m-s.
- *Solution steps:* Initially apply Eq. (6.114) by guessing, from Fig. 6.42, that $C_d \approx 0.98$. From Fig. 6.45, for a nozzle with $p_2/p_1 = 0.7$ and $\beta = 0.6$, read $Y \approx 0.80$. Then

$$\dot{m} = C_d\, Y A_t \sqrt{\frac{2\rho_1(p_1 - p_2)}{1 - \beta^4}} \approx (0.98)(0.80)\,\frac{\pi}{4}\,(0.06 \text{ m})^2 \sqrt{\frac{2(1.87 \text{ kg/m}^3)(60{,}000 \text{ Pa})}{1 - (0.6)}}$$

$$\approx 1.13\,\frac{\text{kg}}{\text{s}}$$

Now estimate Re_d, putting it in the convenient mass flow form:

$$\text{Re}_d = \frac{\rho V d}{\mu} = \frac{4\,\dot{m}}{\pi \mu d} = \frac{4(1.13 \text{ kg/s})}{\pi(2.17 \text{ E-5 kg/m} - \text{s})(0.06 \text{ m})} \approx 1.11 \text{ E6}$$

Returning to Fig. 6.42, we could read a slightly better $C_d \approx 0.99$. Thus our final estimate is

$$\dot{m} \approx 1.14 \text{ kg/s} \qquad\qquad\qquad Ans.$$

- *Comments:* Figure 6.45 is not just a "chart" for engineers to use casually. It is based on the compressible flow theory of Chap. 9. There, we may reassign this example as a *theory*.

Summary

This chapter has been concerned with internal pipe and duct flows, which are probably the most common problems encountered in engineering fluid mechanics. Such flows are very sensitive to the Reynolds number and change from laminar to transitional to turbulent flow as the Reynolds number increases.

The various Reynolds number regimes were outlined, and a semiempirical approach to turbulent flow modeling was presented. The chapter then made a detailed analysis of flow through a straight circular pipe, leading to the famous Moody chart (Fig. 6.13) for the friction factor. Possible uses of the Moody chart were discussed for flow rate and sizing problems, as well as the application of the Moody chart to noncircular ducts using an equivalent duct "diameter." The addition of minor losses due to valves, elbows, fittings, and other devices was presented in the form of loss coefficients to be incorporated along with Moody-type friction losses. Multiple-pipe systems were discussed briefly and were seen to be quite complex algebraically and appropriate for computer solution.

Diffusers are added to ducts to increase pressure recovery at the exit of a system. Their behavior was presented as experimental data, since the theory of real diffusers is still not well developed. The chapter ended with a discussion of flowmeters, especially the pitot-static tube and the Bernoulli obstruction type of meter. Flowmeters also require careful experimental calibration.

Problems

Most of the problems herein are fairly straightforward. More difficult or open-ended assignments are labeled with an asterisk. Problems labeled with a computer icon 💻 may require the use of a computer. The standard end-of-chapter problems P6.1 to P6.163 (categorized in the problem list here) are followed by word problems W6.1 to W6.4, fundamentals of engineering exam problems FE6.1 to FE6.15, comprehensive problems C6.1 to C6.9, and design projects D6.1 and D6.2.

Problem Distribution

Section	Topic	Problems
6.1	Reynolds number regimes	P6.1–P6.5
6.2	Internal and external flow	P6.6–P6.8
6.3	Head loss—friction factor	P6.9–P6.11
6.4	Laminar pipe flow	P6.12–P6.33
6.5	Turbulence modeling	P6.34–P6.40
6.6	Turbulent pipe flow	P6.41–P6.62
6.7	Flow rate and sizing problems	P6.63–P6.85
6.8	Noncircular ducts	P6.86–P6.98
6.9	Minor or local losses	P6.99–P6.110
6.10	Series and parallel pipe systems	P6.111–P6.120
6.10	Three-reservoir and pipe network systems	P6.121–P6.130
6.11	Diffuser performance	P6.131–P6.134
6.12	The pitot-static tube	P6.135–P6.139
6.12	Flowmeters: the orifice plate	P6.140–P6.148
6.12	Flowmeters: the flow nozzle	P6.149–P6.153
6.12	Flowmeters: the venturi meter	P6.154–P6.159
6.12	Flowmeters: other designs	P6.160–P6.161
6.12	Flowmeters: compressibility correction	P6.162–P6.163

Reynolds number regimes

P6.1 An engineer claims that the flow of SAE 30W oil, at 20°C, through a 5-cm-diameter smooth pipe at 1 million N/h, is laminar. Do you agree? A million newtons is a lot, so this sounds like an awfully high flow rate.

P6.2 The present pumping rate of crude oil through the Alaska Pipeline, with an ID of 48 in, is 550,000 barrels per day (1 barrel = 42 U.S. gallons). (a) Is this a turbulent flow? (b) What would be the maximum rate if the flow were constrained to be laminar? Assume that Alaskan oil fits Fig. A.1 of the Appendix at 60°C.

P6.3 The Keystone Pipeline in the chapter opener photo has a maximum proposed flow rate of 1.3 million barrels of crude oil per day. Estimate the Reynolds number and whether the flow is laminar. Assume that Keystone crude oil fits Fig. A.1 of the Appendix at 40°C.

P6.4 For flow of SAE 30 oil through a 5-cm-diameter pipe, from Fig. A.1, for what flow rate in m^3/h would we expect transition to turbulence at (a) 20°C and (b) 100°C?

P6.5 In flow past a body or wall, early transition to turbulence can be induced by placing a trip wire on the wall across the flow, as in Fig. P6.5. If the trip wire in Fig. P6.5 is placed where the local velocity is U, it will trigger turbulence if $Ud/\nu = 850$, where d is the wire diameter [3, p. 388]. If the sphere diameter is 20 cm and transition is observed at $Re_D = 90,000$, what is the diameter of the trip wire in mm?
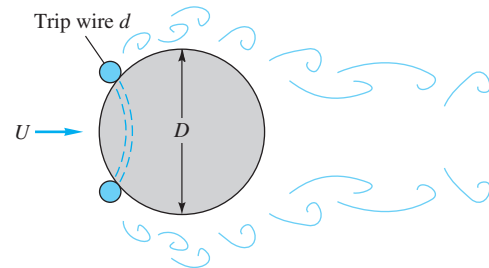
P6.5

Internal and external flow

P6.6 For flow of a uniform stream parallel to a sharp flat plate, transition to a turbulent boundary layer on the plate may occur at $Re_x = \rho Ux/\mu \approx 1$ E6, where U is the approach velocity and x is distance along the plate. If $U = 2.5$ m/s, determine the distance x for the following fluids at 20°C and 1 atm: (a) hydrogen, (b) air, (c) gasoline, (d) water, (e) mercury, and (f) glycerin.

P6.7 SAE 10W30 oil at 20°C flows from a tank into a 2-cm-diameter tube 40 cm long. The flow rate is 1.1 m^3/hr. Is the entrance length region a significant part of this tube flow?

P6.8 When water at 20°C is in steady turbulent flow through an 8-cm-diameter pipe, the wall shear stress is 72 Pa. What is the axial pressure gradient ($\partial p/\partial x$) if the pipe is (a) horizontal and (b) vertical with the flow up?

Head loss—friction factor

P6.9 A light liquid ($\rho \approx 950$ kg/m^3) flows at an average velocity of 10 m/s through a horizontal smooth tube of diameter 5 cm. The fluid pressure is measured at 1-m intervals along the pipe, as follows:

x, m	0	1	2	3	4	5	6
p, kPa	304	273	255	240	226	213	200

Estimate (a) the total head loss, in meters; (b) the wall shear stress in the fully developed section of the pipe; and (c) the overall friction factor.

P6.10 Water at 20°C flows through an inclined 8-cm-diameter pipe. At sections A and B the following data are taken: $p_A = 186$ kPa, $V_A = 3.2$ m/s, $z_A = 24.5$ m, and $p_B = 260$ kPa, $V_B = 3.2$ m/s, $z_B = 9.1$ m. Which way is the flow going? What is the head loss in meters?

P6.11 Water at 20°C flows upward at 4 m/s in a 6-cm-diameter pipe. The pipe length between points 1 and 2 is 5 m, and point 2 is 3 m higher. A mercury manometer, connected between 1 and 2, has a reading $h = 135$ mm, with p_1 higher. (a) What is the pressure change $(p_1 - p_2)$? (b) What is the head loss, in meters? (c) Is the manometer reading proportional to head loss? Explain. (d) What is the friction factor of the flow?

In Probs. 6.12 to 6.99, neglect minor losses.

Laminar pipe flow—no minor losses

P6.12 A 5-mm-diameter capillary tube is used as a viscometer for oils. When the flow rate is 0.071 m³/h, the measured pressure drop per unit length is 375 kPa/m. Estimate the viscosity of the fluid. Is the flow laminar? Can you also estimate the density of the fluid?

P6.13 A soda straw is 20 cm long and 2 mm in diameter. It delivers cold cola, approximated as water at 10°C, at a rate of 3 cm³/s. (a) What is the head loss through the straw? What is the axial pressure gradient $\partial p/\partial x$ if the flow is (b) vertically up or (c) horizontal? Can the human lung deliver this much flow?

P6.14 Water at 20°C is to be siphoned through a tube 1 m long and 2 mm in diameter, as in Fig. P6.14. Is there any height H for which the flow might not be laminar? What is the flow rate if $H = 50$ cm? Neglect the tube curvature.
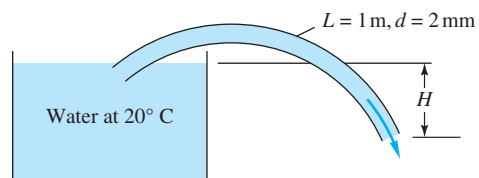
P6.14

P6.15 Professor Gordon Holloway and his students at the University of New Brunswick went to a fast-food emporium and tried to drink chocolate shakes ($\rho \approx 1200$ kg/m³, $\mu \approx 6$ kg/m-s) through fat straws 8 mm in diameter and 30 cm long. (a) Verify that their human lungs, which can develop approximately 3000 Pa of vacuum pressure, would be unable to drink the milkshake through the vertical straw. (b) A student cut 15 cm from his straw and proceeded to drink happily. What rate of milkshake flow was produced by this strategy?

P6.16 Fluid flows steadily, at volume rate Q, through a large pipe and then divides into two small pipes, the larger of which

has an inside diameter of 25 mm and carries three times the flow of the smaller pipe. Both small pipes have the same length and pressure drop. If all flows are laminar, estimate the diameter of the smaller pipe.

P6.17 A *capillary viscometer* measures the time required for a specified volume v of liquid to flow through a small-bore glass tube, as in Fig. P6.17. This transit time is then correlated with fluid viscosity. For the system shown, (a) derive an approximate formula for the time required, assuming laminar flow with no entrance and exit losses. (b) If $L = 12$ cm, $l = 2$ cm, $v = 8$ cm³, and the fluid is water at 20°C, what capillary diameter D will result in a transit time t of 6 seconds?
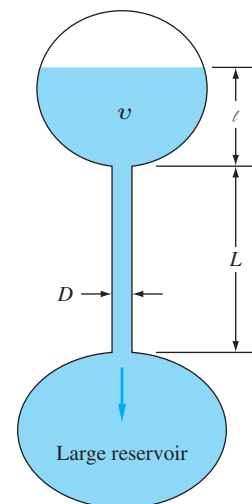
P6.17

P6.18 SAE 50W oil at 20°C flows from one tank to another through a tube 160 cm long and 5 cm in diameter. Estimate the flow rate in m³/hr if $z_1 = 2$ m and $z_2 = 0.8$ m.
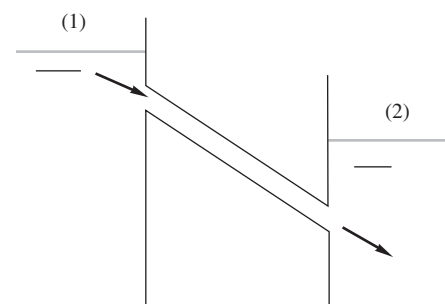
P6.18

P6.19 An oil (SG = 0.9) issues from the pipe in Fig. P6.19 at $Q = 35$ ft³/h. What is the kinematic viscosity of the oil in ft³/s? Is the flow laminar?

P6.19

P6.22
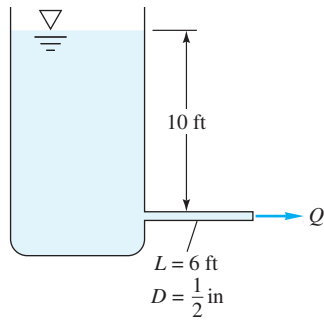
P6.20 The oil tanks in Tinyland are only 160 cm high, and they discharge to the Tinyland oil truck through a smooth tube 4 mm in diameter and 55 cm long. The tube exit is open to the atmosphere and 145 cm below the tank surface. The fluid is medium fuel oil, $\rho = 850$ kg/m^3 and $\mu = 0.11$ kg/(m · s). Estimate the oil flow rate in cm^3/h.

P6.21 In Tinyland, houses are less than a foot high! The rainfall is laminar! The drainpipe in Fig. P6.21 is only 2 mm in diameter. (*a*) When the gutter is full, what is the rate of draining? (*b*) The gutter is designed for a sudden rainstorm of up to 5 mm per hour. For this condition, what is the maximum roof area that can be drained successfully? (*c*) What is Re$_d$?

P6.23 SAE 10 oil at 20°C flows in a vertical pipe of diameter 2.5 cm. It is found that the pressure is constant throughout the fluid. What is the oil flow rate in m^3/h? Is the flow up or down?

P6.24 Two tanks of water at 20°C are connected by a capillary tube 4 mm in diameter and 3.5 m long. The surface of tank 1 is 30 cm higher than the surface of tank 2. (*a*) Estimate the flow rate in m^3/h. Is the flow laminar? (*b*) For what tube diameter will Re$_d$ be 500?

P6.25 For the configuration shown in Fig. P6.25, the fluid is ethyl alcohol at 20°C, and the tanks are very wide. Find the flow rate which occurs in m^3/h. Is the flow laminar?

P6.25

P6.21

P6.22 A steady push on the piston in Fig. P6.22 causes a flow rate $Q = 0.15$ cm^3/s through the needle. The fluid has $\rho = 900$ kg/m^3 and $\mu = 0.002$ kg/(m · s). What force F is required to maintain the flow?
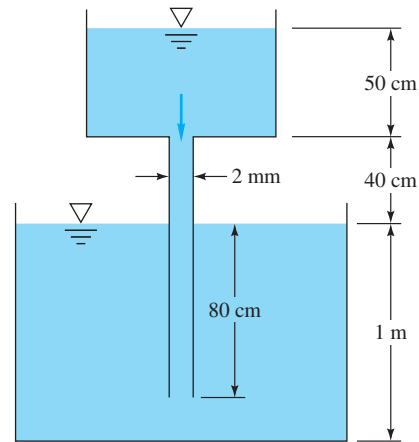
P6.26 Two oil tanks are connected by two 9-m-long pipes, as in Fig. P6.26. Pipe 1 is 5 cm in diameter and is 6 m higher than pipe 2. It is found that the flow rate in pipe 2 is twice as large as the flow in pipe 1. (*a*) What is the diameter of pipe 2? (*b*) Are both pipe flows laminar? (*c*) What is the flow rate in pipe 2 (m^3/s)? Neglect minor losses.

P6.26

P6.28
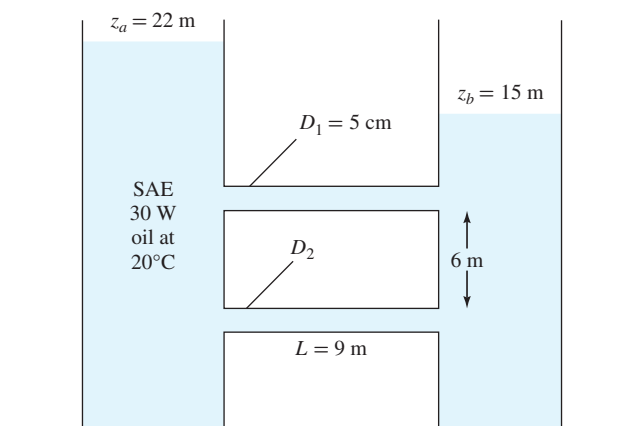
*__P6.27__ Let us attack Prob. P6.25 in symbolic fashion, using Fig. P6.27. All parameters are constant except the upper tank depth $Z(t)$. Find an expression for the flow rate $Q(t)$ as a function of $Z(t)$. Set up a differential equation, and solve for the time t_0 to drain the upper tank completely. Assume quasi-steady laminar flow.
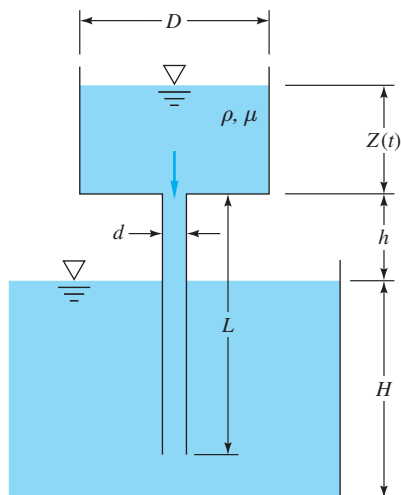
P6.27

P6.28 For straightening and smoothing an airflow in a 50-cm-diameter duct, the duct is packed with a "honeycomb" of thin straws of length 30 cm and diameter 4 mm, as in Fig. P6.28. The inlet flow is air at 110 kPa and 20°C, moving at an average velocity of 6 m/s. Estimate the pressure drop across the honeycomb.
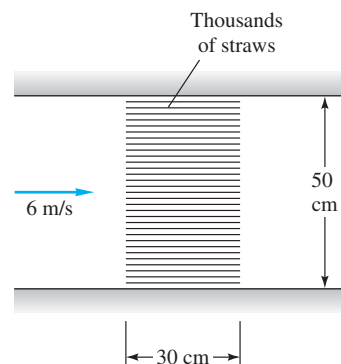
P6.29 SAE 30W oil at 20°C flows through a straight pipe 25 m long, with diameter 4 cm. The average velocity is 2 m/s. (*a*) Is the flow laminar? Calculate (*b*) the pressure drop and (*c*) the power required. (*d*) If the pipe diameter is doubled, for the same average velocity, by what percent does the required power increase?

P6.30 SAE 10 oil at 20°C flows through the 4-cm-diameter vertical pipe of Fig. P6.30. For the mercury manometer reading $h = 42$ cm shown, (*a*) calculate the volume flow rate in m^3/h and (*b*) state the direction of flow.
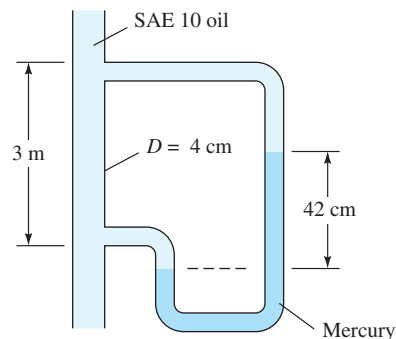
P6.30

P6.31 A *laminar flow element* (LFE) (Meriam Instrument Co.) measures low gas-flow rates with a bundle of capillary tubes or ducts packed inside a large outer tube. Consider oxygen at 20°C and 1 atm flowing at 84 ft^3/min in a 4-in-diameter pipe. (*a*) Is the flow turbulent when approaching the element? (*b*) If there are 1000 capillary tubes, $L = 4$ in, select a tube diameter to keep Re_d below 1500 and also to keep the tube pressure drop no greater than 0.5 lbf/in^2. (*c*) Do the tubes selected in part (*b*) fit nicely within the approach pipe?

P6.32 SAE 30 oil at 20°C flows in the 3-cm-diameter pipe in Fig. P6.32, which slopes at 37°. For the pressure measurements shown, determine (a) whether the flow is up or down and (b) the flow rate in m³/h.

$p_B = 180$ kPa

15 m

$p_A = 500$ kPa

37°

20 m
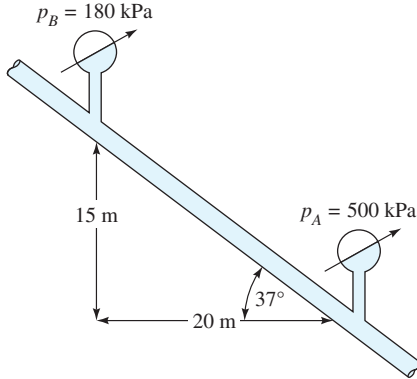
P6.32

P6.33 Water at 20°C is pumped from a reservoir through a vertical tube 10 ft long and 1/16th in in diameter. The pump provides a pressure rise of 11 lbf/in² to the flow. Neglect entrance losses. (a) Calculate the exit velocity. (b) Approximately how high will the exit water jet rise? (c) Verify that the flow is laminar.

Turbulence modeling

P6.34 Derive the time-averaged x-momentum equation (6.21) by direct substitution of Eqs. (6.19) into the momentum equation (6.14). It is convenient to write the convective acceleration as

$$\frac{du}{dt} = \frac{\partial}{\partial x}(u^2) + \frac{\partial}{\partial y}(uv) + \frac{\partial}{\partial z}(uw)$$

which is valid because of the continuity relation, Eq. (6.14).

P6.35 In the overlap layer of Fig. 6.9a, turbulent shear is large. If we neglect viscosity, we can replace Eq. (6.24) with the approximate velocity-gradient function

$$\frac{du}{dy} = fcn(y, \tau_w, \rho)$$

Show by dimensional analysis that this leads to the logarithmic overlap relation (6.28).

P6.36 The following turbulent flow velocity data $u(y)$, for air at 75°F and 1 atm near a smooth flat wall were taken in the University of Rhode Island wind tunnel:

y, in	0.025	0.035	0.047	0.055	0.065
u, ft/s	51.2	54.2	56.8	57.6	59.1

Estimate (a) the wall shear stress and (b) the velocity u at $y = 0.22$ in.

P6.37 Two infinite plates a distance h apart are parallel to the xz plane with the upper plate moving at speed V, as in Fig. P6.37. There is a fluid of viscosity μ and constant pressure between the plates. Neglecting gravity and assuming incompressible turbulent flow $u(y)$ between the plates, use the logarithmic law and appropriate boundary conditions to derive a formula for dimensionless wall shear stress versus dimensionless plate velocity. Sketch a typical shape of the profile $u(y)$.

ν

u h

y

x

Fixed
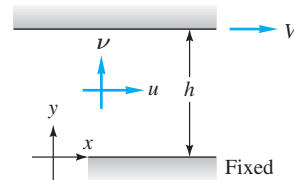
P6.37

P6.38 Suppose in Fig. P6.37 that $h = 3$ cm, the fluid in water at 20°C, and the flow is turbulent, so that the logarithmic law is valid. If the shear stress in the fluid is 15 Pa, what is V in m/s?

P6.39 By analogy with laminar shear, $\tau = \mu\, du/dy$, T. V. Boussinesq in 1877 postulated that turbulent shear could also be related to the mean velocity gradient $\tau_{turb} = \varepsilon\, du/dy$, where ε is called the *eddy viscosity* and is much larger than μ. If the logarithmic overlap law, Eq. (6.28), is valid with $\tau_{turb} \approx \tau_w$, show that $\varepsilon \approx \kappa \rho u^* y$.

P6.40 Theodore von Kármán in 1930 theorized that turbulent shear could be represented by $\tau_{turb} = \varepsilon\, du/dy$, where $\varepsilon = \rho\kappa^2 y^2 |du/dy|$ is called the *mixing-length eddy viscosity* and $\kappa \approx 0.41$ is Kármán's dimensionless *mixing-length constant* [2, 3]. Assuming that $\tau_{turb} \approx \tau_w$ near the wall, show that this expression can be integrated to yield the logarithmic overlap law, Eq. (6.28).

Turbulent pipe flow—no minor losses

P6.41 Two reservoirs, which differ in surface elevation by 40 m, are connected by 350 m of new pipe of diameter 8 cm. If the desired flow rate is at least 130 N/s of water at 20°C, can the pipe material be made of (a) galvanized iron, (b) commercial steel, or (c) cast iron? Neglect minor losses.

P6.42 Fluid flows steadily, at volume rate Q, through a large horizontal pipe and then divides into two small pipes, the larger of which has an inside diameter of 25 mm and carries three times the flow of the smaller pipe. Both small pipes have the same length and pressure drop. If all flows are turbulent, at Re$_D$ near 10^4, estimate the diameter of the smaller pipe.

P6.43 A reservoir supplies water through 100 m of 30-cm-diameter cast iron pipe to a turbine that extracts 80 hp from the flow. The water then exhausts to the atmosphere.

$z_1 = 35$ m

Water at 20°C

Cast iron pipe

$z_2 = 5$ m

P6.43   Turbine
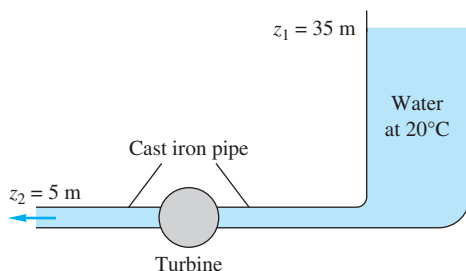
Neglect minor losses. (a) Assuming that $f \approx 0.019$, find the flow rate (which results in a cubic polynomial). Explain why there are *two* legitimate solutions. (b) For extra credit, solve for the flow rates using the actual friction factors.

P6.44 Mercury at 20°C flows through 4 m of 7-mm-diameter glass tubing at an average velocity of 5 m/s. Estimate the head loss in m and the pressure drop in kPa.

P6.45 Oil, SG = 0.88 and $\nu = 4$ E-5 m²/s, flows at 400 gal/min through a 6-in asphalted cast iron pipe. The pipe is 0.5 mi long and slopes upward at 8° in the flow direction. Compute the head loss in ft and the pressure change.

P6.46 The Keystone Pipeline in the chapter opener photo has a diameter of 36 inches and a design flow rate of 590,000 barrels per day of crude oil at 40°C. If the pipe material is new steel, estimate the pump horsepower required per mile of pipe.

P6.47 The gutter and smooth drainpipe in Fig. P6.47 remove rainwater from the roof of a building. The smooth drainpipe is 7 cm in diameter. (a) When the gutter is full, estimate the rate of draining. (b) The gutter is designed for a sudden rainstorm of up to 5 inches per hour. For this condition, what is the maximum roof area that can be drained successfully?

Water

4.2 m
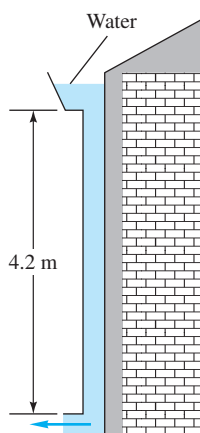
P6.47

P6.48 Follow up Prob. P6.46 with the following question. If the total Keystone pipeline length, from Alberta to Texas, is 2147 miles, how much flow, in barrels per minute, will result if the total available pumping power is 8,000 hp?

P6.49 The tank–pipe system of Fig. P6.49 is to deliver at least 11 m³/h of water at 20°C to the reservoir. What is the maximum roughness height ε allowable for the pipe?

Water at 20°C

4 m

2 m

$L = 5$ m, $d = 3$ cm
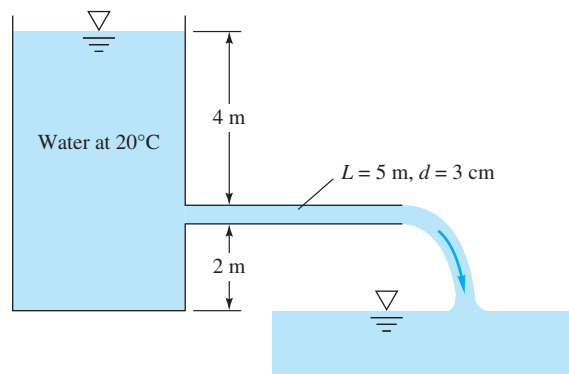
P6.49

P6.50 Ethanol at 20°C flows at 125 U.S. gal/min through a horizontal cast iron pipe with $L = 12$ m and $d = 5$ cm. Neglecting entrance effects, estimate (a) the pressure gradient dp/dx, (b) the wall shear stress τ_w, and (c) the percentage reduction in friction factor if the pipe walls are polished to a smooth surface.

P6.51 The viscous sublayer (Fig. 6.9) is normally less than 1 percent of the pipe diameter and therefore very difficult to probe with a finite-sized instrument. In an effort to generate a thick sublayer for probing, Pennsylvania State University in 1964 built a pipe with a flow of glycerin. Assume a smooth 12-in-diameter pipe with $V = 60$ ft/s and glycerin at 20°C. Compute the sublayer thickness in inches and the pumping horsepower required at 75 percent efficiency if $L = 40$ ft.

P6.52 The pipe flow in Fig. P6.52 is driven by pressurized air in the tank. What gage pressure p_1 is needed to provide a 20°C water flow rate $Q = 60$ m³/h?

30 m

Smooth pipe: $d = 5$ cm

Q Open jet

p_1

10 m

80 m

P6.52   60 m
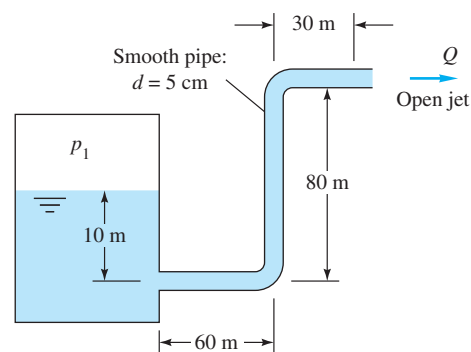
P6.53   Water at 20°C flows by gravity through a smooth pipe from one reservoir to a lower one. The elevation difference is 60 m. The pipe is 360 m long, with a diameter of 12 cm. Calculate the expected flow rate in m^3/h. Neglect minor losses.

***P6.54**   A swimming pool W by Y by h deep is to be emptied by gravity through the long pipe shown in Fig. P6.54. Assuming an average pipe friction factor f_{av} and neglecting minor losses, derive a formula for the time to empty the tank from an initial level h_o.
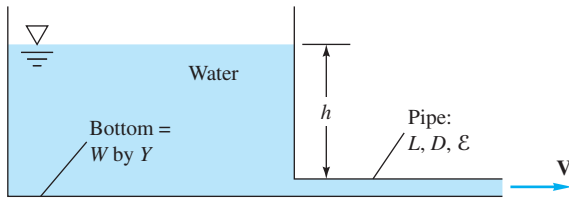
P6.54

P6.55   The reservoirs in Fig. P6.55 contain water at 20°C. If the pipe is smooth with $L = 4500$ m and $d = 4$ cm, what will the flow rate in m^3/h be for $\Delta z = 100$ m?
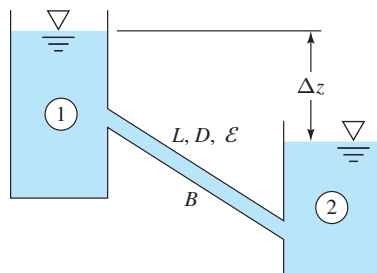
P6.55

P6.56   The Alaska Pipeline in the chapter opener photo has a design flow rate of 4.4 E7 gallons per day of crude oil at 60°C (see Fig. A.1). (a) Assuming a galvanized-iron wall, estimate the total pressure drop required for the 800-mile trip. (b) If there are nine equally spaced pumps, estimate the horsepower each pump must deliver.

P6.57   Apply the analysis of Prob. P6.54 to the following data. Let $W = 5$ m, $Y = 8$ m, $h_o = 2$ m, $L = 15$ m, $D = 5$ cm, and $\varepsilon = 0$. (a) By letting $h = 1.5$ m and 0.5 m as representative depths, estimate the average friction factor. Then (b) estimate the time to drain the pool.

P6.58   For the system in Prob. 6.53, a pump is used at night to drive water back to the upper reservoir. If the pump delivers 15,000 W to the water, estimate the flow rate.

P6.59   The following data were obtained for flow of 20°C water at 20 m^3/h through a badly corroded 5-cm-diameter pipe that slopes downward at an angle of 8°: $p_1 = 420$ kPa, $z_1 = 12$ m, $p_2 = 250$ kPa, $z_2 = 3$ m. Estimate (a) the roughness ratio of the pipe and (b) the percentage change in head loss if the pipe were smooth and the flow rate the same.

P6.60   In the spirit of Haaland's explicit pipe friction factor approximation, Eq. (6.49), Jeppson [20] proposed the following explicit formula:

$$\frac{1}{\sqrt{f}} \approx -2.0 \log_{10}\left(\frac{\varepsilon/d}{3.7} + \frac{5.74}{Re_d^{0.9}}\right)$$

(a) Is this identical to Haaland's formula with just a simple rearrangement? Explain. (b) Compare Jeppson's formula to Haaland's for a few representative values of (turbulent) Re_d and ε/d and their errors compared to the Colebrook formula (6.48). Discuss briefly.

P6.61   What level h must be maintained in Fig. P6.61 to deliver a flow rate of 0.015 ft^3/s through the $\frac{1}{2}$-in commercial steel pipe?
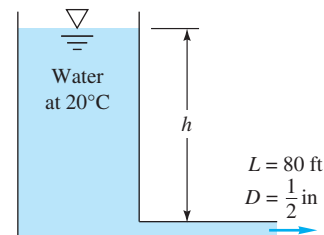
P6.61

P6.62   Water at 20°C is to be pumped through 2000 ft of pipe from reservoir 1 to 2 at a rate of 3 ft^3/s, as shown in Fig. P6.62. If the pipe is cast iron of diameter 6 in and the pump is 75 percent efficient, what horsepower pump is needed?
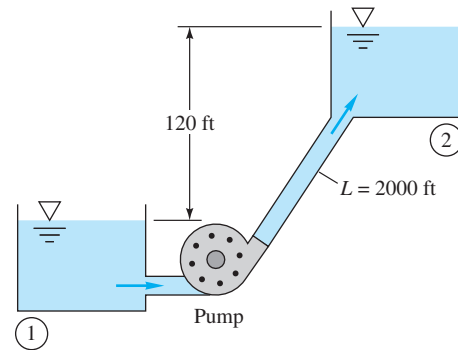
P6.62

Flow rate and sizing problems

P6.63   A tank contains 1 m^3 of water at 20°C and has a drawn-capillary outlet tube at the bottom, as in Fig. P6.63. Find the outlet volume flux Q in m^3/h at this instant.

P6.64   For the system in Fig. P6.63, solve for the flow rate in m^3/h if the fluid is SAE 10 oil at 20°C. Is the flow laminar or turbulent?

P6.63

$L = 80$ cm
$D = 4$ cm

Q

1 m
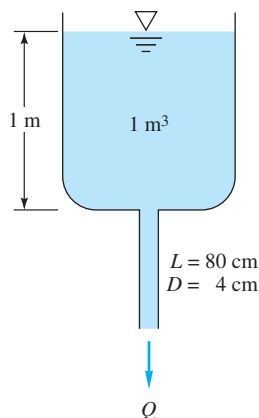
1 m³

P6.65 In Prob. P6.63 the initial flow is turbulent. As the water drains out of the tank, will the flow revert to laminar motion as the tank becomes nearly empty? If so, at what tank depth? Estimate the time, in h, to drain the tank completely.

P6.66 Ethyl alcohol at 20°C flows through a 10-cm horizontal drawn tube 100 m long. The fully developed wall shear stress is 14 Pa. Estimate (a) the pressure drop, (b) the volume flow rate, and (c) the velocity u at $r = 1$ cm.

P6.67 A straight 10-cm commercial-steel pipe is 1 km long and is laid on a constant slope of 5°. Water at 20°C flows downward, due to gravity only. Estimate the flow rate in m³/h. What happens if the pipe length is 2 km?

*P6.68 The Moody chart cannot find V directly, since V appears in both ordinate and abscissa. (a) Arrange the variables (h_f, d, g, L, ν) into a single dimensionless group, with $h_f d^3$ in the numerator, denoted as ξ, which equals ($f \text{Re}_d^2/2$). (b) Rearrange the Colebrook formula (6.48) to solve for Re_d in terms of ξ. (c) For extra credit, solve Example 6.9 with this new formula.

P6.69 For Prob. P6.62 suppose the only pump available can deliver 80 hp to the fluid. What is the proper pipe size in inches to maintain the 3 ft³/s flow rate?

P6.70 Ethylene glycol at 20°C flows through 80 m of cast iron pipe of diameter 6 cm. The measured pressure drop is 250 kPa. Neglect minor losses. Using a noniterative formulation, estimate the flow rate in m³/h.

*P6.71 It is desired to solve Prob. 6.62 for the most economical pump and cast iron pipe system. If the pump costs $125 per horsepower delivered to the fluid and the pipe costs $7000 per inch of diameter, what are the minimum cost and the pipe and pump size to maintain the 3 ft³/s flow rate? Make some simplifying assumptions.

P6.72 Modify Prob. P6.57 by letting the diameter be unknown. Find the proper pipe diameter for which the pool will drain in about two hours flat.

P6.73 For 20°C water flow in a smooth, horizontal 10-cm pipe, with $\Delta p/L = 1000$ Pa/m, the writer computed a flow rate of 0.030 m³/s. (a) Verify, or disprove, the writer's answer. (b) If verified, use the power-law friction factor relation, Eq. (6.41), to estimate the pipe diameter that will triple this flow rate. (c) For extra credit, use the more exact friction factor relation, Eq. (6.38), to solve part (b).

P6.74 Two reservoirs, which differ in surface elevation by 40 m, are connected by a new commercial steel pipe of diameter 8 cm. If the desired flow rate is 200 N/s of water at 20°C, what is the proper length of the pipe?

P6.75 You wish to water your garden with 100 ft of $\frac{5}{8}$-in-diameter hose whose roughness is 0.011 in. What will be the delivery, in ft³/s, if the gage pressure at the faucet is 60 lbf/in²? If there is no nozzle (just an open hose exit), what is the maximum horizontal distance the exit jet will carry?

P6.76 The small turbine in Fig. P6.76 extracts 400 W of power from the water flow. Both pipes are wrought iron. Compute the flow rate Q in m³/h. Why are there two solutions? Which is better?

Water
20°C

20 m

Turbine

Q

10 m
$D = 6$ cm

30 m
$D = 4$ cm
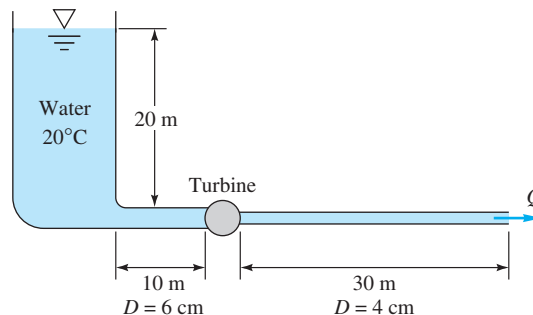
P6.76

*P6.77 Modify Prob. P6.76 into an economic analysis, as follows: Let the 40 m of wrought iron pipe have a uniform diameter d. Let the steady water flow available be $Q = 30$ m³/h. The cost of the turbine is $4 per watt developed, and the cost of the piping is $75 per centimeter of diameter. The power generated may be sold for $0.08 per kilowatt-hour. Find the proper pipe diameter for minimum *payback time*—that is, the minimum time for which the power sales will equal the initial cost of the system.

P6.78 In Fig. P6.78 the connecting pipe is commercial steel 6 cm in diameter. Estimate the flow rate, in m³/h, if the fluid is water at 20°C. Which way is the flow?

P6.79 A garden hose is to be used as the return line in a waterfall display at a mall. In order to select the proper pump, you need to know the roughness height inside the garden hose. Unfortunately, roughness information is not supplied by the hose manufacturer. So you devise a simple experiment

to measure the roughness. The hose is attached to the drain of an above-ground swimming pool, the surface of which is 3.0 m above the hose outlet. You estimate the minor loss coefficient of the entrance region as 0.5, and the drain valve has a minor loss equivalent length of 200 diameters when fully open. Using a bucket and stopwatch, you open the valve and measure the flow rate to be 2.0×10^{-4} m³/s for a hose that is 10.0 m long and has an inside diameter of 1.50 cm. Estimate the roughness height in mm inside the hose.
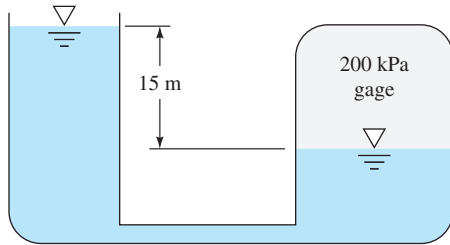
P6.78 $L = 50$ m

P6.80 The head-versus-flow-rate characteristics of a centrifugal pump are shown in Fig. P6.80. If this pump drives water at 20°C through 120 m of 30-cm-diameter cast iron pipe, what will be the resulting flow rate, in m³/s?

P6.80 0   Q   2m³/s
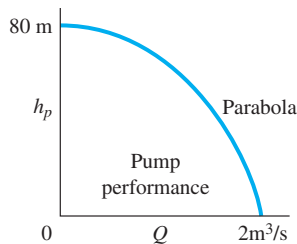
P6.81 The pump in Fig. P6.80 is used to deliver gasoline at 20°C through 350 m of 30-cm-diameter galvanized iron pipe. Estimate the resulting flow rate, in m³/s. (Note that the pump head is now in meters of gasoline.)

P6.82 Fluid at 20°C flows through a horizontal galvanized-iron pipe 20 m long and 8 cm in diameter. The wall shear stress is 90 Pa. Calculate the flow rate in m³/h if the fluid is (a) glycerin and (b) water.

P6.83 For the system of Fig. P6.55, let $\Delta z = 80$ m and $L = 185$ m of cast iron pipe. What is the pipe diameter for which the flow rate will be 7 m³/h?

P6.84 It is desired to deliver 60 m³/h of water at 20°C through a horizontal asphalted cast iron pipe. Estimate the pipe diameter that will cause the pressure drop to be exactly 40 kPa per 100 m of pipe length.

P6.85 For the system in Prob. P6.53, a pump, which delivers 15,000 W to the water, is used at night to refill the upper reservoir. The pipe diameter is increased from 12 cm to provide more flow. If the resultant flow rate is 90 m³/h, estimate the new pipe size.

Noncircular ducts

P6.86 SAE 10 oil at 20°C flows at an average velocity of 2 m/s between two smooth parallel horizontal plates 3 cm apart. Estimate (a) the centerline velocity, (b) the head loss per meter, and (c) the pressure drop per meter.

P6.87 A commercial steel annulus 40 ft long, with $a = 1$ in and $b = \frac{1}{2}$ in, connects two reservoirs that differ in surface height by 20 ft. Compute the flow rate in ft³/s through the annulus if the fluid is water at 20°C.

P6.88 An oil cooler consists of multiple parallel-plate passages, as shown in Fig. P6.88. The available pressure drop is 6 kPa, and the fluid is SAE 10W oil at 20°C. If the desired total flow rate is 900 m³/h, estimate the appropriate number of passages. The plate walls are hydraulically smooth.
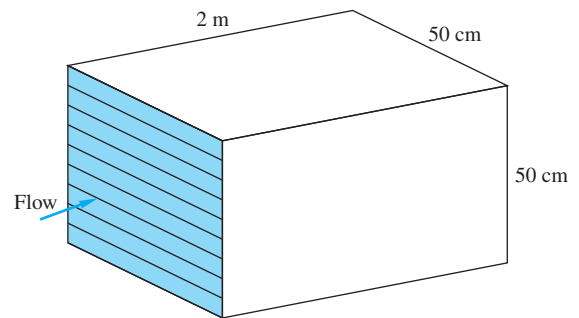
P6.88

P6.89 An annulus of narrow clearance causes a very large pressure drop and is useful as an accurate measurement of viscosity. If a smooth annulus 1 m long with $a = 50$ mm and $b = 49$ mm carries an oil flow at 0.001 m³/s, what is the oil viscosity if the pressure drop is 250 kPa?

P6.90 A rectangular sheet-metal duct is 200 ft long and has a fixed height $H = 6$ in. The width B, however, may vary from 6 to 36 in. A blower provides a pressure drop of 80 Pa of air at 20°C and 1 atm. What is the optimum width B that will provide the most airflow in ft³/s?

P6.91 Heat exchangers often consist of many triangular passages. Typical is Fig. P6.91, with $L = 60$ cm and an isosceles-triangle cross section of side length $a = 2$ cm and included angle $\beta = 80°$. If the average velocity is $V = 2$ m/s and the fluid is SAE 10 oil at 20°C, estimate the pressure drop.
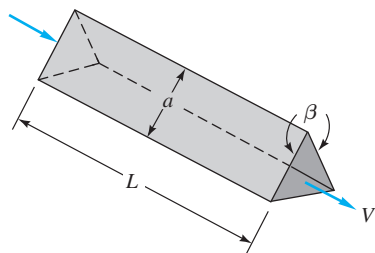
P6.91

P6.92 A large room uses a fan to draw in atmospheric air at 20°C through a 30-cm by 30-cm commercial-steel duct 12 m long, as in Fig. P6.92. Estimate (a) the airflow rate in m^3/h if the room pressure is 10 Pa vacuum and (b) the room pressure if the flow rate is 1200 m^3/h. Neglect minor losses.

30 cm by 30 cm

Room

Fan

p_{atm}

12 m
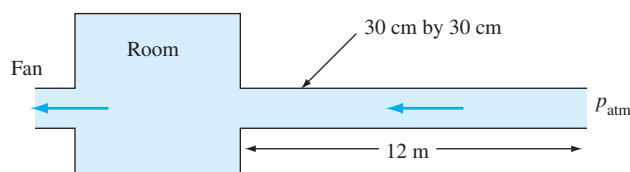
P6.92

P6.93 In Moody's Example 6.6, the 6-inch diameter, 200-ft-long asphalted cast iron pipe has a pressure drop of about 280 lbf/ft^2 when the average water velocity is 6 ft/s. Compare this to an *annular* cast iron pipe with an inner diameter of 6 in and the same annular average velocity of 6 ft/s. (a) What outer diameter would cause the flow to have the same pressure drop of 280 lbf/ft^2? (b) How do the cross-section areas compare, and why? Use the hydraulic diameter approximation.

P6.94 Air at 20°C flows through a smooth duct of diameter 20 cm at an average velocity of 5 m/s. It then flows into a smooth square duct of side length a. Find the square duct size a for which the pressure drop per meter will be exactly the same as the circular duct.

P6.95 Although analytical solutions are available for laminar flow in many duct shapes [34], what do we do about ducts of arbitrary shape? Bahrami et al. [57] propose that a better approach to the pipe result, $f\mathrm{Re} = 64$, is achieved by replacing the hydraulic diameter D_h with $\sqrt{A}$, where A is the area of the cross section. Test this idea for the isosceles triangles of Table 6.4. If time is short, at least try 10°, 50°, and 80°. What do you conclude about this idea?

P6.96 A fuel cell [59] consists of air (or oxygen) and hydrogen micro ducts, separated by a membrane that promotes proton exchange for an electric current, as in Fig. P6.96. Suppose that the air side, at 20°C and approximately 1 atm, has five 1 mm by 1 mm ducts, each 1 m long. The total flow

rate is 1.5 E-4 kg/s. (a) Determine if the flow is laminar or turbulent. (b) Estimate the pressure drop. *(Problem courtesy of Dr. Pezhman Shirvanian.)*

Hydrogen
flow

Air
flow

1 mm by 1 mm by 1m

Anode   Cathode

P6.96   PEM membrane
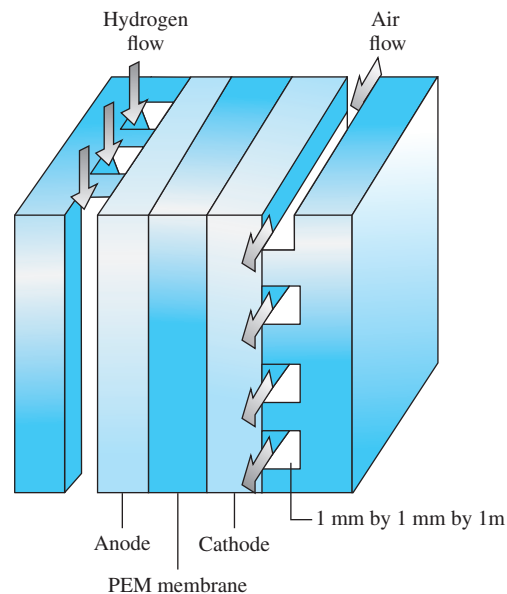
P6.97 A heat exchanger consists of multiple parallel-plate passages, as shown in Fig. P6.97. The available pressure drop is 2 kPa, and the fluid is water at 20°C. If the desired total flow rate is 900 m^3/h, estimate the appropriate number of passages. The plate walls are hydraulically smooth.

2 m

50 cm

50 cm
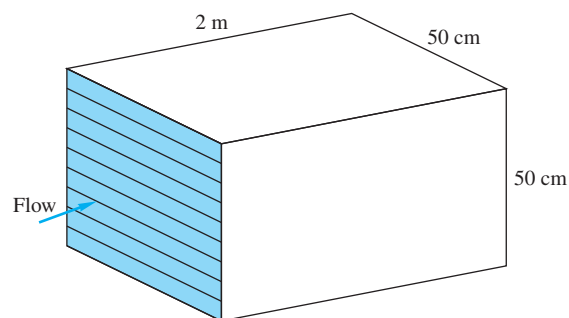
Flow

P6.97

P6.98 A rectangular heat exchanger is to be divided into smaller sections using sheets of commercial steel 0.4 mm thick, as sketched in Fig. P6.98. The flow rate is 20 kg/s of water at 20°C. Basic dimensions are $L = 1$ m, $W = 20$ cm, and $H = 10$ cm. What is the proper number of *square* sections if the overall pressure drop is to be no more than 1600 Pa?
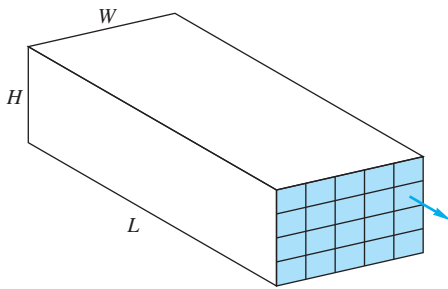
P6.98

Minor or local losses

P6.99 In Sec. 6.11 it was mentioned that Roman aqueduct customers obtained extra water by attaching a diffuser to their pipe exits. Fig. P6.99 shows a simulation: a smooth inlet pipe, with or without a 15° conical diffuser expanding to a 5-cm-diameter exit. The pipe entrance is sharp-edged. Calculate the flow rate (a) without and (b) with the diffuser.
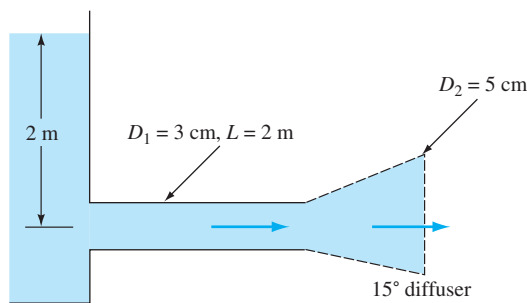

P6.99

*P6.100 Modify Prob. P6.55 as follows: Assume a pump can deliver 3 kW to pump the water back up to reservoir 1 from reservoir 2. Accounting for an open flanged globe valve and sharp-edged entrance and exit, estimate the predicted flow rate, in m^3/h.

P6.101 In Fig. P6.101 a thick filter is being tested for losses. The flow rate in the pipe is 7 m^3/min, and the upstream pressure is 120 kPa. The fluid is air at 20°C. Using the water manometer reading, estimate the loss coefficient K of the filter.
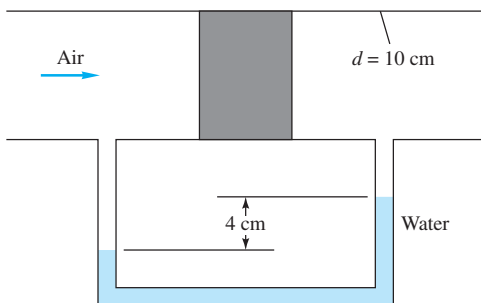
P6.101

*P6.102 A 70 percent efficient pump delivers water at 20°C from one reservoir to another 20 ft higher, as in Fig. P6.102. The piping system consists of 60 ft of galvanized iron 2-in pipe, a reentrant entrance, two screwed 90° long-radius elbows, a screwed-open gate valve, and a sharp exit. What is the input power required in horsepower with and without a 6° well-designed conical expansion added to the exit? The flow rate is 0.4 ft^3/s.
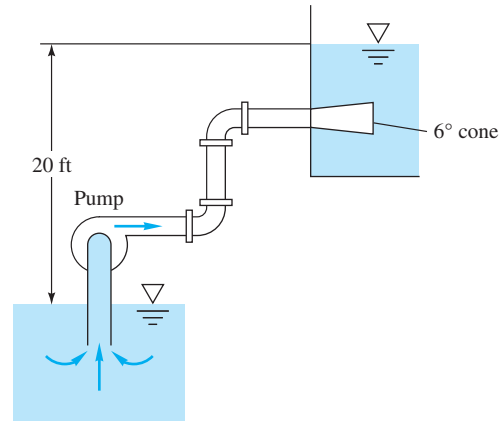
P6.102

P6.103 The reservoirs in Fig. P6.103 are connected by cast iron pipes joined abruptly, with sharp-edged entrance and exit. Including minor losses, estimate the flow of water at 20°C if the surface of reservoir 1 is 45 ft higher than that of reservoir 2.
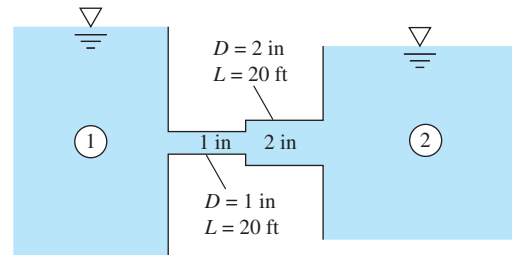
P6.103

P6.104 Consider a 20°C flow at 2 m/s through a smooth 3-mm diameter microtube which consists of a straight run of 10 cm, a long radius bend, and another straight run of 10 cm. Compute the total pressure drop if the fluid is (a) water; and (b) ethylene glycol.

P6.105 The system in Fig. P6.105 consists of 1200 m of 5 cm cast iron pipe, two 45° and four 90° flanged long-radius elbows, a fully open flanged globe valve, and a sharp exit into a reservoir. If the elevation at point 1 is 400 m, what gage pressure is required at point 1 to deliver 0.005 m^3/s of water at 20°C into the reservoir?
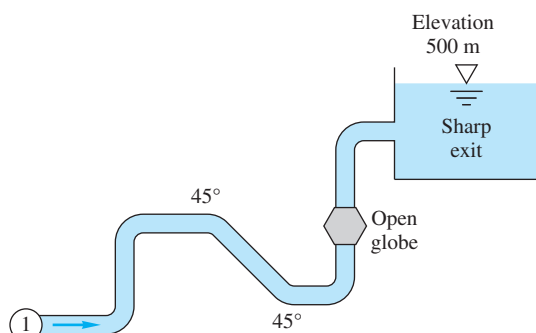
P6.105

P6.106 The water pipe in Fig. P6.106 slopes upward at 30°. The pipe has a 1-in diameter and is smooth. The flanged globe valve is fully open. If the mercury manometer shows a 7-in deflection, what is the flow rate in ft³/s?
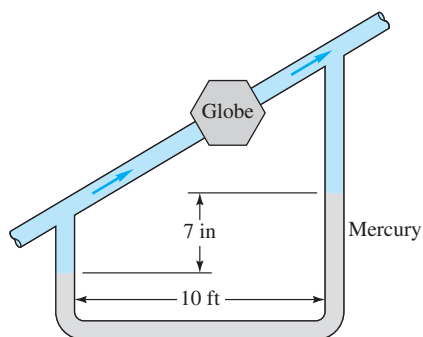

P6.106

*P6.107 A tank of water 4 m in diameter and 7 m deep is to be drained by a 5-cm-diameter exit pipe at the bottom, as in Fig. P6.107. In design (1), the pipe extends out for 1 m and into the tank for 10 cm. In design (2), the interior pipe is removed and the entrance beveled, Fig. 6.21, so that $K \approx 0.1$ in the entrance. (a) An engineer claims that design (2) will drain 25 percent faster than design (1). Is this claim true? (b) Estimate the time to drain of design (2), assuming $f \approx 0.020$.
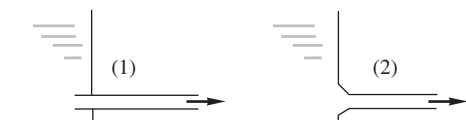
P6.107

P6.108 The water pump in Fig. P6.108 maintains a pressure of 6.5 psig at point 1. There is a filter, a half-open disk valve, and two regular screwed elbows. There are 80 ft of 4-in diameter commercial steel pipe. (a) If the flow rate is 0.4 ft³/s, what is the loss coefficient of the filter? (b) If the disk valve is wide open and $K_{filter} = 7$, what is the resulting flow rate?
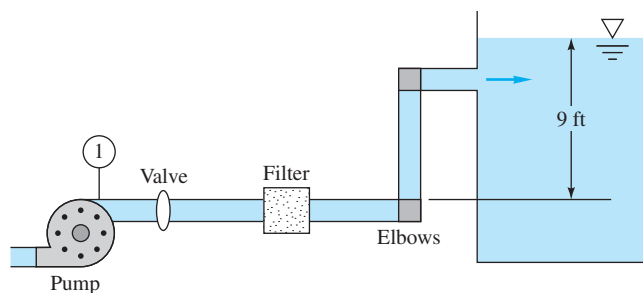
P6.108

P6.109 In Fig. P6.109 there are 125 ft of 2-in pipe, 75 ft of 6-in pipe, and 150 ft of 3-in pipe, all cast iron. There are three 90° elbows and an open globe valve, all flanged. If the exit elevation is zero, what horsepower is extracted by the turbine when the flow rate is 0.16 ft³/s of water at 20°C?
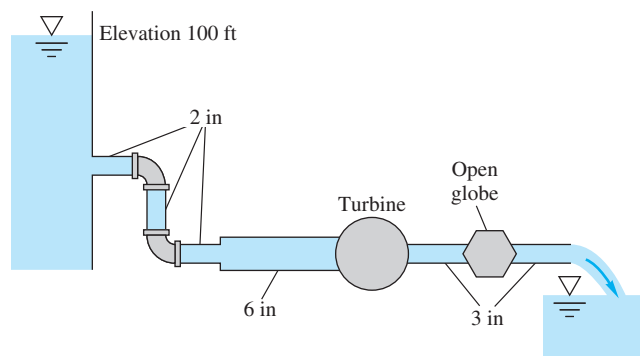
P6.109

P6.110 In Fig. P6.110 the pipe entrance is sharp-edged. If the flow rate is 0.004 m³/s, what power, in W, is extracted by the turbine?
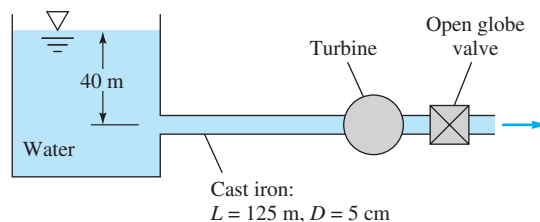
P6.110

Series and parallel pipe systems

**P6.111** For the parallel-pipe system of Fig. P6.111, each pipe is cast iron, and the pressure drop $p_1 - p_2 = 3$ lbf/in². Compute the total flow rate between 1 and 2 if the fluid is SAE 10 oil at 20°C.
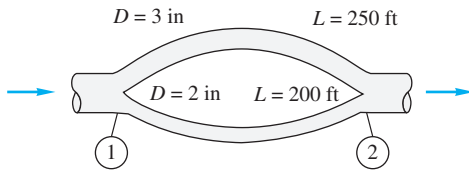
P6.111

P6.112 If the two pipes in Fig. P6.111 are instead laid in series
with the same total pressure drop of 3 lbf/in², what will the
flow rate be? The fluid is SAE 10 oil at 20°C.

P6.113 The parallel galvanized iron pipe system of Fig. P6.113
delivers water at 20°C with a total flow rate of 0.036 m³/s.
If the pump is wide open and not running, with a loss coef-
ficient $K = 1.5$, determine (a) the flow rate in each pipe and
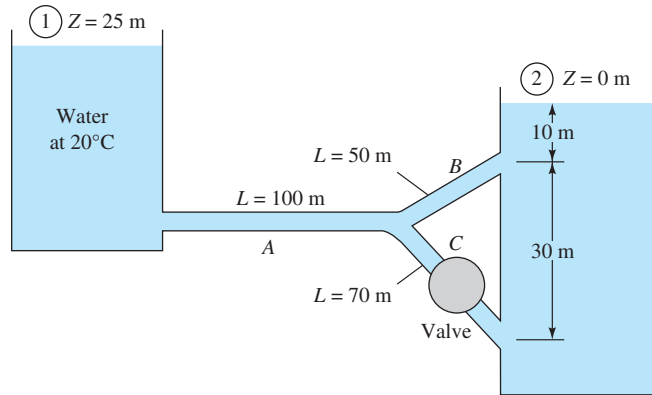(b) the overall pressure drop.
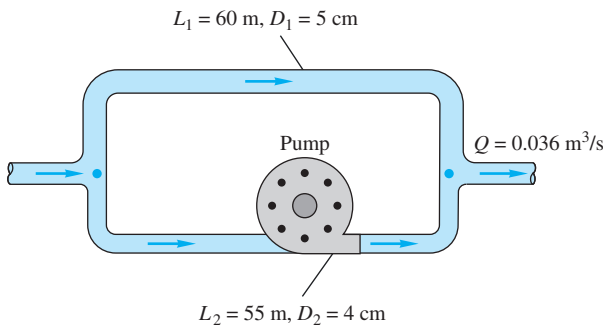
P6.113

*P6.114 A blower supplies standard air to a plenum that feeds two
horizontal square sheet-metal ducts with sharp-edged en-
trances. One duct is 100 ft long, with a cross-section 6 in by
6 in. The second duct is 200 ft long. Each duct exhausts to
the atmosphere. When the plenum pressure is 5.0 lbf/ft²
(gage) the volume flow in the longer duct is three times the
flow in the shorter duct. Estimate both volume flows and
the cross-section size of the longer duct.

P6.115 In Fig. P6.115 all pipes are 8-cm-diameter cast iron. Deter-
mine the flow rate from reservoir 1 if valve C is (a) closed
and (b) open, $K = 0.5$.

P6.116 For the series-parallel system of Fig. P6.116, all pipes are
8-cm-diameter asphalted cast iron. If the total pressure
drop $p_1 - p_2 = 750$ kPa, find the resulting flow rate Q m³/h
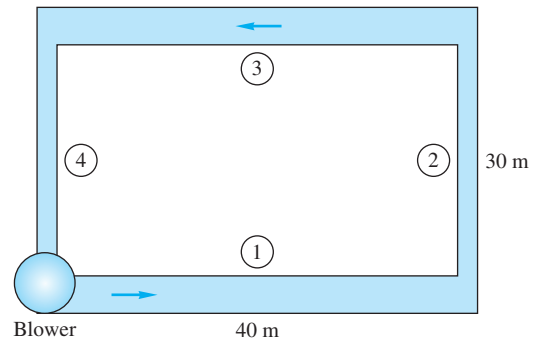for water at 20°C. Neglect minor losses.

P6.117 A blower delivers air at 3000 m³/h to the duct circuit in
Fig. P6.117. Each duct is commercial steel and of square
cross section, with side lengths $a_1 = a_3 = 20$ cm and
$a_2 = a_4 = 12$ cm. Assuming sea-level air conditions, esti-
mate the power required if the blower has an efficiency of
75 percent. Neglect minor losses.

P6.115
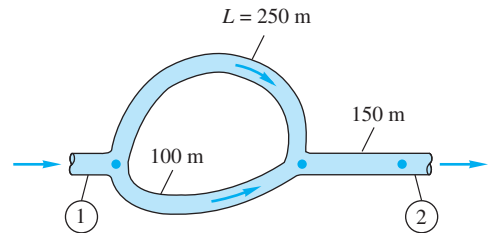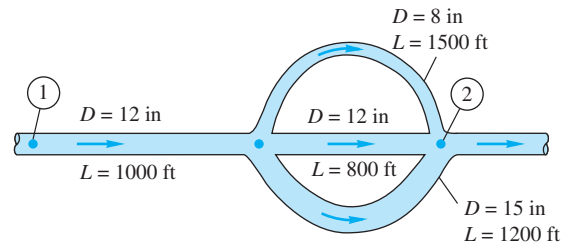

P6.116

P6.117

P6.118 For the piping system of Fig. P6.118, all pipes are concrete
with a roughness of 0.04 in. Neglecting minor losses, com-
pute the overall pressure drop $p_1 - p_2$ in lbf/in² if
$Q = 20$ ft³/s. The fluid is water at 20°C.

P6.118

P6.119 For the piping system of Prob. P6.111, let the fluid be gasoline at 20°C, with both pipes cast iron. If the flow rate in the 2-in pipe (*b*) is 1.2 ft³/min, estimate the flow rate in the 3-in pipe (*a*), in ft³/min.

P6.120 Three cast iron pipes are laid in parallel with these dimensions:

Pipe	Length, m	Diameter, cm
1	800	12
2	600	8
3	900	10

The total flow rate is 200 m³/h of water at 20°C. Determine (*a*) the flow rate in each pipe and (*b*) the pressure drop across the system.

Three-reservoir and pipe network systems

P6.121 Consider the three-reservoir system of Fig. P6.121 with the following data:

$$L_1 = 95\text{m} \quad L_2 = 125 \text{ m} \quad L_3 = 160 \text{ m}$$

$$z_1 = 25 \text{ m} \quad z_2 = 115 \text{ m} \quad z_3 = 85 \text{ m}$$

All pipes are 28-cm-diameter unfinished concrete ($\varepsilon = 1$ mm). Compute the steady flow rate in all pipes for water at 20°C.
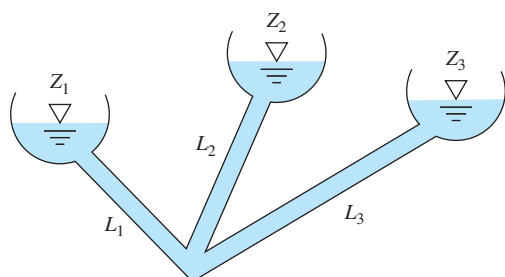
P6.121

P6.122 Modify Prob. P6.121 as follows: Reduce the diameter to 15 cm (with $\varepsilon = 1$ mm), and compute the flow rates for water at 20°C. These flow rates distribute in nearly the same manner as in Prob. P6.121 but are about 5.2 times lower. Can you explain this difference?

P6.123 Modify Prob. P6.121 as follows: All data are the same except that z_3 is unknown. Find the value of z_3 for which the flow rate in pipe 3 is 0.2 m³/s toward the junction. (This problem requires iteration and is best suited to a computer.)

P6.124 The three-reservoir system in Fig. P6.124 delivers water at 20°C. The system data are as follows:

$$D_1 = 8 \text{ in} \quad D_2 = 6 \text{ in} \quad D_3 = 9 \text{ in}$$

$$L_1 = 1800 \text{ ft} \quad L_2 = 1200 \text{ ft} \quad L_3 = 1600 \text{ ft}$$

All pipes are galvanized iron. Compute the flow rate in all pipes.
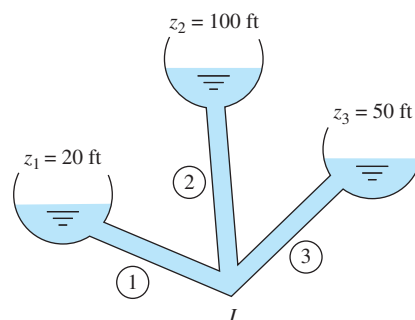
P6.124

P6.125 Suppose that the three cast iron pipes in Prob. P6.120 are instead connected to meet smoothly at a point *B*, as shown in Fig. P6.125. The inlet pressures in each pipe are

$$p_1 = 200 \text{ kPa} \quad p_2 = 160 \text{ kPa} \quad p_3 = 100 \text{ kPa.}$$

The fluid is water at 20°C. Neglect minor losses. Estimate the flow rate in each pipe and whether it is toward or away from point *B*.
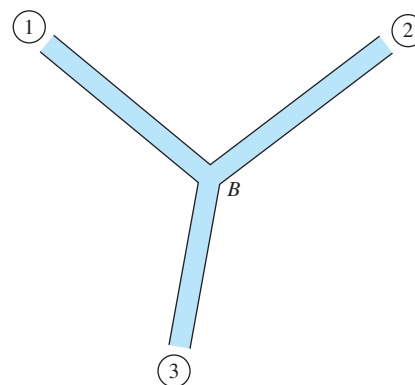

P6.125

P6.126 Modify Prob. P6.124 as follows: Let all data be the same except that pipe 1 is fitted with a butterfly valve (Fig. 6.19*b*). Estimate the proper valve opening angle (in degrees) for the flow rate through pipe 1 to be reduced to 1.5 ft³/s toward reservoir 1. (This problem requires iteration and is best suited to a computer.)

P6.127 In the five-pipe horizontal network of Fig. P6.127, assume that all pipes have a friction factor $f = 0.025$. For the given inlet and exit flow rate of 2 ft³/s of water at

20°C, determine the flow rate and direction in all pipes. If p_A = 120 lbf/in^2 gage, determine the pressures at points B, C, and D.
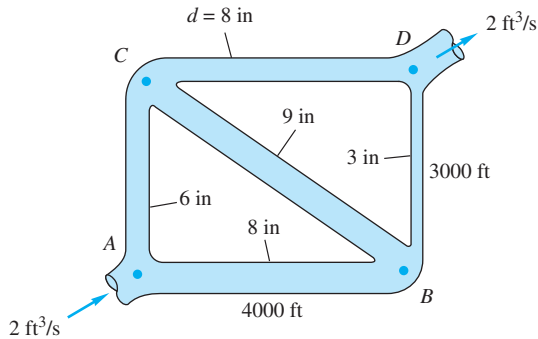

P6.127

P6.128 Modify Prob. P6.127 as follows: Let the inlet flow rate at A and the exit flow at D be unknown. Let $p_A - p_B$ = 100 lbf/in^2. Compute the flow rate in all five pipes.

P6.129 In Fig. P6.129 all four horizontal cast iron pipes are 45 m long and 8 cm in diameter and meet at junction a, delivering water at 20°C. The pressures are known at four points as shown:

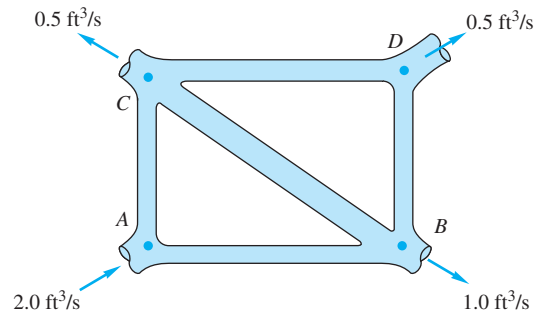$$p_1 = 950 \text{ kPa} \quad p_2 = 350 \text{ kPa}$$

$$p_3 = 675 \text{ kPa} \quad p_4 = 100 \text{ kPa}$$

Neglecting minor losses, determine the flow rate in each pipe.
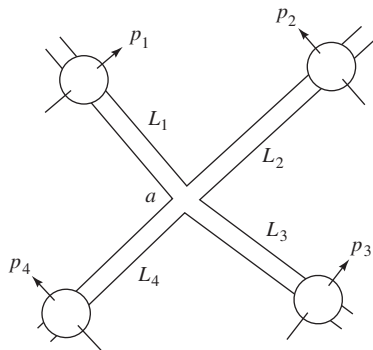
P6.129

P6.130 In Fig. P6.130 lengths AB and BD are 2000 and 1500 ft, respectively. The friction factor is 0.022 everywhere, and p_A = 90 lbf/in^2 gage. All pipes have a diameter of 6 in. For water at 20°C, determine the flow rate in all pipes and the pressures at points B, C, and D.

P6.130

Diffuser performance

P6.131 A water tunnel test section has a 1-m diameter and flow properties V = 20 m/s, p = 100 kPa, and T = 20°C. The boundary layer blockage at the end of the section is 9 percent. If a conical diffuser is to be added at the end of the section to achieve maximum pressure recovery, what should its angle, length, exit diameter, and exit pressure be?

P6.132 For Prob. P6.131 suppose we are limited by space to a total diffuser length of 10 m. What should the diffuser angle, exit diameter, and exit pressure be for maximum recovery?

P6.133 A wind tunnel test section is 3 ft square with flow properties V = 150 ft/s, p = 15 lbf/in^2 absolute, and T = 68°F. Boundary layer blockage at the end of the test section is 8 percent. Find the angle, length, exit height, and exit pressure of a flat-walled diffuser added onto the section to achieve maximum pressure recovery.

P6.134 For Prob. P6.133 suppose we are limited by space to a total diffuser length of 30 ft. What should the diffuser angle, exit height, and exit pressure be for maximum recovery?

The pitot-static tube

P6.135 An airplane uses a pitot-static tube as a velocimeter. The measurements, with their uncertainties, are a static temperature of (-11 ± 3)°C, a static pressure of 60 ± 2 kPa, and a pressure difference $(p_o - p_s)$ = 3200 ± 60 Pa. (a) Estimate the airplane's velocity and its uncertainty. (b) Is a compressibility correction needed?

P6.136 For the pitot-static pressure arrangement of Fig. P6.136, the manometer fluid is (colored) water at 20°C. Estimate (a) the centerline velocity, (b) the pipe volume flow, and (c) the (smooth) wall shear stress.

P6.137 For the 20°C water flow of Fig. P6.137, use the pitot-static arrangement to estimate (a) the centerline velocity and (b) the volume flow in the 5-in-diameter smooth pipe. (c) What error in flow rate is caused by neglecting the 1-ft elevation difference?

P6.136

**P6.137**   Mercury
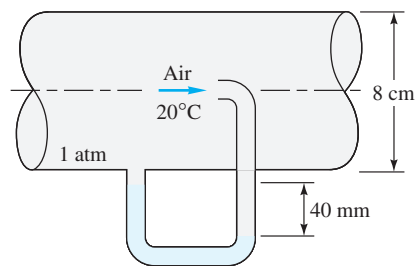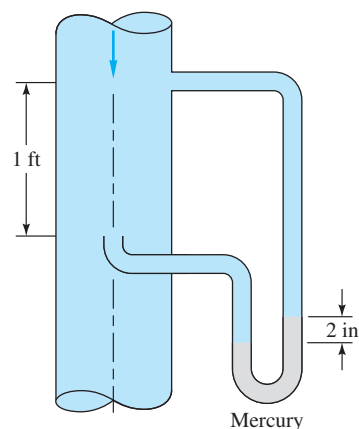
P6.138 An engineer who took college fluid mechanics on a pass–fail basis has placed the static pressure hole far upstream of the stagnation probe, as in Fig. P6.138, thus contaminating the pitot measurement ridiculously with pipe friction losses. If the pipe flow is air at 20°C and 1 atm and the manometer fluid is Meriam red oil (SG = 0.827), estimate the air centerline velocity for the given manometer reading of 16 cm. Assume a smooth-walled tube.
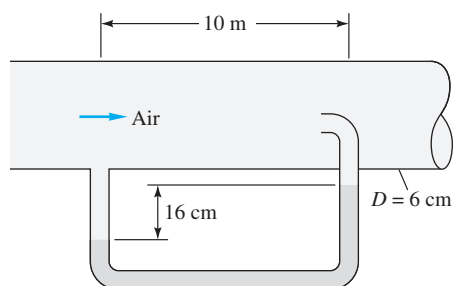
P6.138

P6.139 Professor Walter Tunnel needs to measure the flow velocity in a water tunnel. Due to budgetary restrictions, he cannot

afford a pitot-static probe, but instead inserts a total head probe and a static pressure probe, as shown in Fig. P6.139, a distance h_1 apart from each other. Both probes are in the main free stream of the water tunnel, unaffected by the thin boundary layers on the sidewalls. The two probes are connected as shown to a U-tube manometer. The densities and vertical distances are shown in Fig. P6.139. (*a*) Write an expression for velocity V in terms of the parameters in the problem. (*b*) Is it critical that distance h_1 be measured accurately? (*c*) How does the expression for velocity V differ from that which would be obtained if a pitot-static probe had been available and used with the same U-tube manometer?
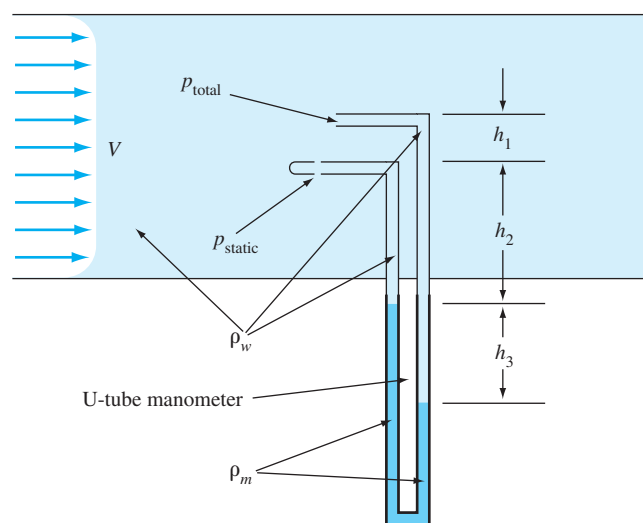

P6.139

Flowmeters: the orifice plate

P6.140 Gasoline at 20°C flows at 3 m³/h in a 6-cm-diameter pipe. A 4-cm-diameter thin-plate orifice with corner taps is installed. Estimate the measured pressure drop, in Pa.

P6.141 Gasoline at 20°C flows at 105 m³/h in a 10-cm-diameter pipe. We wish to meter the flow with a thin-plate orifice and a differential pressure transducer that reads best at about 55 kPa. What is the proper β ratio for the orifice?

P6.142 The shower head in Fig. P6.142 delivers water at 50°C. An orifice-type flow reducer is to be installed. The upstream pressure is constant at 400 kPa. What flow rate, in gal/min, results without the reducer? What reducer orifice diameter would decrease the flow by 40 percent?

$D = 1.5$ cm

$p = 400$ kPa

Flow reducer

45 holes, 1.5-mm diameter
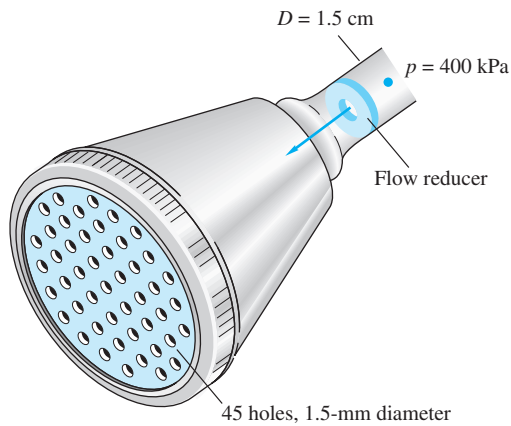
P6.142

P6.143 A 10-cm-diameter smooth pipe contains an orifice plate with $D: \frac{1}{2}D$ taps and $\beta = 0.5$. The measured orifice pressure drop is 75 kPa for water flow at 20°C. Estimate the flow rate, in m³/h. What is the nonrecoverable head loss?

*__P6.144__ Water at 20°C flows through the orifice in Fig. P6.154, which is monitored by a mercury manometer. If $d = 3$ cm, (a) what is h when the flow rate is 20 m³/h and (b) what is Q in m³/h when $h = 58$ cm?

Water

5 cm

d

h

Mercury
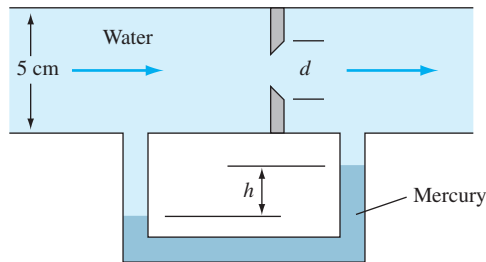
P6.144

P6.145 The 1-m-diameter tank in Fig. P6.145 is initially filled with gasoline at 20°C. There is a 2-cm-diameter orifice in the bottom. If the orifice is suddenly opened, estimate the time for the fluid level $h(t)$ to drop from 2.0 to 1.6 m.

$h(0) = 2$ m

1 m

$h(t)$

P6.145

$Q(t)$
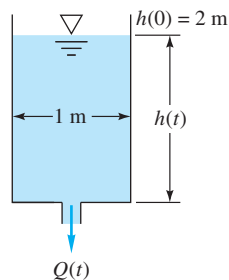
P6.146 A pipe connecting two reservoirs, as in Fig. P6.146, contains a thin-plate orifice. For water flow at 20°C, estimate (a) the volume flow through the pipe and (b) the pressure drop across the orifice plate.

20 m

$L = 100$ m
$D = 5$ cm

3-cm
orifice
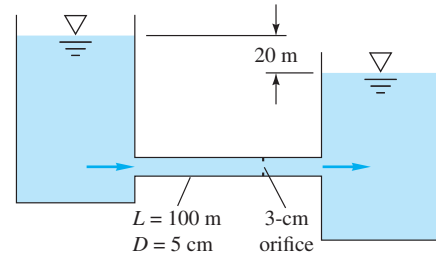
P6.146

P6.147 Air flows through a 6-cm-diameter smooth pipe that has a 2-m-long perforated section containing 500 holes (diameter 1 mm), as in Fig. P6.147. Pressure outside the pipe is sea-level standard air. If $p_1 = 105$ kPa and $Q_1 = 110$ m³/h, estimate p_2 and Q_2, assuming that the holes are approximated by thin-plate orifices. (*Hint:* A momentum control volume may be very useful.)

500 holes (diameter 1 mm)

1

2

2 m

$D = 6$ cm
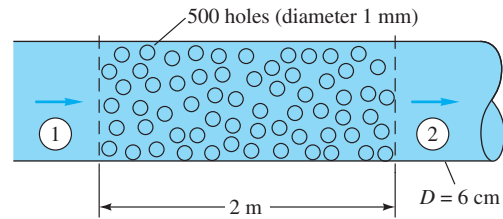
P6.147

P6.148 A smooth pipe containing ethanol at 20°C flows at 7 m³/h through a Bernoulli obstruction, as in Fig. P6.148. Three piezometer tubes are installed, as shown. If the obstruction is a thin-plate orifice, estimate the piezometer levels (a) h_2 and (b) h_3.

h_3

h_2

$h_1 = 1$ m

5 m

$D = 5$ cm

$d = 3$ cm
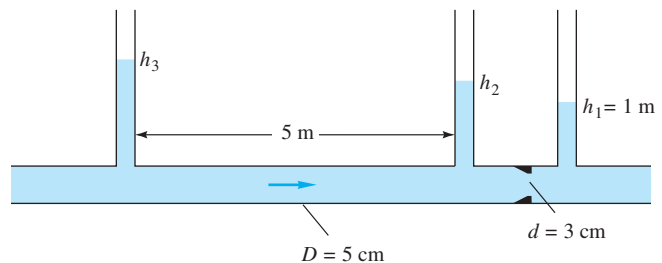
P6.148

Flowmeters: the flow nozzle

P6.149 In a laboratory experiment, air at 20°C flows from a large tank through a 2-cm-diameter smooth pipe into a sea-level atmosphere, as in Fig. P6.149. The flow is metered by a long-radius nozzle of 1-cm diameter, using a manometer with Meriam red oil (SG = 0.827). The pipe is 8 m long. The measurements of tank pressure and manometer height are as follows:

p_{tank}, Pa(gage):	60	320	1200	2050	2470	3500	4900
h_{mano}, mm:	6	38	160	295	380	575	820

Use these data to calculate the flow rates Q and Reynolds numbers Re_D and make a plot of measured flow rate versus tank pressure. Is the flow laminar or turbulent? Compare the data with theoretical results obtained from the Moody chart, including minor losses. Discuss.
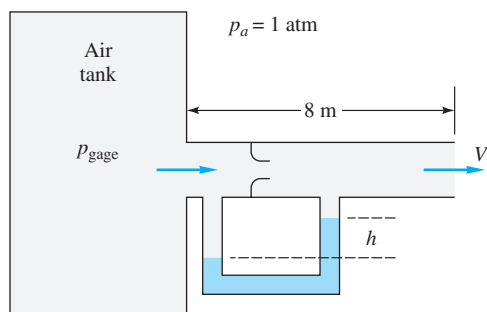

P6.149

P6.150 Gasoline at 20°C flows at 0.06 m³/s through a 15-cm pipe and is metered by a 9-cm long-radius flow nozzle (Fig. 6.40a). What is the expected pressure drop across the nozzle?

P6.151 An engineer needs to monitor a flow of 20°C gasoline at about 250 ± 25 gal/min through a 4-in-diameter smooth pipe. She can use an orifice plate, a long-radius flow nozzle, or a venturi nozzle, all with 2-in-diameter throats. The only differential pressure gage available is accurate in the range 6 to 10 lbf/in². Disregarding flow losses, which device is best?

P6.152 Kerosene at 20°C flows at 20 m³/h in an 8-cm-diameter pipe. The flow is to be metered by an ISA 1932 flow nozzle so that the pressure drop is 7000 Pa. What is the proper nozzle diameter?

P6.153 Two water tanks, each with base area of 1 ft², are connected by a 0.5-in-diameter long-radius nozzle as in Fig. P6.153. If $h = 1$ ft as shown for $t = 0$, estimate the time for $h(t)$ to drop to 0.25 ft.
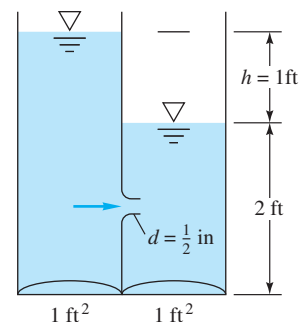

P6.153

Flowmeters: the venturi meter

P6.154 Gasoline at 20°C flows through a 6-cm-diameter pipe. It is metered by a modern venturi nozzle with $d = 4$ cm. The measured pressure drop is 8.5 kPa. Estimate the flow rate in gallons per minute.

P6.155 It is desired to meter methanol at 20°C flowing through a 5-in-diameter pipe. The expected flow rate is about 300 gal/min. Two flowmeters are available: a venturi nozzle and a thinplate orifice, each with $d = 2$ in. The differential pressure gage on hand is most accurate at about 12–15 lbs/in². Which meter is better for this job?

P6.156 Ethanol at 20°C flows down through a modern venturi nozzle as in Fig. P6.156. If the mercury manometer reading is 4 in, as shown, estimate the flow rate, in gal/min.
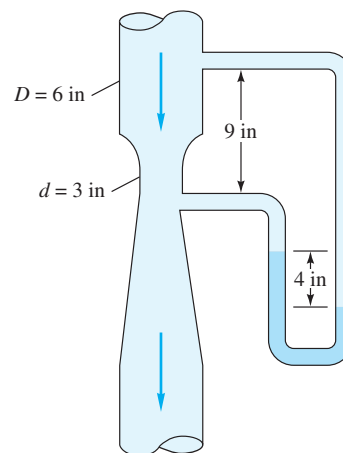
P6.156

P6.157 Modify Prob. P6.156 if the fluid is air at 20°C, entering the venturi at a pressure of 18 lbf/in². Should a compressibility correction be used?

P6.158 Water at 20°C flows in a long horizontal commercial steel 6-cm-diameter pipe that contains a classical Herschel venturi with a 4-cm throat. The venturi is connected to a mercury manometer whose reading is $h = 40$ cm. Estimate

(*a*) the flow rate, in m³/h, and (*b*) the total pressure difference between points 50 cm upstream and 50 cm downstream of the venturi.

P6.159 A modern venturi nozzle is tested in a laboratory flow with water at 20°C. The pipe diameter is 5.5 cm, and the venturi throat diameter is 3.5 cm. The flow rate is measured by a weigh tank and the pressure drop by a water–mercury manometer. The mass flow rate and manometer readings are as follows:

$\dot{m}$, kg/s	0.95	1.98	2.99	5.06	8.15
h, mm	3.7	15.9	36.2	102.4	264.4

Use these data to plot a calibration curve of venturi discharge coefficient versus Reynolds number. Compare with the accepted correlation, Eq. (6.114).

Flowmeters: other designs

P6.160 An instrument popular in the beverage industry is the *target flowmeter* in Fig. P6.160. A small flat disk is mounted in the center of the pipe, supported by a strong but thin rod. (*a*) Explain how the flowmeter works. (*b*) If the bending moment *M* of the rod is measured at the wall, derive a formula for the estimated velocity of the flow. (*c*) List a few advantages and disadvantages of such an instrument.

Flow
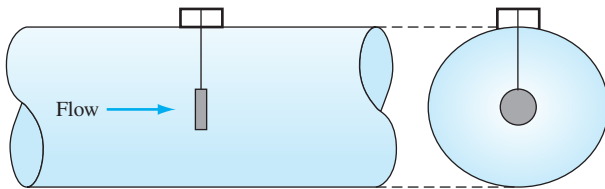
P6.160

P6.161 An instrument popular in the water supply industry, sketched in Fig. P6.161, is the single jet water meter. (*a*) How does it work? (*b*) What do you think a typical calibration curve would look like? (*c*) Can you cite further details, for example, reliability, head loss, cost [58]?
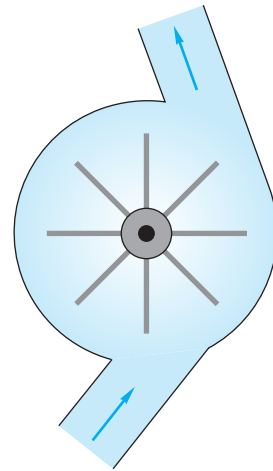

P6.161

Flowmeters: compressibility correction

P6.162 Air flows at high speed through a Herschel venturi monitored by a mercury manometer, as shown in Fig. P6.162. The upstream conditions are 150 kPa and 80°C. If $h = 37$ cm, estimate the mass flow in kg/s. (*Hint:* The flow is compressible.)

P6.163 Modify Prob. P6.162 as follows: Find the manometer reading h for which the mass flow through the venturi is approximately 0.4 kg/s. (*Hint:* The flow is compressible.)

$D = 6$ cm

$d = 4$ cm

Air

h

Mercury
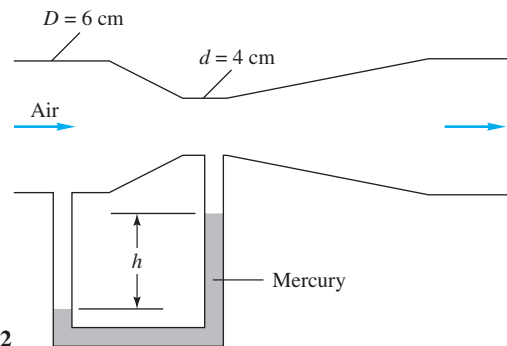
P6.162

Word Problems

W6.1 In fully developed straight-duct flow, the velocity profiles do not change (why?), but the pressure drops along the pipe axis. Thus there is pressure work done on the fluid. If, say, the pipe is insulated from heat loss, where does this energy go? Make a thermodynamic analysis of the pipe flow.

W6.2 From the Moody chart (Fig. 6.13), rough surfaces, such as sand grains or ragged machining, do not affect laminar flow.

Can you explain why? They *do* affect turbulent flow. Can you develop, or suggest, an analytical–physical model of turbulent flow near a rough surface that might be used to predict the known increase in pressure drop?

W6.3 Differentiation of the laminar pipe flow solution, Eq. (6.40), shows that the fluid shear stress $\tau(r)$ varies linearly from zero at the axis to τ_w at the wall. It is claimed that this

is also true, at least in the time mean, for fully developed *turbulent* flow. Can you verify this claim analytically?

W6.4   A porous medium consists of many tiny tortuous passages, and Reynolds numbers based on pore size are usually very low, of order unity. In 1856 H. Darcy proposed that the pressure gradient in a porous medium was directly proportional to the volume-averaged velocity **V** of the fluid:

$$\nabla p = -\frac{\mu}{K}\mathbf{V}$$

where K is termed the *permeability* of the medium. This is now called *Darcy's law* of porous flow. Can you make a

Poiseuille flow model of porous-media flow that verifies Darcy's law? Meanwhile, as the Reynolds number increases, so that $VK^{1/2}/\nu > 1$, the pressure drop becomes nonlinear, as was shown experimentally by P. H. Forscheimer as early as 1782. The flow is still decidedly laminar, yet the pressure gradient is quadratic:

$$\nabla p = -\frac{\mu}{K}\mathbf{V} - C|V|\mathbf{V} \quad \text{Darcy-Forscheimer law}$$

where C is an empirical constant. Can you explain the reason for this nonlinear behavior?

## Fundamentals of Engineering Exam Problems

FE6.1   In flow through a straight, smooth pipe, the diameter Reynolds number for transition to turbulence is generally taken to be
(*a*) 1500, (*b*) 2300, (*c*) 4000, (*d*) 250,000, (*e*) 500,000

FE6.2   For flow of water at 20°C through a straight, smooth pipe at 0.06 m³/h, the pipe diameter for which transition to turbulence occurs is approximately
(*a*) 1.0 cm, (*b*) 1.5 cm, (*c*) 2.0 cm, (*d*) 2.5 cm, (*e*) 3.0 cm

FE6.3   For flow of oil [$\mu = 0.1$ kg/(m · s), SG = 0.9] through a long, straight, smooth 5-cm-diameter pipe at 14 m³/h, the pressure drop per meter is approximately
(*a*) 2200 Pa, (*b*) 2500 Pa, (*c*) 10,000 Pa, (*d*) 160 Pa, (*e*) 2800 Pa

FE6.4   For flow of water at a Reynolds number of 1.03 E6 through a 5-cm-diameter pipe of roughness height 0.5 mm, the approximate Moody friction factor is
(*a*) 0.012, (*b*) 0.018, (*c*) 0.038, (*d*) 0.049, (*e*) 0.102

FE6.5   Minor losses through valves, fittings, bends, contractions, and the like are commonly modeled as proportional to
(*a*) total head, (*b*) static head, (*c*) velocity head, (*d*) pressure drop, (*e*) velocity

FE6.6   A smooth 8-cm-diameter pipe, 200 m long, connects two reservoirs, containing water at 20°C, one of which has a surface elevation of 700 m and the other a surface elevation of 560 m. If minor losses are neglected, the expected flow rate through the pipe is
(*a*) 0.048 m³/h, (*b*) 2.87 m³/h, (*c*) 134 m³/h, (*d*) 172 m³/h, (*e*) 385 m³/h

FE6.7   If, in Prob. FE6.6 the pipe is rough and the actual flow rate is 90 m³/h, then the expected average roughness height of the pipe is approximately
(*a*) 1.0 mm, (*b*) 1.25 mm, (*c*) 1.5 mm, (*d*) 1.75 mm, (*e*) 2.0 mm

FE6.8   Suppose in Prob. FE6.6 the two reservoirs are connected, not by a pipe, but by a sharp-edged orifice of diameter 8 cm. Then the expected flow rate is approximately
(*a*) 90 m³/h, (*b*) 579 m³/h, (*c*) 748 m³/h, (*d*) 949 m³/h, (*e*) 1048 m³/h

FE6.9   Oil [$\mu = 0.1$ kg/(m · s), SG = 0.9] flows through a 50-m-long smooth 8-cm-diameter pipe. The maximum pressure drop for which laminar flow is expected is approximately
(*a*) 30 kPa, (*b*) 40 kPa, (*c*) 50 kPa, (*d*) 60 kPa, (*e*) 70 kPa

FE6.10   Air at 20°C and approximately 1 atm flows through a smooth 30-cm-square duct at 1500 ft³/min. The expected pressure drop per meter of duct length is
(*a*) 1.0 Pa, (*b*) 2.0 Pa, (*c*) 3.0 Pa, (*d*) 4.0 Pa, (*e*) 5.0 Pa

FE6.11   Water at 20°C flows at 3 m³/h through a sharp-edged 3-cm-diameter orifice in a 6-cm-diameter pipe. Estimate the expected pressure drop across the orifice.
(*a*) 440 Pa, (*b*) 680 Pa, (*c*) 875 Pa, (*d*) 1750 Pa, (*e*) 1870 Pa

FE6.12   Water flows through a straight 10-cm-diameter pipe at a diameter Reynolds number of 250,000. If the pipe roughness is 0.06 mm, what is the approximate Moody friction factor?
(*a*) 0.015, (*b*) 0.017, (*c*) 0.019, (*d*) 0.026, (*e*) 0.032

FE6.13   What is the hydraulic diameter of a rectangular air-ventilation duct whose cross section is 1 m by 25 cm?
(*a*) 25 cm, (*b*) 40 cm, (*c*) 50 cm, (*d*) 75 cm, (*e*) 100 cm

FE6.14   Water at 20°C flows through a pipe at 300 gal/min with a friction head loss of 45 ft. What is the power required to drive this flow?
(*a*) 0.16 kW, (*b*) 1.88 kW, (*c*) 2.54 kW, (*d*) 3.41 kW, (*e*) 4.24 kW

FE6.15   Water at 20°C flows at 200 gal/min through a pipe 150 m long and 8 cm in diameter. If the friction head loss is 12 m, what is the Moody friction factor?
(*a*) 0.010, (*b*) 0.015, (*c*) 0.020, (*d*) 0.025, (*e*) 0.030

Comprehensive Problems

C6.1 A pitot-static probe will be used to measure the velocity distribution in a water tunnel at 20°C. The two pressure lines from the probe will be connected to a U-tube manometer that uses a liquid of specific gravity 1.7. The maximum velocity expected in the water tunnel is 2.3 m/s. Your job is to select an appropriate U-tube from a manufacturer that supplies manometers of heights 8, 12, 16, 24, and 36 in. The cost increases significantly with manometer height. Which of these should you purchase?

*__C6.2__ A pump delivers a steady flow of water (ρ, μ) from a large tank to two other higher-elevation tanks, as shown in Fig. C6.2. The same pipe of diameter d and roughness ε is used throughout. All minor losses *except through the valve* are neglected, and the partially closed valve has a loss coefficient K_{valve}. Turbulent flow may be assumed with all kinetic energy flux correction coefficients equal to 1.06. The pump net head H is a known function of Q_A and hence also of $V_A = Q_A/A_{pipe}$; for example, $H = a - bV_A^2$, where a and b are constants. Subscript J refers to the junction point at the tee where branch A splits into B and C. Pipe length L_C is much longer than L_B. It is desired to predict the pressure at J, the three pipe velocities and friction factors, and the pump head. Thus there are eight variables: H, V_A, V_B, V_C, f_A, f_B, f_C, p_J. Write down the eight equations needed to resolve this problem, but *do not solve,* since an elaborate iteration procedure would be required.
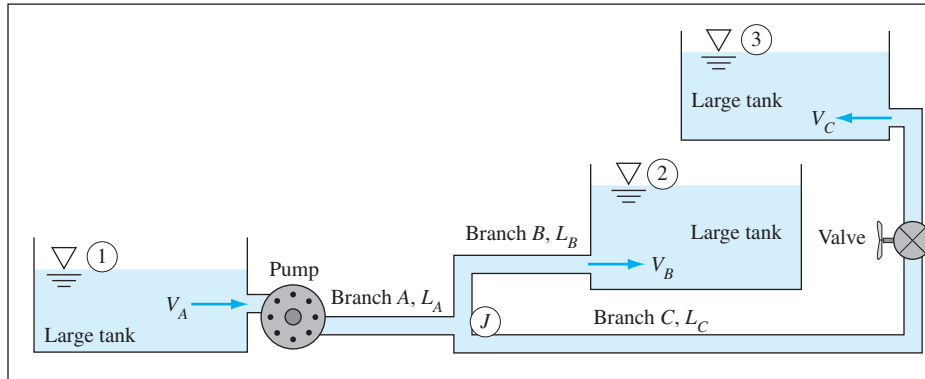

C6.2

C6.3 A small water slide is to be installed inside a swimming pool. See Fig. C6.3. The slide manufacturer recommends a continuous water flow rate Q of 1.39×10^{-3} m³/s (about 22 gal/min) down the slide, to ensure that the customers do not burn their bottoms. A pump is to be installed under the slide, with a 5.00-m-long, 4.00-cm-diameter hose supplying swimming pool water for the slide. The pump is 80 percent efficient and will rest fully submerged 1.00 m below the water surface. The roughness inside the hose is about 0.0080 cm. The hose discharges the water at the top of the slide as a free jet open to the atmosphere. The hose outlet is 4.00 m above the water surface. For fully developed turbulent pipe flow, the kinetic energy flux correction factor is about 1.06. Ignore any minor losses here. Assume that $\rho = 998$ kg/m³ and $v = 1.00 \times 10^{-6}$ m²/s for this water. Find the brake horsepower (that is, the actual shaft power in watts) required to drive the pump.

*__C6.4__ Suppose you build a rural house where you need to run a pipe to the nearest water supply, which is fortunately at an elevation of about 1000 m above that of your house. The pipe will be 6.0 km long (the distance to the water supply), and the gage pressure at the water supply is 1000 kPa. You require a minimum of 3.0 gal/min of water when the end of your pipe is open to the atmosphere. To minimize cost, you want to buy the smallest-diameter pipe possible. The pipe you will use is extremely smooth. (*a*) Find the total head loss from the pipe inlet to its exit. Neglect any minor losses due to valves, elbows, entrance lengths, and so on, since the length is so long here and major losses dominate. Assume the outlet of the pipe is open to the atmosphere. (*b*) Which is more important in this problem, the head loss due to elevation difference or the head loss due to pressure drop in the pipe? (*c*) Find the minimum required pipe diameter.

C6.5 Water at room temperature flows at the *same* volume flow rate, $Q = 9.4 \times 10^{-4}$ m³/s, through two ducts, one a round pipe and one an annulus. The cross-sectional area A of the two ducts is identical, and all walls are made of commercial steel. Both ducts are the same length. In the cross sections shown in Fig. C6.5 $R = 15.0$ mm and $a = 25.0$ mm.
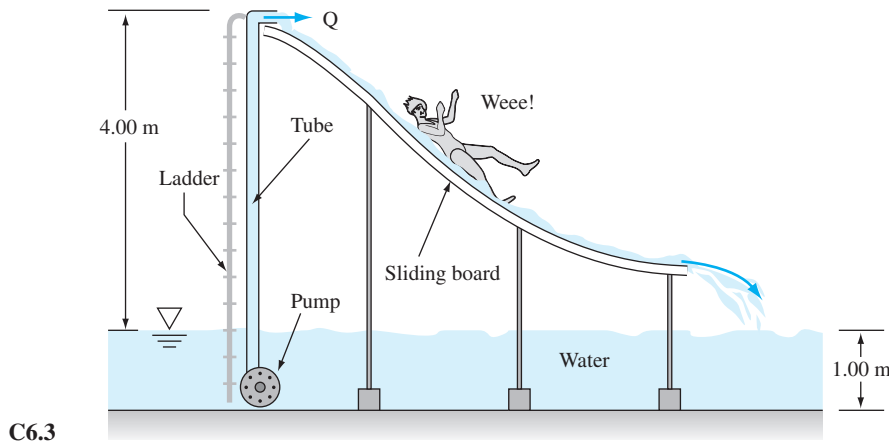
C6.3
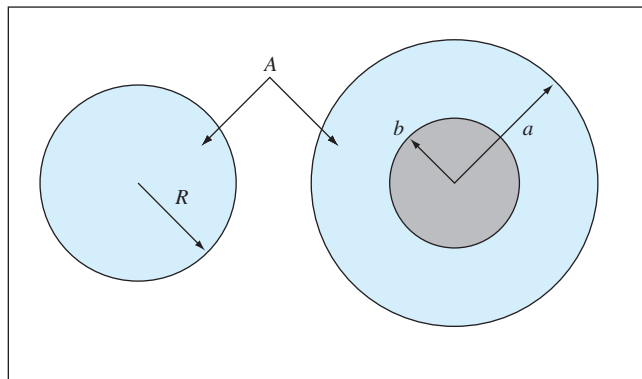
C6.5

(*a*) What is the radius *b* such that the cross-sectional areas of the two ducts are identical? (*b*) Compare the frictional head loss h_f per unit length of pipe for the two cases, assuming fully developed flow. For the annulus, do both a quick estimate (using the hydraulic diameter) and a more accurate estimate (using the effective diameter correction), and compare. (*c*) If the losses are different for the two cases, explain why. Which duct, if any, is more "efficient"?

C6.6   John Laufer (*NACA Tech Rep*. 1174, 1954) gave velocity data 20°C airflow in a smooth 24.7-cm-diameter pipe at Re ≈ 5 E5:

u/u_{CL}	1.0	0.997	0.988	0.959	0.908	0.847	0.818	0.771	0.690
r/R	0.0	0.102	0.206	0.412	0.617	0.784	0.846	0.907	0.963

Source: John Laufer (NASA Tech Rep. 1174, 1954)

The centerline velocity u_{CL} was 30.5 m/s. Determine (*a*) the average velocity by numerical integration and (*b*) the wall shear stress from the log law approximation. Compare with the Moody chart and with Eq. (6.43).

C6.7   Consider energy exchange in fully developed laminar flow between parallel plates, as in Eqs. (6.60). Let the pressure drop over a length L be Δp. Calculate the rate of work done by this pressure drop on the fluid in the region ($0 < x < L$, $-h < y < +h$) and compare with the integrated energy dissipated due to the viscous function Φ from Eq. (4.50) over this same region. The two should be equal. Explain why this is so. Can you relate the viscous drag force and the wall shear stress to this energy result?

C6.8   This text has presented the traditional correlations for the turbulent smooth-wall friction factor, Eq. (6.38), and the law of the wall, Eq. (6.28). Recently, groups at Princeton and Oregon [56] have made new friction measurements and suggest the following smooth-wall friction law:
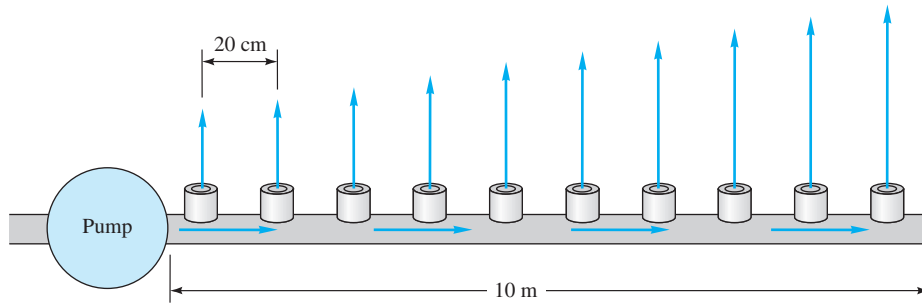
$$\frac{1}{\sqrt{f}} = 1.930 \log_{10}(\mathrm{Re}_D \sqrt{f}) - 0.537$$

In earlier work, they also report that better values for the constants κ and B in the log-law, Eq. (6.28), are $\kappa \approx 0.421 \pm 0.002$ and $B \approx 5.62 \pm 0.08$. (*a*) Calculate a few values of f in the range 1 E4 ≤ Re_D ≤ 1 E8 and see how the two formulas differ. (*b*) Read Ref. 56 and briefly check the five papers in its bibliography. Report to the class on the general results of this work.

C6.9   A pipeline has been proposed to carry natural gas 1715 miles from Alaska's North Slope to Calgary, Alberta, Canada. The (assumed smooth) pipe diameter will be 52 in. The gas will be at high pressure, averaging 2500 lbs/in². (*a*) Why? The proposed flow rate is 4 billion cubic feet per day at sea-level conditions. (*b*) What volume flow rate, at 20°C, would carry the same mass at the high pressure? (*c*) If natural gas is assumed to be methane (CH_4), what is the total pressure drop? (*d*) If each pumping station can deliver 12,000 hp to the flow, how many stations are needed?

Design Projects

D6.1 A hydroponic garden uses the 10-m-long perforated-pipe system in Fig. D6.1 to deliver water at 20°C. The pipe is 5 cm in diameter and contains a circular hole every 20 cm. A pump delivers water at 75 kPa (gage) at the entrance, while the other end of the pipe is closed. If you attempted, for example, Prob. P3.125, you know that the pressure near the closed end of a perforated "manifold" is surprisingly high, and there will be too much flow through the holes near that end. One remedy is to vary the hole size along the pipe axis. Make a design analysis, perhaps using a personal computer, to pick the optimum hole size distribution that will make the discharge flow rate as uniform as possible along the pipe axis. You are constrained to pick hole sizes that correspond only to commercial (numbered) metric drill-bit sizes available to the typical machine shop.

D6.2 It is desired to design a pump-piping system to keep a 1-million-gallon capacity water tank filled. The plan is to use a modified (in size and speed) version of the model 1206 centrifugal pump manufactured by Taco Inc., Cranston, Rhode Island. Test data have been provided to us by Taco Inc. for a small model of this pump: $D = 5.45$ in, $\Omega = 1760$ r/min, tested with water at 20°C:

Q, gal/min	0	5	10	15	20	25	30	35	40	45	50	55	60
H, ft	28	28	29	29	28	28	27	26	25	23	21	18	15
Efficiency, %	0	13	25	35	44	48	51	53	54	55	53	50	45

The tank is to be filled daily with rather chilly (10°C) groundwater from an aquifer, which is 0.8 mi from the tank and 150 ft lower than the tank. Estimated daily water use is 1.5 million gal/day. Filling time should not exceed 8 h per day. The piping system should have four "butterfly" valves

D6.1

with variable openings (see Fig. 6.19), 10 elbows of various angles, and galvanized iron pipe of a size to be selected in the design. The design should be economical—both in capital costs and operating expense. Taco Inc. has provided the following cost estimates for system components:

Pump and motor	$3500 plus $1500 per inch of impeller size
Pump speed	Between 900 and 1800 r/min
Valves	$300 + $200 per inch of pipe size
Elbows	$50 plus $50 per inch of pipe size
Pipes	$1 per inch of diameter per foot of length
Electricity cost	10¢ per kilowatt-hour

Your design task is to select an economical pipe size and pump impeller size and speed for this task, using the pump test data in nondimensional form (see Prob. P5.61) as design data. Write a brief report (five to six pages) showing your calculations and graphs.

References

1. P. S. Bernard and J. M. Wallace, *Turbulent Flow: Analysis, Measurement, and Prediction,* Wiley, New York, 2002.
2. H. Schlichting et al., *Boundary Layer Theory*, Springer, New York, 2000.
3. F. M. White, *Viscous Fluid Flow,* 3d ed., McGraw-Hill, New York, 2005.
4. O. Reynolds, "An Experimental Investigation of the Circumstances which Determine Whether the Motion of Water Shall Be Direct or Sinuous and of the Law of Resistance in Parallel Channels," *Phil. Trans. R. Soc.,* vol. 174, 1883, pp. 935–982.
5. P. G. Drazin and W. H. Reid, *Hydrodynamic Stability*, 2d ed., Cambridge University Press, New York, 2004.

6. H. Rouse and S. Ince, *History of Hydraulics,* Iowa Institute of Hydraulic Research, State University of Iowa, Iowa City, 1957.

7. J. Nikuradse, "Strömungsgesetze in Rauhen Rohren," *VDI Forschungsh.* 361, 1933; English trans., *NACA Tech. Mem.* 1292.

8. L. F. Moody, "Friction Factors for Pipe Flow," *ASME Trans.,* vol. 66, pp. 671–684, 1944.

9. C. F. Colebrook, "Turbulent Flow in Pipes, with Particular Reference to the Transition between the Smooth and Rough Pipe Laws," *J. Inst. Civ. Eng. Lond.,* vol. 11, 1938–1939, pp. 133–156.

10. O. C. Jones, Jr., "An Improvement in the Calculations of Turbulent Friction in Rectangular Ducts," *J. Fluids Eng.,* June 1976, pp. 173–181.

11. R. Berker, *Handbuch der Physik,* vol. 7, no. 2, pp. 1–384, Springer-Verlag, Berlin, 1963.

12. R. M. Olson, *Essentials of Engineering Fluid Mechanics*, Literary Licensing LLC, Whitefish, MT, 2012.

13. P. A. Durbin and B. A. Pettersson, *Statistical Theory and Modeling for Turbulent Flows*, 2d ed., Wiley, New York, 2010.

14. P. W. Runstadler, Jr., et al., "Diffuser Data Book," *Creare Inc. Tech. Note* 186, Hanover, NH, 1975.

15. "*Flow of Fluids through Valves, Fittings, and Pipes,*" Tech. Paper 410, Crane Valve Group, Long Beach, CA, 1957 (now updated as a CD-ROM; see < http://www.cranevalves.com >).

16. E. F. Brater, H. W. King, J. E. Lindell, and C. Y. Wei, *Handbook of Hydraulics,* 7th ed., McGraw-Hill, New York, 1996.

17. H. Cross, "Analysis of Flow in Networks of Conduits or Conductors," *Univ. Ill. Bull.* 286, November 1936.

18. P. K. Swamee and A. K. Sharma, *Design of Water Supply Pipe Networks*, Wiley-Interscience, New York, 2008.

19. D. C. Wilcox, *Turbulence Modeling for CFD*, 3d ed., DCW Industries, La Cañada, CA, 2006.

20. R. W. Jeppson, *Analysis of Flow in Pipe Networks,* Butterworth-Heinemann, Woburn, MA, 1976.

21. R. W. Fox and S. J. Kline, "Flow Regime Data and Design Methods for Curved Subsonic Diffusers," *J. Basic Eng.,* vol. 84, 1962, pp. 303–312.

22. R. C. Baker, *Flow Measurement Handbook: Industrial Designs, Operating Principles, Performance, and Applications*, Cambridge University Press, New York, 2005.

23. R. W. Miller, *Flow Measurement Engineering Handbook,* 3d edition, McGraw-Hill, New York, 1997.

24. B. Warren and C. Wunsch (eds.), *Evolution of Physical Oceanography,* M.I.T. Press, Cambridge, MA, 1981.

25. U.S. Department of Commerce, *Tidal Current Tables,* National Oceanographic and Atmospheric Administration, Washington, DC, 1971.

26. J. A. Shercliff, *Electromagnetic Flow Measurement,* Cambridge University Press, New York, 1962.

27. J. A. Miller, "A Simple Linearized Hot-Wire Anemometer," *J. Fluids Eng.,* December 1976, pp. 749–752.

28. R. J. Goldstein (ed.), *Fluid Mechanics Measurements,* 2d ed., Hemisphere, New York, 1996.

29. D. Eckardt, "Detailed Flow Investigations within a High Speed Centrifugal Compressor Impeller," *J. Fluids Eng.,* September 1976, pp. 390–402.

30. H. S. Bean (ed.), *Fluid Meters: Their Theory and Application,* 6th ed., American Society of Mechanical Engineers, New York, 1971.

31. "Measurement of Fluid Flow by Means of Orifice Plates, Nozzles, and Venturi Tubes Inserted in Circular Cross Section Conduits Running Full," *Int. Organ. Stand. Rep.* DIS-5167, Geneva, April 1976.

32. P. Sagaut and C. Meneveau, *Large Eddy Simulation for Incompressible Flows: An Introduction*, 3d ed., Springer, New York, 2006.

33. S. E. Haaland, "Simple and Explicit Formulas for the Friction Factor in Turbulent Pipe Flow," *J. Fluids Eng.,* March 1983, pp. 89–90.

34. R. K. Shah and A. L. London, *Laminar Flow Forced Convection in Ducts,* Academic, New York, 1979.

35. P. L. Skousen, *Valve Handbook,* 3d ed. McGraw-Hill, New York, 2011.

36. W. Li, W.-X. Chen, and S.-Z. Xie, "Numerical Simulation of Stress-Induced Secondary Flows with Hybrid Finite Analytic Method," *Journal of Hydrodynamics,* vol. 14, no. 4, December 2002, pp. 24–30.

37. *ASHRAE Handbook—2012 Fundamentals,* ASHRAE, Atlanta, GA, 2012.

38. F. Durst, A. Melling, and J. H. Whitelaw, *Principles and Practice of Laser-Doppler Anemometry,* 2d ed., Academic, New York, 1981.

39. A. P. Lisitsyn et al., *Laser Doppler and Phase Doppler Measurement Techniques,* Springer-Verlag, New York, 2003.

40. J. E. Amadi-Echendu, H. Zhu, and E. H. Higham, "Analysis of Signals from Vortex Flowmeters," *Flow Measurement and Instrumentation,* vol. 4, no. 4, Oct. 1993, pp. 225–231.

41. G. Vass, "Ultrasonic Flowmeter Basics," *Sensors,* vol. 14, no. 10, Oct. 1997, pp. 73–78.

42. ASME Fluid Meters Research Committee, "The ISO-ASME Orifice Coefficient Equation," *Mech. Eng.* July 1981, pp. 44–45.

43. R. D. Blevins, *Applied Fluid Dynamics Handbook,* Van Nostrand Reinhold, New York, 1984.

44. O. C. Jones, Jr., and J. C. M. Leung, "An Improvement in the Calculation of Turbulent Friction in Smooth Concentric Annuli," *J. Fluids Eng.,* December 1981, pp. 615–623.

45. P. R. Bandyopadhyay, "Aspects of the Equilibrium Puff in Transitional Pipe Flow," *J. Fluid Mech.,* vol. 163, 1986, pp. 439–458.

46. I. E. Idelchik, *Handbook of Hydraulic Resistance,* 3d ed., CRC Press, Boca Raton, FL, 1993.

47. S. Klein and W. Beckman, *Engineering Equation Solver (EES),* University of Wisconsin, Madison, WI, 2014.

48. R. D. Coffield, P. T. McKeown, and R. B. Hammond, "Irrecoverable Pressure Loss Coefficients for Two Elbows in Series with Various Orientation Angles and Separation Distances," *Report WAPD-T-3117,* Bettis Atomic Power Laboratory, West Mifflin, PA, 1997.

49. H. Ito, "Pressure Losses in Smooth Pipe Bends," *Journal of Basic Engineering,* March 1960, pp. 131–143.

50. A. H. Gibson, "On the Flow of Water through Pipes and Passages," *Proc. Roy. Soc. London,* Ser. A, vol. 83, 1910, pp. 366–378.

51. M. Raffel et al., *Particle Image Velocimetry: A Practical Guide,* 2d ed., Springer, New York, 2007.

52. Crane Co., *Flow of Fluids through Valves, Fittings, and Pipe*, Crane, Stanford, CT, 2009.

53. S. A. Berger, L. Talbot, and L.-S. Yao, "Flow in Curved Pipes," *Annual Review of Fluid Mechanics,* vol. 15, 1983, pp. 461–512.

54. P. L. Spedding, E. Benard, and G. M. McNally, "Fluid Flow through 90° Bends," *Developments in Chemical Engineering and Mineral Processing,* vol. 12, nos. 1–2, 2004, pp. 107–128.

55. R. R. Kerswell, "Recent Progress in Understanding the Transition to Turbulence in a Pipe," *Nonlinearity,* vol. 18, 2005, pp. R17–R44.

56. B. J. McKeon et al., "Friction Factors for Smooth Pipe Flow," *J. Fluid Mech.,* vol. 511, 2004, pp. 41–44.

57. M. Bahrami, M. M. Yovanovich, and J. R. Culham, "Pressure Drop of Fully-Developed Laminar Flow in Microchannels of Arbitrary Cross-Section," *J. Fluids Engineering,* vol. 128, Sept. 2006, pp. 1036–1044.

58. G. S. Larraona, A. Rivas, and J. C. Ramos, "Computational Modeling and Simulation of a Single-Jet Water Meter," *J. Fluids Engineering,* vol. 130, May 2008, pp. 0511021–05110212.

59. C. Spiegel, *Designing and Building Fuel Cells,* McGraw-Hill, New York, 2007.

60. B. A. Finlayson et al., *Microcomponent Flow Characterization*, Chap. 8 of *Micro Instrumentation*, M. V. Koch (Ed.), John Wiley, Hoboken, NJ, 2007.